DOCTORAL DISSERTATION
SHIBAURA INSTITUTE OF TECHNOLOGY

DEVELOPMENT OF WOODCERAMICS ORIGINATED

FROM BIOMASS, AND THEIR APPLICATIONS

MARCH 2015

DON KAEWDOOK

SHIBAURA INSTITUTE OF TECHNOLOGY

DEVELOPMENT OF WOODCERAMICS ORIGINATED FROM BIOMASS, AND THEIR APPLICATIONS

By

DON KAEWDOOK

A THESIS SUBMITTED TO

SHIBAURA INSTITUTE OF TECHNOLOGY

IN PARTIAL FULFILLMENT OF THE REQUIREMENTS FOR THE DEGREE OF

DOCTOR OF ENGINEERING

GRADUATE SCHOOL OF ENGINEERING AND SCIENCE

MARCH 2015

Declaration of Authorship

I, DON KAEWDOOK, declare that this thesis titled, DEVELOPMENT OF WOODCERAMICS ORIGINATED FROM BIOMASS, AND THEIR APPLICATIONS and the work presented in it are my own. I confirm that:

- This work was done wholly or mainly while in candidate for a research degree at Shibaura Institute of Technology.
- Where any part of this thesis has previously been submitted for a degree or any other qualification at Shibaura Institute of Technology or any other institution, this has been clearly stated.
- Where I have consulted the published work of others, this is always clearly attributed.
- Where I have quoted from the work of others, the source is always given. With the exception of such quotations, this thesis is entirely my own work.
- I have acknowledged all main sources of help.
- Where the thesis is based on work done by myself jointly with another, I have made clear exactly what was done by others and what I have contributed myself.

Signed: _____

(Don KAEWDOOK)

Certified by: _____

(Prof.Dr.Akito TAKASAKI)

Date: _____

ABSTRACT

The increasing world population causes an increasing consumption of resources and the increased generation of waste, which leads to the need for development of new materials made from renewable resources harmless to the natural environment. Thailand has plenty of such renewable resources since its economy is largely based on agriculture, and biomass residues from crops progressively increase as the Thai government promotes the production of crops and high volume exports. Currently, natural rubber is a plant of economic importance to Thailand. The region is the largest producer and exporter of natural rubber in Asia and Thailand has a top of global market share. The natural rubber wood constitutes a large part of its biomass as rubber trees have a productive life of 20-25 years. Once this period of time has been completed, the farmers need to cut down the old trees for replanting. The large volume of waste and biomass from old rubber trees is a problem that needs to be addressed. To use the biomass waste effectively I focus on woodceramics which were developed in Japan.

Woodceramics (WCMs) is a new technical innovation with superb functionalities and high additional value. WCMs are carbon-based hybrid materials consisting of amorphous and glassy carbon (organic carbon resulting from carbonized wood waste) with porous structure.

In this research, I employed diverse techniques developed in Japan to fabricate WCMs. One objective of this research is to explore the potential to use biomass from natural rubber trees and wastes from coconut shells in Thailand to fabricate WCMs. These techniques will be environmentally safe and save operation costs to dispose of agricultural wastes.

This study examined the use of biomass charcoal made from carbonized residues of rubber wood and or coconut shell, mixed with phenolic resin and carbonized in a vacuum. The microstructure and physical characterization has been performed by several techniques, namely, X-ray diffraction (XRD), scanning electron microscope with energy dispersive X-ray analysis (SEM/EDX) and mechanical test. The results showed that the high weight ratio of phenolic resin increased compressive and bending strength of WCMs and high carbonization temperature affected the microstructure, surface porosity, density and increasing the purity of the graphite of WCMs.

I have studied three main applications of WCMs fabricated from biomass charcoal originated from rubber tree in Thailand, (1) production of amorphous carbon (a-C) films using woodceramics as a target material, (2) electrochemical deposition of nickel and/or copper on woodceramics and (3) fabrication of eco-composites using biomass charcoal with waste melamine formaldehyde. For production of amorphous carbon (a-C) films, the synthesis of the films onto a silicon wafer as substrate was successfully fabricated by a RF magnetron sputtering method using wood ceramics as a target. The a-C films possess carbon turbostratic structure or amorphous with electron configurations of type sp^2 and sp^3. For electrochemical deposition, in order to improve the compressive strength of WCMs, a metallic film was electrochemically deposited using copper sulfate ($CuSO_4$) and/or nickel sulfate ($NiSO_4$) solutions. As a result, the compressive strength was increased to 35 MPa and 43 MPa after being deposited in $CuSO_4$ and $NiSO_4$ solutions, respectively. Without this deposition process, the compressive strength was 28 MPa. For eco-composite, they were fabricated using charcoal powder obtained from rubber tree wood, waste melamine formaldehyde resin (WMF) powder and phenolic resin as binder material. A mixing ratio of WMF lower than 50 wt.% was used in the fabrication of eco-composites. The highest compressive strength of 35.7 MPa was obtained when the mixing ratio: WMF/Biomass charcoal/Phenolic resin was: 50/30/20.

ACKNOWLEDGEMENTS

Contents

List of Figures

List of Tables

Abbreviations

$\dot{A}$	Angstrom
CO_2	Carbon dioxide
$CuSO_4$	Copper Sulfate
CRP	Carbon fiber reinforced plastic
DLC	Diamond like Carbon
EDX	Energy-dispersive X-ray spectroscopy
JIS	Japan Industrial Standard
NR	Natural Rubber
$NiSO_4$	Nickel Sulfate
O_2	Oxygen
PMF	Pure of Virgin Melamine Formaldehyde
P_{atm}	Atmosphere pressure
R_T	Room temperature, ambient temperature
SEM	Scanning electron microscope
TG	Thermo gravimetric
T	Temperature
WMF	Waste Melamine Formaldehyde Resins
WCMs	Woodceramics
XRD	X-ray Diffraction
XPS	X-ray photoelectron spectroscopy

Physical Contents

Angstrom	$\mathring{A}$	=	$1.00001495 \times 10^{-10}$ m
X-ray values	CuK_α	=	$1.00207697 \times 10^{-13}$ m
Atomic mass constant	m_u	=	$1.660538921 \times 10^{-27}$ kg
Standard gravity	g	=	9.80665 m$\cdot$s^{-2}

Dedicated to my beloved parents, brothers, sisters, and all my best

friends for their endless love, support and encouragement

Chapter 1

Introduction

1.1 Current status of biomass residue in Thailand

Thailand is an agricultural country located in the center of Southeast Asia bordered by Myanmar, Lao PDR, Cambodia and Malaysia as shown in Figure 1.1. The total area is approximately 514,000 square kilometers [1], and the population in 2014 was estimated to have increased to 67.2 million. The main Gross Domestic Product (GDP) of Thailand extended to 0.60 percent in the third quarter of 2014 over the same quarter of 2013. Average GDP Annual Growth Rate in Thailand was 3.68 Percent from 1994 until 2014, reach to 19.10 percent in the fourth quarter of 2012 [2]. Thailand is divided into 77 provinces, covering the agricultural sector with 24.86 million people working on farms (39 percent of the total population) [3].

Figure 1.1 Thailand geographical locations [4]

The traditional of Thailand is an agricultural country, with regards to 10 percent of GDP is coming from the agricultural sector [5]. Agricultural products in Thailand have not only growth them for their own consumption, however,their are major source of economic income from exporting. The value of agricultural exports are slightly increase every year and acting as a main product of export earnings. The Thai government is attempting to enhance agricultural productivity, which is essential to raisraising incomes and improving the population's standard of living. After harvesting there will be a large amount of agricultural waste left which could be used as biomass energy.

The recent dramatic economic growth brought new environmental challenges. The country presently faces the prospect of air and water pollution, declining wildlife populations, deforestation, soil erosion, water scarcity, and hazardous waste issues growing into a serious problem in Thailand in 2013. The survey from the pollution control department, Ministry of Natural Resourcesand Environment of Thailand indicated that total waste generated in 2013 was found to be 26.77 million tons; an increase from 2012 which was about 2 million tons [6, 7].

This is a national problem where all agencies need to cooperate in order to brainstorm solutions. It warned scientists to assess its impacts on present ecosystem function and to provide valuable knowledge to establish green innovation which involves adaptation to mitigate climate change.

1.1.1 Biomass resources in Thailand

The biomass waste reprocessing project has objectives to reduce pressure on Thailand's natural forests and to reduce climate change and greenhouse gas emissions. Biomass is organic matter including forest and mill residues which are categorized broadly as waste coming from wood, non wood, and from animal droppings. The biomass from wood comprises forests, agroindustry plantation, bush trees, urban trees and fast growing trees. The woody biomass is generally a value commodious and has several advantage application such as timber, raw material for pulp and paper, the pencil and matchstick industries, and heat source cooking. Nonwoody biomass comprise of crop residues like straw, leaves, and plant stems, processing residues like saw dust, bagasse,

nutshells and husks, and domestic wastes (food, rubbish and sewage). Animal waste constitutes the wastes from animal husbandry [8, 9]. The assessment of biomass application potential including biomass residue and forestry biomass in Thailand was carried out taking into account the amount of biomass residue which was already demonstrate and the possibility of biomass energy estate farm in accordant with the National Plan of the Thai Government as,

- Agricultural crops such as sugarcane, cassava, corn, etc.
- Agricultural residues such as rice husk/straw from rice fields, cassava rhizome, corncobs, etc.
- Woody biomass residues from forest plantation, fast grawing trees, natural rubber trees, wood waste from wood mill, pulp and paper mill, palm oil extraction plants, etc.
- Waste of wood from furniture manufactory (barks, sawdust, etc.)
- The bio energy source for ethanol production (cassava, sugar cane, etc.)
- Raw materials for biodiesel production (palm oil, jatropha oil, etc.)
- Residues process from from agroindustry
- Livestock manure
- Solid waste from municipal and sewage.

Figure 1.2 Rice farm growth in Thailand [10]

Figure 1.3 Natural rubber product farm in Thailand [11-14].

The local areas in Thailand are main sources of biomass from paddy field as shown in Figure 1.2. Recently, most of woody biomass coming from natural rubber trees since the expanding production area to all regions of Thailand as economics trees as shown in Figure 1.3.

1.1.2 Biomass utilization in Thailand

Generally, the biomass shown in Table 1.1 is matter that is derived from the plant which is suitable for use as source materials for renewable energy, which makes them useful for large scale energy plantations. Biomass specially means agricultural wastes such as rice straw/husk, forestry waste, fast growing trees, economic trees as natural rubber trees. The utilization of biomass ranges from local usage to well established technology. Major technologies using biomass in Thailand are gasification, combustion, pyrolysis and biogas. However, the characteristics of biomass, availability of planting area, crop patterns, and storage and transportation, are main factors of efficient biomass utilization in Thailand. The utilization of biomass are mainly consumed from 2 sectors. The first is the residential sector, which use about 56%. The second is the mafacturing sector

which use about 44% in 2002 [15]. The biomass consumption indicates that the trend of biomass demand has increased .

Table 1.1 Agricultural product and Biomass ratio [16].

Agricultural Product	Biomass	Biomass Ratio (%)
Paddy	Rice husk	21.00
	Rice straw	49.00
Sugar cane	Bagasse	28.00
	Leaf, Top of Sugar cane	17.00
Cassava	Cassava waste	37.00
	Cassava peel	0.06
	Cassava rhizome	20.00
Corn	Corncob	24.00
	Corn stem	82.00
Coconut	Shell	81.56
Rubber wood	Waste wood	87

1.1.3 Thai rubber statistic

Thailand is the leading producer and exporter of natural rubber in South East Asia. The region is the largest producer and exporter of natural rubber in Asian country and the world with a market share of 80%. Among the region, Thailand is the top of global market share (33.1%), followed by Indonesia, Malaysia and Vietnam. The total amount of natural rubber produced and exported generates over 678,000 ton per year, involving no less than 6 million people as shown in Table 1.2 and Figure 1.4 [17, 18].

Table 1.2 Productivity of natural rubber in Thailand since 1993-2013.

Year	Quantity of Production	Quantity of Export	Domestic Consumption
1993	1,553,384	1,396,783	130,236
1994	1,717,861	1,604,964	132,195
1995	1,804,788	1,635,533	153,159
1996	1,970,265	1,762,989	173,671
1997	2,032,714	1,837,148	182,020
1998	2,075,950	1,839,396	186,379
1999	2,154,560	1,886,339	226,917
2000	2,346,487	2,166,153	242,549
2001	2,319,549	2,042,079	253,105
2002	2,615,104	2,354,416	278,355
2003	2,876,005	2,573,450	298,699
2004	2,984,293	2,637,096	318,649
2005	2,937,158	2,632,398	334,649
2006	3,136,993	2,771,673	320,885
2007	3,056,005	2,703,762	373,659
2008	3,089,751	2,675,283	397,595
2009	3,164,379	2,726,193	399,415
2010	3,252,135	2,866,447	458,637
2011	3,569,033	2,952,381	486,745
2012	3,778,010	3,121,332	505,052
2013	4,170,428	3,664,941	520,628
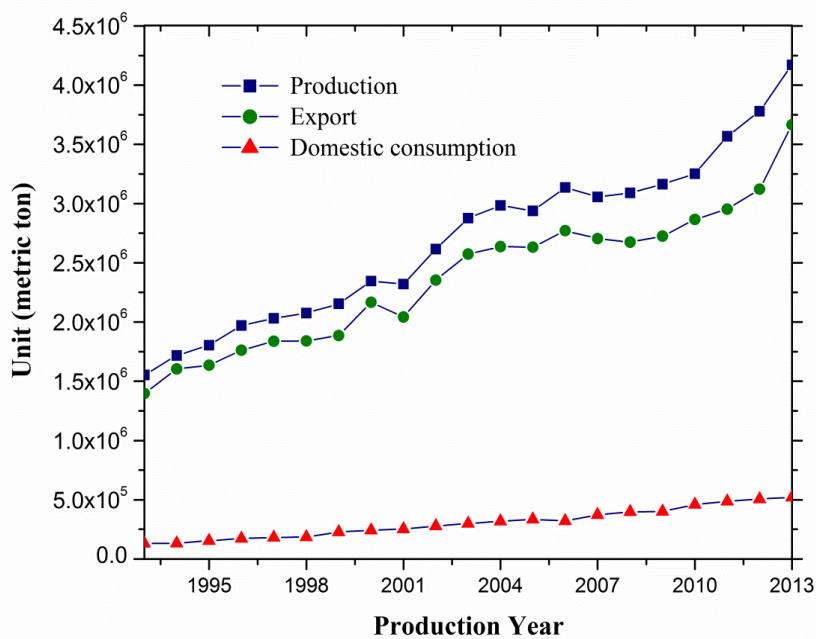
Figure 1.4 Production capacity of para rubber in Thailand during 1993–2013

1.1.4 Recent Status of Biomass Management

The Pollution Control Department (PCD) of Thailand's responsible assessment survey suggests that waste management has needs across a wide range of areas. The government of Thailand has made it a priority to treat the problem and aims to promote and support effective and appropriate technology. Biomass provides simple heat energy for cooking and processing in traditional industries of Thailand. Nowadays, in Thailand, biomass is an important source material as renewable materials used to generated electricity in power plants, and liquid fuels such as ethanol that can reduce amount of fuels derived from fossil fuel.

This study covers agricultural organic waste treatment and utilization techniques. Agricultural organic waste can be properly treated, thus reducing its impacts on environment and climate.

1.2 Wooceramics and their applications

1.2.1 What are Woodceramics

Woodceramics (WCMs) are new carbon materials obtained by carbonizing wood or woody materials impreginated with phenolic resin and carbonization in vacuum furnace [19] . The microstructure of WCMs are carbon-carbon composite originated from carbonized woody mixing with phenolic resin. The cell structure of WCMs was carbon reinforced by glassy carbon from phenolic resin which was changed after high temperature carbonization to increase its mechanical properties. The design of WCMs is to support society by carrying advantages and conveniences to human daily life. They also impose a wide various of problems on the environment through each and every step of production, processing, circulation, consumption, use, recycling and disposal [20]. A schematic diagram of the fabrication process is shown in Figure 1.5. Waste of wood such as sawdust from residues woody, and small trees architecture waste can also be used as raw materials. The second step is impregnation or mixing with
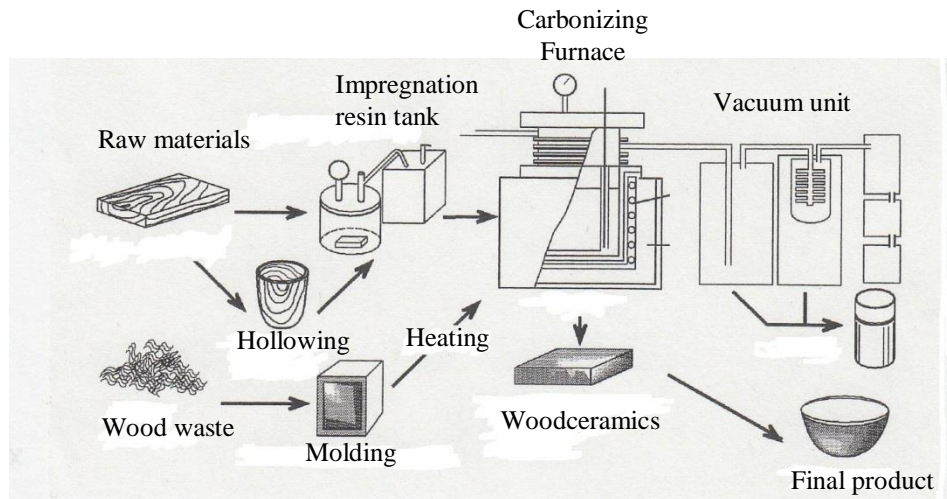
Figure 1.5 Schematic process to fabricate woodceramics [21]

phenolic resin. The third step is the most important process, which is carbonization to change structure of phenolic resin to glassy carbon structure. The final result is WCMs which needs an additional process before making a final product [21, 22].

In general, land-growing plants in the form of trees, shrubs, and agricultural crops are formed by catalytic conversion of carbon dioxide to an organic mass mainly consisting of the elements C-O(-N)-H. Wood typically contains 10 to 20 wt.% of hemicellulose,10 to 30 wt.% of lignin, and 30 to 55 wt.% of cellulose (and less than 2 wt.% of ash including minerals) as shown in Figure 1.6 [23].
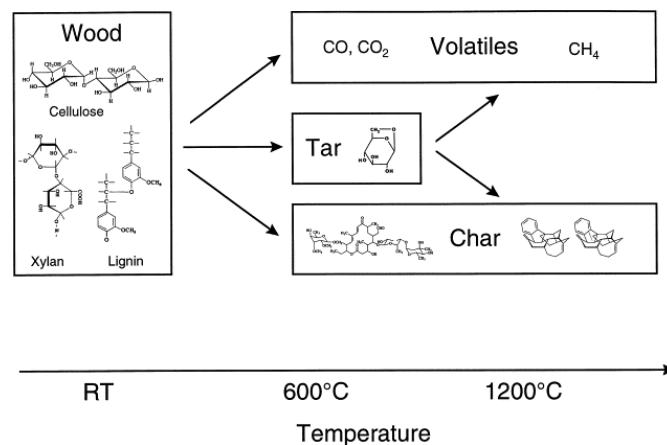
Figure 1.6 Thermal decomposition products of the major molecular constituents of wood [24].

Heating wood under vacuum atmosphere at temperature above 600 °C results in decomposition of the polyaromatic constitutents to form a carbon residue which reproduces the original cellular structure.

1.2.2 Proposed application of woodceramics

The WCMs are a new porous carbon material developed with the aim of adding superb functionality and value to carbon materials using biomass such as organic waste. These are one of the eco-materials, because they can be made from any kind of biomass with special physical properties such as high porosity, lightweight, low friction and increased wear resistance. The WCMs also have quite good properties of heat resistance, thermal shock toughness, small thermal expansion, chemical stability, electrical resistance, electromagnetic shielding and infrared radiation, and are being expected to be used widely in industrial fields. Therefore, it has great potential use in various applications such as heaters, gas filters, absorbents, humidity and temperature sensors, catalyst carrier materials, self-lubrication materials, heat insulating materials, damping materials, electromagnetic shielding, light structure ceramics, etc [25-28].

1.2.3 Recent researches in woodceramics

Woodceramics are carbon materials synthesized from natural wood or biomass, and are carbon composite or ceramic structure. The biomass provided by organic carbon from varieties of wood combined with phenolic resin create a composite with different mechanical properties and thermal stability [20, 29-31].

The development of bean-curd refuse origin ceramic materials for infrared radiators was successful. Therefore, an efficient recycling method for bean curd has been produced in view of lessening the environmental effect and reducing the costs in disposal. The methodology starts from carbonizing bean-curd to charcoal and mixing it with phenolic resin, forming and carbonizing under vacuum atmosphere. The ceramic materials exhibited a high inrfrared emissivity compared to commercial product [21].

The recycling of wastepapers following the ways of WCMs were successfully applied. The results indicated that high performance in electric and magnetic shielding were equivalent to general WCMS made from medium density fiberboard, whose were electric shielding effectiveness is 30 dB for 100 MHz, 43 dB for 300 MHz and 30dB for 100 MHz, 37dB for 400 MHz respectively [27].

The carbonizing temperature had the effect of changing the properties of WCMs. The different heating rate changes dimension shrinkage and weight loss, density, compressive, tensile strength and specific surface area. The dimension shrinkage and weight loss increased with increase of heating rate, while the mechanical strength decreased. Therefore, when increased carbonization temperature the ration of carbon to oxygen in WCMs were increased. The carbonization temperature higher than 650 °C, then space of crystalline (R-value) increased, the (002) interplaanar have turbostatic structure with cracks and internal stress [32, 33].

Hydrogen absorption and adsorption properties of WCMs made from radiate pine wood fiberboards were investigated. The high temperature enhances graphitization of WCMs, then decreased capacities of hydrogen adsorption and absorption in WCMs [26].

Damping properties of WCMs can increase by being infiltrated with magnesium alloy. After infiltration, WCMs have interpenetrating network structure. So that the mechanical strength and damping characteristics were increased [34].

The Aluminum-silicon alloy liquid infiltration to WCMs at high pressure vacuum conditions can improve tribological properties of WCMs, which improves dry sliding friction and wear behavior as well as mechanical properties [28].

The WCMs can be derived from tobacco stems with different contents of phenolic resin and different cabonizing temperature. Raman spectroscopy indicated that R-value decreased with an increased carboning temperature and increased content of phenol resin. The carbonizing temperature of 973 K is the turning point for preparing WCMs. The crystalline size (L_a) was low, which was microcrystalline between 1.85 and 5.40 nm [35].

The natural wood, after carbonizing at 800-1800 °C is infiltrated with liquid silicon and re-cabonizing at 1600 °C then converted to an original structure of silicon carbide (SiC). The anisotropy of their mechanical and physical properties generally increased with porosity and great differences in strength, strain to failure and toughness [24].

1.3 Study motivation

WCMs are environmentally conscious (eco-materials) composite materials dedesigned to reduce impact to the environment and create ideal recycling as shown in Figure 1.7. The WCMs are materials that friendly to the environmental and improvement throughout the whole life cycle although maintaining accountable performance. Regarding on the basic properties of WCMs background, the fundamental concept of eco-materials are showing as below.
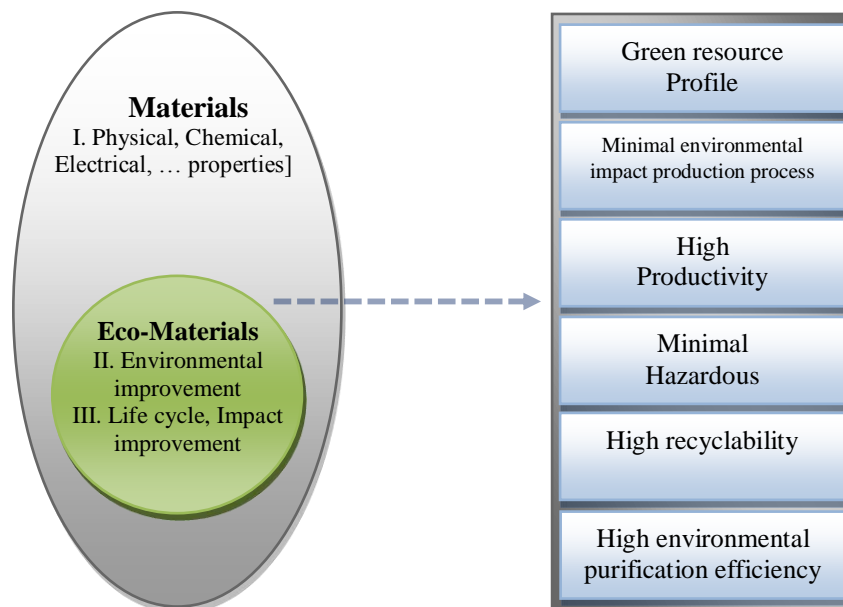
Figure 1.7 Conceptual model of Eco-materials within concept of materials science [36, 37].

This study is to explore potentials for value addition to biomass produced in Thailand. The objective of this research work focuses on the possibility to produce WCMs using Thai biomass waste such as rubber trees and coconut shell, and on new applications of WCMs;

I.   *Fabrication of Woodceramics from biomass in Thailand* : The biomass from residues of natural rubber trees and coconut shell have been chosen for WCMs fabrication in this research. The basic properties of biomass are low density and low mechanical strength which is not suitable for use as structural material. However , it includes a high percentage of carbon with some chemical element that supports an increase in the mechanical properties of WCMs. Also, the biomass from the waste of coconut shell that is very high in porosity microstructure, has excellent advantages to use as raw materials to fabricate high porosity WCMs for gas adsorption or absorption materials. The fundamental properties of coconut shell after carbonizing have excellent natural structure, high density and low ash content.

II. *Production of Amorphous Carbon Films using Woodceramics*: To design the low cost fabrication of amorphous carbon (a-C) thin films were deposited on silicon wafers by RF magnetron sputtering technique using woodceramics as a target. The amorphous carbon (a-C) thin films that are used as optically transparent films with low friction, wear resistance, hardness, high thermal conductivity and electrical resistance are technologically important. Radio frequency magnetron sputtering is a process that is used to make thin film with solid carbon target. In this process, WCMs are used instead of graphite materials to make thin film on a substrate that is placed in a vacuum chamber.

III. *Electrochemical Deposition of Ni and Cu on Woodceramics:* Electroplating is primarily used to change the surface properties of an object. To imrove surface resistance, physical and mechanical strength of WCMs, the electrochemical deposition were applied for coating metal objects with a thin layer of copper or nickel on WCMs surface.

IV. *Fabrication of Eco-composite using charcoal from biomass and used melamine formaldehyde:* The mission of fabricating eco-composite is to design new solutions for the disposal of biomass residues from natural rubber trees and used melamine formaldehyde to save disposal cost and minimizing the environmental impacts.

1.4 Thesis Outline and Contribution

Chapter 1: Introduction

The chapter introduces the current biomass situation in Thailand, and in detail explains the resources and current utilization of biomass including natural rubber economic production area in Thailand. The properties of WCMs, fabrication techniques and current research and applications are also explained. Finally given about research objectives and outline of this research study were explained.

Chapter 2: Characterization of woodceramics

In this chapter, the theory for evalution and analysis methods for WCMs are described. The crystalline strucuture, microstructure, chemical content and mechanical properties were determined by X-ray diffraction (XRD) , scanning electron microscope (SEM), energy dispersive X-Ray spectroscope, thermogravimetric analysis (TGA), raman spectroscopy and mechanical testing.

Chapter 3: Fabrication of Woodceramics from biomass in Thailand

This chapter discusses on the preparation of raw materials for fabrication of new WCMs from biomass residues (rubber trees and coconut shell) in Thailand. The designed forming parameters and carbonization parameters were also discussed. The basic properties of WCMS such as chemical copositions, microstructure, physical properties, and mechanical properties are investigated.

Chapter 4: Production of Amorphous Carbon Films using Woodceramics

This chapter introduces a new application of WCMs in the field of fabrication of amorphous carbon (a-C) thin films by an RF magnetron sputtering. The theory of amorphous carbon films and its application were introduced. The conditions to fabrication of a-C films and characterizing methods were explained. The main characterizing method were X-ray diffraction, raman spectroscopy and X-ray photoelectron spectroscopy. Fundamental mechanical properties such as hardness and friction coefficient were also measured.

Chapter 5: Electrochemical Deposition of Ni and Cu Woodceramics

This chapter introduces new techniques to improve the mechanical properties of woodceramics. In this study we attempted to deposit metallic (Cu or Ni) layers electrochemically on the woodceramics, in copper sulfate (CuSO4) or nickel sulfate (NiSO4) solutions. The concentration of the solutions and deposition times were varied. The microstructures and the character of depopsited films as well as compressive strength were investigated by means of X-ray diffraction, scanning electron microscopy, and compression test respectively. The compression test of samples before and after metallic deposition was also performed.

Chapter 6: Concluding Remarks and Future Works

The final chapter concludes all the studies that have been conducted. In addition to additional studies on optimization of design, the possibility of new biomass materials to fabricate WCMs, properties analyses and those application, new possible commercial expansions are suggested in this chapter.

Appendix : Fabrication of Eco-Composite using charcoal from biomass

This chapter investigates new eco-composite materials which consists of biomass charcoal from natural rubber trees and used waste melamine formaldehyde, and/or virgin melamine formaldehyde with phenol resin as a combinder material. The design parameters of each element and fabrication conditions were introduced. The

characterization of eo-composite, microstructure, crystalline and mechanical properties were also investigated. The future applications of eco-composite were also discussed in this chapter.

References

[1]   "Ministry of Natural Resources and Environment," Ministry of Natural Resources and Environment Thailand, 2011. [Online]. Available: http://www.mnre.go.th/main.php?filename=Links. [Diakses 20 November 2014].

[2]   T. ECONOMICS, "Thailand GDP Annual Growth Rate," TRADING ECONOMICS, 2014. [Online]. Available: http://www.tradingeconomics.com/thailand/gdp-growth-annual. [Diakses 20 November 2014].

[3]   The United Nation, "Thailand Population 2014," World Population Review, 2014. [Online]. Available: http://worldpopulationreview.com/countries/thailand-population/. [Diakses 20 November 2014].

[4]   T. C. Thailand, "Map of Thailand," [Online]. Available: http://www.teflcoursethailand.com/images/thailand_map.gif. [Diakses 26 December 2014].

[5]   H. Leturque, S. Wiggins, "Thailand Progress in Agriculture," Overseas Development Institute, London, UK, 2011.

[6]   X. Ping, "Environment Problems and Green Lifestyles in Thailand," June 2011. [Online]. Available: http://www.nanzan-u.ac.jp/English/aseaccu/venue/pdf/2011_05.pdf. [Diakses 10 September 2014].

[7]   C. Visvanathan, "Solid waste and climate change : Perceptions and possibilities," dalam *The International Conference on Solid Waste MAnagement* , Khulna, Bangladesh, 2009.

[8]   U.K. Mirza, N. Ahmad and T. Majeed, "An overview of biomass energy utilization in Pakistan," *Renewable and Sustainable Energy Reviews,* vol. 12, no. 7, pp. 1988-1996, 2008.

[9]   T. U. D. o. E. National Renewable Energy LAboratory, "Biomass Characterization Capabilities," NREL, 29 July 2014. [Online]. Available: http://www.nrel.gov/biomass/biomass_characterization.html. [Diakses 26 December 2014].

[10]   1. P. Stock, "thai farmer is harvesting the rice in the paddy field," [Online]. Available: http://www.123rf.com/photo_17803403_thai-farmer-is-harvesting-the-rice-in-the-paddy-field-chiangmai-thailand.html. [Diakses 26 December 2014].

[11]   THAIPUBLICA, "Rubber pricing strategy," ThaiPublica.org , [Online]. Available: http://thaipublica.org/2013/01/rubber-pricing-strategy/. [Accessed 20 January 2015].

[12] P. Link, "Rubber tree Yala Province Thailand," PNYlink, [Online]. Available: http://www.pnylink.com. [Accessed 21 January 2015].

[13] Nongpaya, "ศูนย์รวมกล้าพันธ์ุไม้มาตรฐาน," [Online]. Available: http://www.takuyak.com/index.php?mo=14&newsid=208347. [Accessed 21 January 2015].

[14] T. Klaharn, "Rubber production in Thailand," [Online]. Available: http://www.zimbio.com/pictures/sg947RjmXmW/Rubber+production+In+Thailand/PRGkVlpbtmX/Thongshin+Klaharn. [Accessed 21 January 2015].

[15] S. Papong, C. Yuvaniyama, P. Lohsomboon and P. Malakul, "Overview of biomass utilization in Thailand," dalam *ASEAN Biomass*, Bangkok, Thailand, 2004.

[16] T. Prapita, "Supply chain management of agricultural waste for biomass utilization and CO2 emission reduction in the lower northern," *Energy Procedia,* vol. 14, pp. 843-848, 2012.

[17] T. R. Assocation, "Thai Rubber Statistic," Thai Rubber Assocation, 3 September 2014. [Online]. Available: http://www.thainr.com/uploadfile/20141024112319.pdf. [Diakses 12 November 2014].

[18] T. T. R. Association, "Production of natural rubber in Thailand," August 2014. [Online]. Available: http://www.thainr.com/en/index.php?detail=stat-thai. [Diakses 12 September 2014].

[19] K. Halada and R. Yamamoto, "The current status of research and development on ecomaterials around the world," *MRS Bulletin,* vol. 26, pp. 871-879, 2001.

[20] T. Okabe, K. Saito and K. Hokkirigawa, "New porous carbon materials, woodceramics: Development and fundamental properties," *Journal of Porous Materials,* vol. 2, pp. 207-213, 1996.

[21] S. Kakuta, H. Ono, M. Kushibuki, T. Okabe, H. Degawa, H. Hatnaka, Y. Iwamoto, M. Ogawa, A. Takasaki and M. Murakami, "Development of bean-Curd Refuse Origin Ceramics Materials," *Trans. Mat. Res. Soc of Japan,* vol. 30, pp. 169-172, 2010.

[22] T. Okabew, K. Kakishita, H. Simizu, K. Ogawa, Y. Nishimoto, A. Takasaki, T. Suda, M. Fushitani, H. Togawa, M. Sata and R. Yamamoto, "Current status and application of woodceramics made from biomass," *Trans. Mat. Res. Soc. of Japan,* vol. 38, pp. 191-194, 2013.

[23] P. Greil, "Biomorphous ceramics from lignocellulosics," *Journal of the European Ceramics Society,* vol. 21, pp. 105-118, 2001.

[24] P. Greil, T. Lifka and A. Kaindl, "Biomorphic Cellular Silicon Carbide Ceramics," *uniivrsity porcessding,* vol. 2, no. 3, pp. 1961-1980, 1998.

[25] A. Takasaki and T. Okabe, "Hydrogen desorption properties of woodceramics," *Trans. Mat. Res. Soc. of Japan,* vol. 34, no. 4, pp. 675-678, 2009.

[26] A. Takasaki, M. Otsuka and T. Okabe, "Hydrogen Absorption and Adsorption Characteristics of Woodceramics," *Trans. of Mat. Research Society of Japan,* vol. 30, no. 4, pp. 1151-1154, 2005.

[27] K. Shibata, T. Okabe, K. Saito, T. Okayama, M. Shimada, A. Yamamura and R. Yamamoto, "Electromagnetic Shielding Properitesd of Woodceramics made from Watespaper," *Journal of Porous MAterials,* vol. 4, pp. 269-275, 1997.

[28] X.Qing, F.T. Xiang, S. Bing-He, Zh. Di, T. Sakata, H. Mori and T. Okabe, "Dry sliding friction and wear behavior of woodceramics/Al-Si composites," *Materials Science and Engineering,* vol. A 342, pp. 287-293, 2003.

[29] A. Shaaban, S.M. Se, N. Merry, M. Mitan and M.F. Dimin, "Characterization of biochar derived from rubber wood sawdust through slow pyrolysis surface porosities and function groups," *Procedia Engineering,* vol. 68, pp. 365-371, 2013.

[30] C. Zollfrank, H. Sieber, "Microstructure and phase morphology of wood derived biomorphous SiSiC-ceramics," *Journal of the European Ceramics Society,* vol. 24, pp. 495-506, 2004.

[31] Z.Kadirova, Y. Kamesshima, A. Nakajima and K. Okada, "Preparatioin and sorption properties of porous materials from refuse paper and plastic fuel (RPF)," *Journal of Hazardous Materials,* vol. B137, pp. 352-358, 2006.

[32] T. Hirose, T. Fujino, T. Fan, H. Endo, T. Okabe and M. Yoshimura, "Effect of carbonization temperature on the structure change of woodecramics impregnated with liquefied wood," *Carbon,* vol. 40, pp. 761-765, 2002.

[33] T. Hirose, T. Fan, T. Okabe and M. Yoshimura, "Effect of Carbonizing Speed on the Property Change of Woodceramics Impregnated with Liquefacient Wood," *Materials Letters,* vol. 52, pp. 229-233, 2002.

[34] X. Qing, F.T. Xiang, Zh. Di and W.R. Jie, "Increasing the mechanical properties of high damping woodceramics by infiltration with a magnesium alloy," *Composites Science and Technology,* vol. 62, pp. 1341-1346, 2002.

[35] L.B. Zhang, W. Li, J.H. Peng, N. Li, J.Zh. Pu, S.M. Zhang and Sh.H. Guo, "Raman spectroscopic investigation of the woodceramics derived from carbonized tabacco stems/phenolic resin composite," *Materials and Design,* vol. 29, pp. 2066-2071, 2008.

[36] K. Halada and R. Yamamoto, "The current status of research and development on ecomaterials around the world," *MRS Bulletin,* vol. 26, pp. 871-879, 2001.

[37] X.H. Nguyen, T. Honda, "Classification of Eco-Materials in the perspectives of sustainability," dalam *The 3 International Symposium on Environmental Conscious Design and Inverse Manufacturing*, Japan, 2003.

Chapter 2

Characterization of woodceramics

2.1 X-ray diffraction (XRD) measurements [1-5]

Woodceramics are solid carbon materials with hybrid structure between glassy carbon and graphite structure in a solid. The structures of crystalline solid material are classified by the constancy of atoms and ions arrangement. Most of this technical method identifies crystalline materials using x-ray diffraction techniques.

The XRD analysis measurement is a versatile, non-destructive technique used for the identification of unknown crystalline materials such as minerals, metal, organic, and inorganic compounds. To identifications of unknown element are critical to studies in geology, environmental science, material science, engineering, and biology field.

X-ray diffraction is based on constructive interference of monochromatic X-rays and a crystalline sample. The X-ray beam generated by a cathode ray tube, filtered to produce monochromatic radiation, collimated to concentrate directly toward the specimen as shown in Figure 2.1 and 2.2. The collaboration of the incident rays with the specimen generated constructive interference when conditions satisfy Bragg's Law as shown in Equation 2.1. This regulation relate to wavelength of electromagnetic radiation to the X-ray diffraction angle and the lattice space in a crystalline of specimen. These diffracted X-rays are then detected, processed and counted by scanning sample through a range of 2θ, all possible diffraction directions of the lattice should be attained due to the random orientation of the powdered material. Convergent of the diffraction peaks to d-spacing identification the mineral because each mineral has a set of unique d-spacing. Essentially, this measurement achieved by comparison of d-spacing with standard reference patterns. The diffraction methods are based on the generation of X-rays in tube.
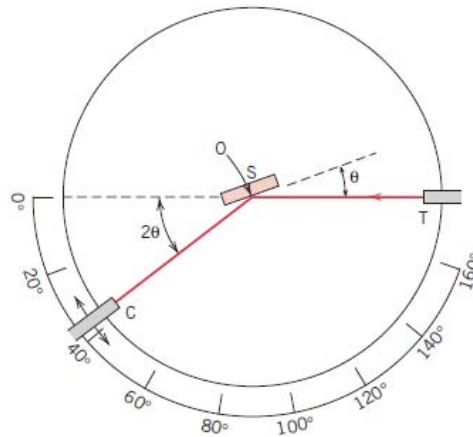
Figure 2.1 Schematic diagram of an XRD, T = x-ray source, S=specimen, C=detector and O=axis between detector and specimen [3].
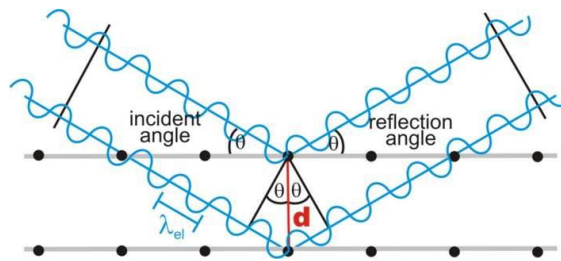
Figure 2.2 Reflection of X-rays from two lattice planes [4].

The divergent beam X-ray are directed at the specimen and the diffracted rays are collected. A main component of all diffraction is the position of angle between the incident and diffracted rays.

The XRD is primarily used for;

    i. Identifying crystalline material.

    ii. Identifying unit cell dimensions

    iii. Identifying different polymorphic forms.

    iv. Distinguishing between amorphous and crystalline material.

    v. Quantifying the percent crystallinity of a sample.

X-rays interaction with the electron in atom. While the x-ray photons collide with electrons, some photons from the incident beam will be diffracted away from the direction where they initially. The process is called elastic scattering (Thompson Scattering) in that only momentum has been transferred in the scattering process. These are the X-rays that one measure in diffraction experiments, as the scattered X-rays carry information about the electron distribution in materials. On the other hand, in the inelastic scattering process (Compton Scattering), X-rays transfer some of their energy to the electrons and the scattered x-rays will have different wavelength than the incident X-rays.

The diffraction waves from different atoms can intervene with each other and the derivable intensity distribution is strongly modulated by the collaboration. The atoms are arranged in a periodic fashion, as in crystals, the diffracted waves will consist of sharp interference maxima (peaks) with the same symmetry as in the distribution of atoms. The analysis of the diffraction pattern therefore allows us to deduce the distribution of atoms in a material.

The peaks in an x-ray diffraction pattern are directly related to atomic distances. For a given set of lattice planes with an inter-plane distance of d, the condition for a diffraction (peak) to occur can be simply written as which is known as the Bragg's law, after W.L. Bragg, who first proposed it. In the Equation 2.1 is the wavelength of the x-ray, q the scattering angle, and 'n' an integer representing the order of the diffraction peak. The Bragg's Law is one of most important laws used for interpreting X-ray diffraction data.

$$2d \sin \emptyset = n\lambda \qquad\qquad (2.1)$$

Where; d = spacing of planes of atoms

θ = diffraction angle

λ = x-ray wave length

n = integer numbers

According to the arrangement of atoms, the unit cell is specific to a crystal lattice, this forms the determination basis of the material crystal structure. Each atom independently has an atomic scattering factor, f_i, on the basis of scattering efficiency of all electrons in the atom. Here we can define a scattering factor of unit cell, F, as Equation 2.2. The sum of the f_i from all the i atoms in the unit cell is obtained

$$F = \sum_{i}^{\infty} f_i \, e^{2\pi i(hx_i+ky+lz_i)} \qquad (2.2)$$

Where; x, y, z = positions of the atom in the unit cell (x,y,z)

h, k, l = specific atomic planes (h,k,l) that make up the crystal structure.

In order to determine structure of powder, a bulk sample and a-C films (XRD method) are used in this work. The XRD equipment is Rigaku Ultima IV using Cu-Kα radiation (wave length of 1.541 Å) with a graphite monochromator at room temperature. However, it has been mentioned that structure of woodceramics and a-C films are noncrystalline called amorphous. Amorphous materials are characterized by an atomic or molecular structure. Ceramic materials include crystalline and noncrystalline structures, whereas others, the inorganic glasses, some structure of composite polymer are amorphous.

2.2 Scanning electron microscope (SEM) [6-8]

The scanning electron microscope (SEM) is a tool for the investigation of specimens with a resolution down to micrometer scale and nanoscale. The principle of SEM using a focused high energy electron beam from cathode and electromagnetic lenses is to generate a signal at the surface of a specimen to create an image as shown in Figure 2.3.

The SEM is routinely used equipment to generate high-resolution images of the shapes of objects. The signals that derive from electron-sample interactions reveal information about the sample including external morphology (texture). In most applications, data is collected over a selected area of the surface of the sample, and a 2-dimensional image is generated that displays spatial variations in these properties.

In the conventional scanning electron microscope, which operates in high vacuum atmosphere, the specimen has to be electrically conductive or has to be coated with a conductive layer (e.g. Carbon, Gold etc.). In the environmental scanning electron microscope (ESEM) two further vacuum states lead to new possibilities. The low vacuum mode allows the imaging of nonconductive specimens such as polymers and biological samples. Microscopy is now recognized as a separate technological field and has become a valuable research tool which is applicable to all modern technologies.
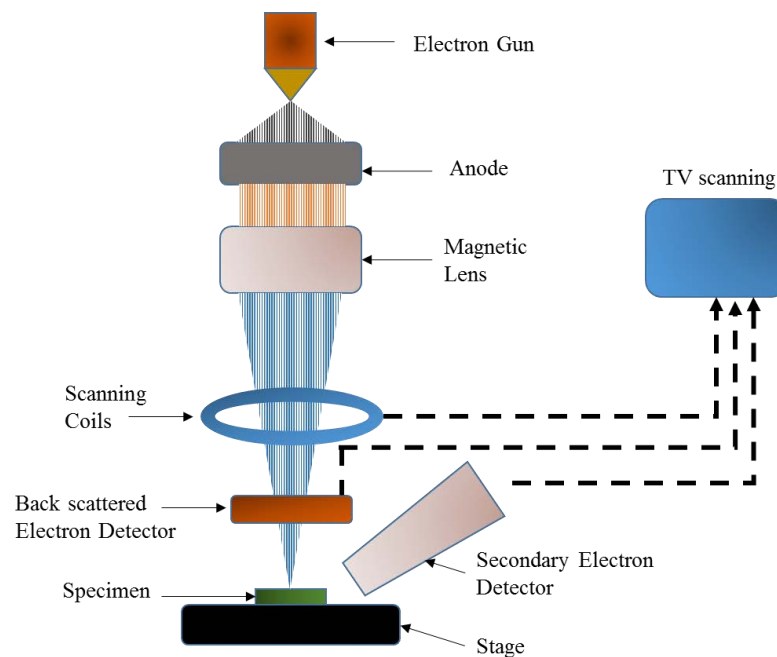
Figure 2.3 Schematic diagram of a Scanning Electron Microscope (SEM).

A beam of high-energy electrons is produced in the electron gun at the top of the column and applies high voltage to a tungsten filament and nearby anode as shown in Figure 2.4. This beam is accelerated down past the anode into the column where it is condensed and aligned by a series of electromagnetic lenses and coils within the column. This focused beam continuously back and forth across the sample. Interactions between the electron beam and the sample result in different types of emissions that are measured by a series of detectors located within the sample chamber. The types of emissions that are measured are: secondary electrons, backscattered electrons, X-rays, and cathode luminescence. X-ray data is sent to the x-ray system where it is translated into elemental

plots. The other three detectors are connected to a 'TV' monitor where the signal generates a clear, green monochrome image of the sample. Secondary electron imaging provides good 3-dimensional topographical views of the sample. Backscattered electron images show less defined topography but clearly display differences in elemental compositions because higher atomic number elements appear brighter. Cathode luminescence imaging highlights chemical variations within individual grains due to trace element variations and zoning.

2.3 Energy Dispersive X-ray spectroscopy (EDS) [9]

The energy dispersive x-ray spectroscopy (EDS or EDX) is a technique that utilizes X-ray emitted from the sample during the bombardment by the electron beam to characterize the elemental composition of material imaged in a SEM. The specimen is bombarded by the electron beam of SEM process, electrons are ejected from the atoms comprising the surface of the specimen. The result of electron vacancy is filled by an electron from a higher shell, and an x-ray is emitted to balance the energy difference between the two electrons. The X-ray detector measures the number of emitted X-ray versus their energy. The energy of the x-ray is characteristic of the element from which the x-ray was emitted. A spectrum of the energy versus relative counts of the detected X-ray is obtained and evaluated for qualitative and quantitative determination of the elements present in the sampled volume. Backscattered electron images in the SEM display compositional contrasts that result from different atomic number elements and their distribution. Energy Dispersive Spectroscopy (EDS) allows one to identify what those particular elements are and their relative proportions in atomic weight percent.

The X-ray generation of EDS, have two basic types of produced inelastic interaction of electron beams with the atoms of a specimen's surface. The hole in an inner shell (here : K shell) of a specimen atom is generated by an incident high energy electron (E_0) that loss the corresponding energy (E) transferred to the ejected electron as shown in Figure 2.4.
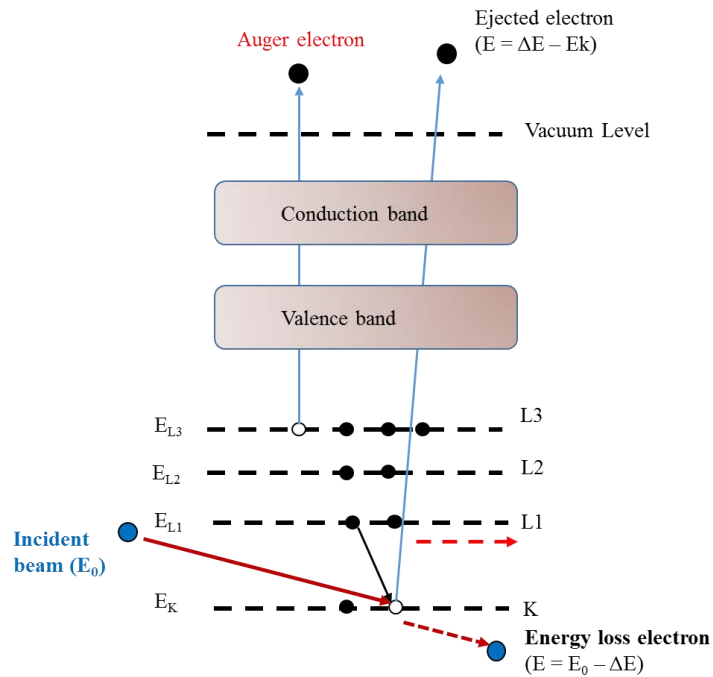
Figure 2.4 Schematic description of x-ray result when the beam electron eject inner shell electron of specimen atoms.

The hole of a shell is subsequently filled by an electron from L1 to L3 shell. The superfluous energy is emitted as a characteristic X-ray quantum. The energy of the X-ray is characteristic of the specimen atomic number from which it is derived. Auger electrons have an energy range of $50 - 2500$ eV and mean free paths within the specimen of $0.1 - 2$ nm. This means that only Auger electrons escaping from a depth of $0.1 - 2$ nm (5-10 atomic layers) will not have undergone additional inelastic interactions with specimen atoms after their generation. Auger spectroscopy is a true surface analysis methodology.

The EDS system is comprised of three main components, an X-ray detector which detects and converts x-ray into electron signals, a pulse processor which measures the electron signals to determine the energy of each x-ray detected, and multiple channel analyzer which displays and interprets the x-ray data of EDS measurement.

2.4 X-ray photoelectron spectroscopy (XPS) [10-13]

X-ray photoelectron spectroscopy (XPS) or Electron Spectroscopy for Chemical Analysis (ESCA) is a technique used to conduct elemental analysis of surfaces or surface chemical analysis technique cause of its relative simplicity in use and data interpretation. The sample is irradiated with mono-energetic X-rays causing photoelectrons to be emitted from the sample surface. An electron energy analyzer determines the binding energy of the photoelectrons. From the binding energy and intensity of a photoelectron peak, the elemental identity, chemical state, and quantity of an element are determined. The information XPS provides about surface layers or thin film structures is of value in many industrial applications including: polymer surface modification, catalysis, corrosion, adhesion, semiconductor and dielectric materials, electronics packaging, magnetic media, and thin film coatings used in a number of industries. The X-ray photon of energy ejection of an electron from a core level, the energy emitted photoelectrons is then analyzed by the electron spectrometer and data presented as a graph of intensity versus electron energy included photoelectron spectrum as shown in Figure 2.5.

- ❖ elemental composition of the surface
- ❖ empirical formula of pure materials
- ❖ elements that contaminate a surface
- ❖ chemical or electronic state of each element in the surface
- ❖ uniformity of elemental composition across the top surface (or line profiling or mapping)
- ❖ uniformity of elemental composition as a function of ion beam etching (or depth profiling)

$$E_b = h_v - E_k - W_f$$
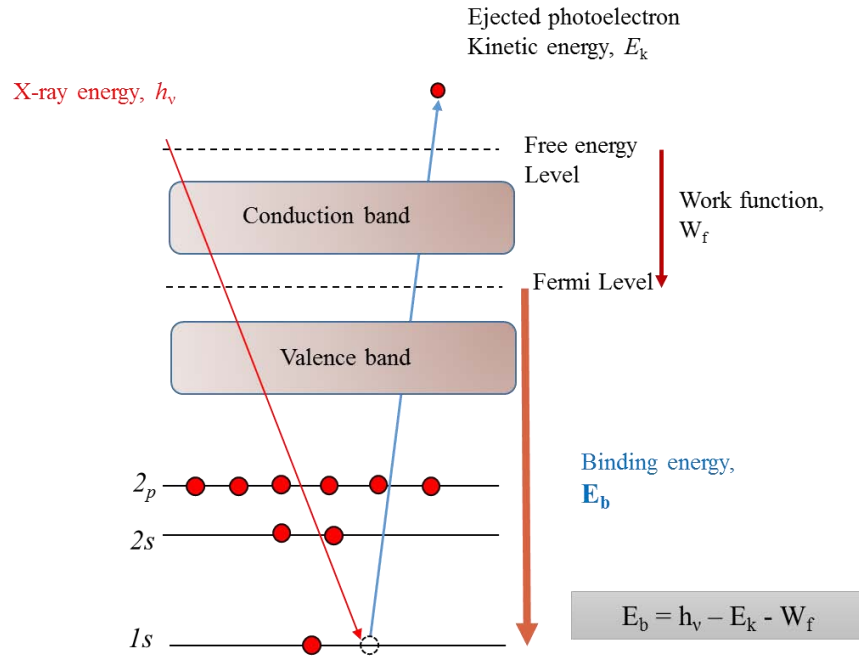
Figure 2.5 Schematic principle process of x-ray photoelectron spectroscopy.
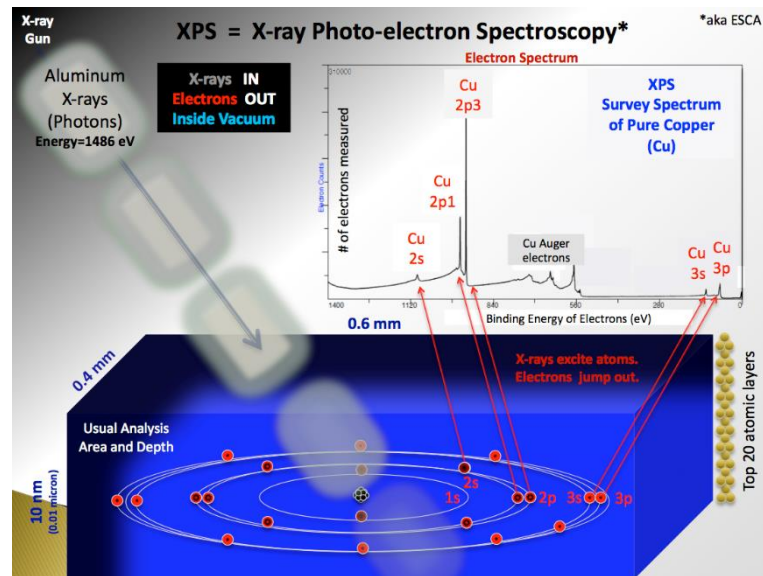
Figure 2.6 Schematic description of Photoelectric effect of XPS instrumentation [13].

XPS detects only those electrons that have actually escaped from the sample into the vacuum of the instrument, and reach the detector as shown in Figure 2.6. In order to escape from the sample into vacuum, a photoelectron must travel through the sample. Photo-emitted electrons can undergo inelastic collisions, recombination, excitation of the sample, recapture or trapping in various excited states within the material, all of which can reduce the number of escaping photoelectrons. These effects appear as an exponential attenuation function as the depth increases, making the signals detected from analysis at the surface much stronger than the signals detected from analysis deeper below the sample surface. Thus, the signal measured by XPS is an exponentially surface-weighted signal, and this fact can be used to estimate analyst depths in layered materials.

2.5 Raman spectroscopy [14-19]

The basics of Raman scattering can be explained using classical physics and quantum mechanical treatise. The phenomenon of inelastic scattering of light, then the phenomenon has been referred to as Raman spectroscopy. Raman spectroscopy are widely used to provide materials information on chemical structure and physical forms, to identify substances from the characteristic spectral patterns and quantitatively or semi-quantitatively the amount of a substance in specimen surface. It has played an important role in the structural characterization of graphitic materials, in particular providing valuable information about defects, stacking of the graphene layers and the finite sizes of the crystallites parallel and perpendicular to the hexagonal axis.

In the original experiment sunlight was focused by a telescope onto a sample which was either a purified liquid or a dust free vapor. A second lens was placed by the sample to collect the scattered radiation. A system of optical filters was used to show the existence of scattered radiation with an altered frequency from the incident light the basic characteristic of Raman spectroscopy.

The main concept of Raman spectroscopies being employed to detect vibrations in molecules is based on the processes of infrared absorption and Raman scattering that provides rich information about the identity of molecular species.
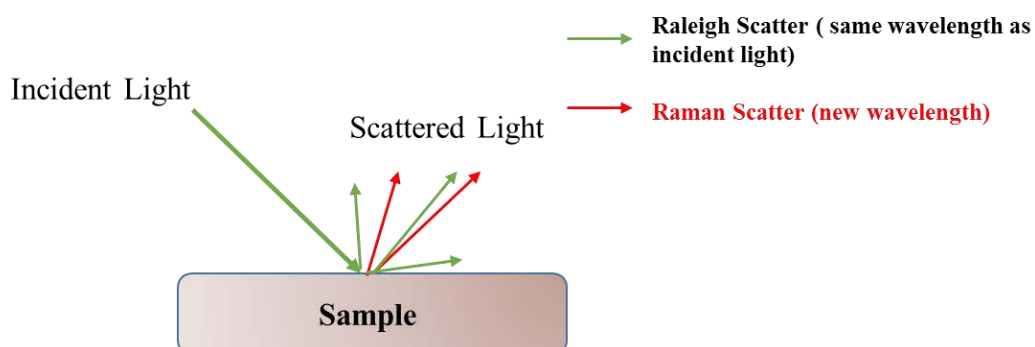
Figure 2.7 Principle scattering of Raman spectroscopy.
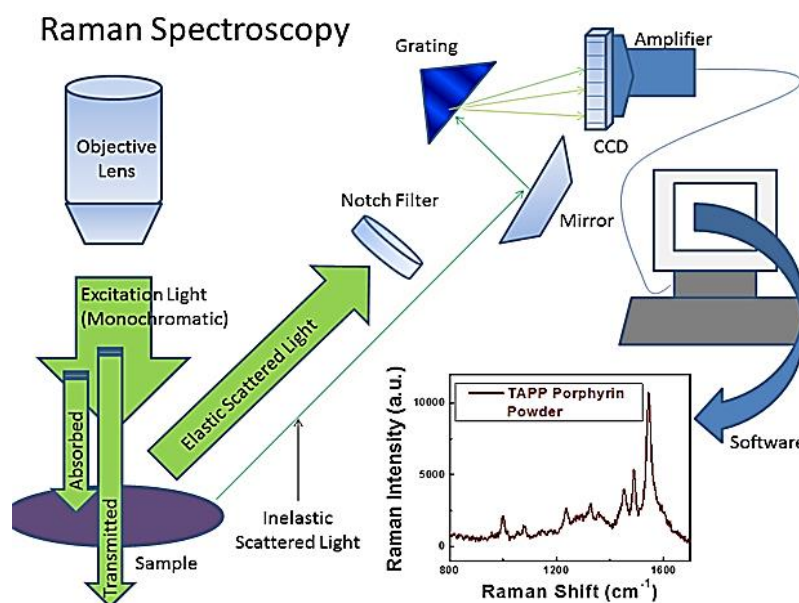
Figure 2.8 Schematic description for process involved in collecting Raman spectra [19].

The majority of scattered light is elastically scattered, meaning it is the same wavelength as the excitation source. A notch filter is used to block elastically scattered light which would otherwise overwhelm the weak signal from the Raman or inelastically scattered photons as shown on Figure 2.7 and 2.8.
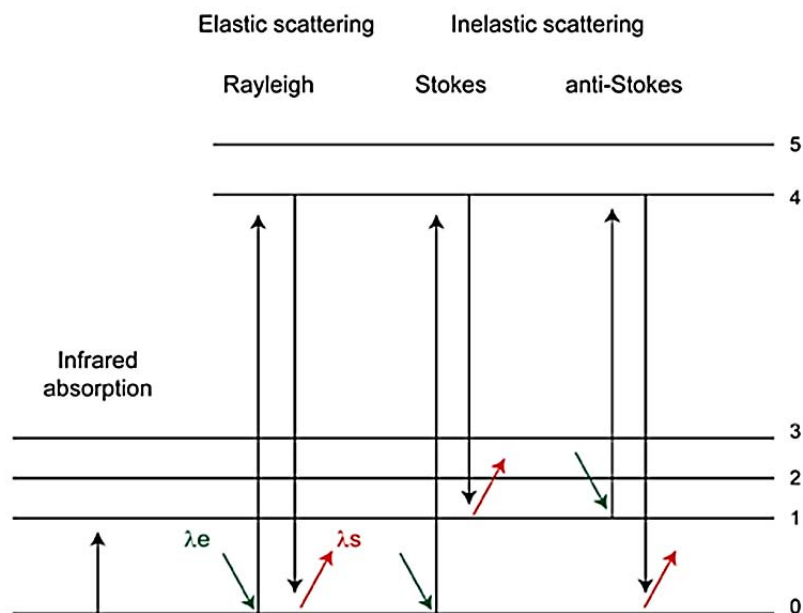
Figure 2.9 Simplified energy level diagram. The shift in wavelength between the excitation light (λe) and the scattered light (λs) is related to Raman shift (ΔV in cm-1) according to: $\Delta V = (1/\lambda e) + (1/\lambda s)$.

When light interacts with matter, the photons which make up the light may be absorbed or scattered, or may not interact with the material and may pass straight through it. The photon energy of this scattered light is equal to that of the incoming light. If the energy of an incident photon corresponds to the energy gap between the ground state of a molecule and an excited state, the photon may be absorbed and the molecule promoted to the higher energy excited state as show in Figure 2.10. It is this change which is measured in absorption spectroscopy by the detection of the loss of that energy of radiation from the light. However, it is also possible for the photon to interact with the molecule and scatter from it. In this case there is no need for the photon to have an energy which matches the difference between two energy levels of the molecule. The scattered photons can be observed by collecting light at an angle to the incident light beam, provided there is no absorption from any electronic transitions which have similar energies to that of the incident light, the efficiency increases as the fourth power of the frequency of the incident light.

This process is called Rayleigh scattering. Scattering is a commonly used technique. For example, it is widely used for measuring particle size and size distribution down to sizes less than 1 mm. A molecule may also fall back from an excited electronic state to an energy state that is higher (Stokes type scattering) or lower (anti-Stokes type scattering) than the original state. The difference in energy between the incoming and scattered photon (Raman shift) corresponds to the energy difference between the vibrational energy levels of the molecule. The different vibrational modes of a molecule can therefore be identified by recognizing Raman shifts (or 'bands') in the inelastically scattered light spectrum.

References

[1]   E.J. Mittemeijer, P. Scardi, Diffraction Analysis of the Microstructure of Materials, Berlin, German: Springer, 2003, Print..

[2]   B.L. Dutrow, Ch.M. Clark, "Geochemical Instrumentation and Analysis,X-ray Powder Diffraction (XRD)," [Online]. Available: http://serc.carleton.edu/research_education/geochemsheets/techniques/XRD.html. [Diakses 2 January 2015].

[3]   D. William and Jr. Callister, Materials Science and Engineering an Introduction, 3rd Ed., New York, United State: John Wiley and Sons, Inc., 1994, Print..

[4]   F.Krumeich, "Bragg's Law of Diffraction," ETH, 4 September 2013. [Online]. Available: http://www.microscopy.ethz.ch/bragg.htm. [Diakses 25 November 2014].

[5]   M. R. Laboratory, "UC Santa Barbara, Materials Research Laboratory," 2014. [Online]. Available: http://www.mrl.ucsb.edu/centralfacilities/x-ray/basics. [Diakses 3 January 2014].

[6]   S. Swapp, "Geochemical Instrumentation and Analysis, Scanning Electron Microscopy (SEM)," [Online]. Available: http://serc.carleton.edu/research_education/geochemsheets/techniques/SEM.html. [Diakses 2 January 2015].

[7]   FELMI-ZFE, "The principles of SEM and Microanalysis," [Online]. Available: http://portal.tugraz.at/portal/page/portal/felmi/research/Scanning%20Electron%20Microscopy/Principles%20of%20SEM. [Diakses 3 January 2015].

[8] J. Goldstein, D.E. Newbury, D.C. Joy, and Ch.E. Lyman, Scanning Electron
      Microscopy and X-Ray Microanalysis 3rd, United States of America:
      Springer, 2003.

[9] B. Hafner, "Energy Dispersive Spectroscopy on the SEM:," [Online].
      Available:
      http://www.charfac.umn.edu/instruments/eds_on_sem_primer.pdf. [Diakses
      3 January 2015].

[10] J.F. Watts, J. Wolstenholme, An Introduction to SURFACE ANALYSIS by
       XPS and AES, London, UK: John Wiley and Sons Ltd., 2003, Print..

[11] L. I. f. S. S. a. M. R. Dresden, "X-Ray Photoelectron Spectroscopy (XPS),"
       [Online]. Available: https://www.ifw-dresden.de/?id=346. [Diakses 3
       January 2015].

[12] P. Electronics dan A. d. o. ULCAV-PHI, "XPS: X-Ray Photoelectron
       Spectroscopy," [Online]. Available: https://www.phi.com/surface-analysis-
       techniques/xps.html. [Diakses 3 January 2015].

[13] "X-ray photoelectron spectroscopy," 14 November 2014. [Online].
       Available: http://en.wikipedia.org/wiki/X-
       ray_photoelectron_spectroscopy#mediaviewer/File:XPS_PHYSICS.png.
       [Diakses 25 November 2014].

[14] M.A. Pimenta, G. Dresselhaus, M.S. Dresselhaus, L.G. Cancado, A. Jorio
       and R. Saito, "Studying disorder in graphite-based systems by Raman
       spectroscopyw," *Phys. Chem. Phys.,* vol. 9, pp. 1276-1291, 2007.

[15] E.Smith and G. Dent, "Introduction, Basic Theory and Principles, in Modern
       Raman," dalam *Modern Raman Spectroscopy*, Chichester, UK, A Practical
       Approach, John Wiley & Sons, Ltd, 2005, pp. 1-20.

[16] J.R. Ferraro, K. Nakamoto, Ch.W. Brown, Introductory Raman
       Spectroscopy, California, United State: Academic Press, 2003, Print..

[17] U.O.N. Dame, "Spectroscopic Characterization," The Prashant Kamat lab at
       the University of Notre Dame, 2012. [Online]. Available:
       http://www3.nd.edu/~kamatlab/facilities_spectroscopy.html. [Diakses 25
       November 2014].

[18] U.O. Bergen, "Raman Spectroscopy - Theory," University of Bergen,
       [Online]. Available: http://www.geo.uib.no/bgf/index.php/raman/ramantech.
       [Diakses 25 November 2014].

[19] U. o. Maryland, "Surface Analysis Center," Dept. of Chemistry &
       Biochemistry, 2014. [Online]. Available:
       http://www.chem.umd.edu/sharedinstrumentation/surface-analysis-center/.
       [Accessed 25 January 2015].

Chapter 3

Fabrication of woodceramics from biomass in Thailand

3.1 Introduction

In general biomass description, they are the matter coming or derived direct or indirect from all plant which is utilized as the energy or material substantial amount. The biomass includes variety of agricultural, forestry and process agroindustrial residues and processed waste, and is quite varied and different in it's the physical and chemical property, content of moisture, and mechanical properties. As Thailand is an agricultural country, there will be a large amount of agricultural waste left which provides potential for biomass. The main agricultural products are rice husk, rice straw, bagasse fiber, corn, cassava, wood residues, coconut shell and palm shell. As reported in Chapter 1, Thailand is a leading producer of natural rubber, the old rubber trees are cut down to grow new plantations. Rubber wood is regarded as a by-product from the production of natural rubber plantation, the original rubber wood is not suitable in wide application due to low natural durability and softwood. The waste generated from old rubber trees usually disposed by being burned or dumped into landfills. The disposal of this waste becomes a major problem. The volume of biomass from rubber trees stemming from roots, stumps and leaves, and rubber tree branches are very high in potential biomass in Thailand. In addition, the coconut production process also generates biomass in Thailand. The coconut grows throughout the year, with harvesting generally 4 times in a year. The biomass from coconut is coconut shell and coconut husk. Base on the environmental concern , the disposal of this materials as solid wastes is a great problem which may lead to environmental effect and toxicological issues. Faced with the protection of the global environment such as the recycling of organic waste from

biomass, the carbon materials are attracting much attention. Therefore, the development of new carbon materials with superb functionality has been expected [1].

New functional carbon materials as woodceramics have been develop by material research group in Japan. The woodceramics are new porosity structure carbon materials, which are made by impregnating woody materials with phenolic resin that are then carbonized in a vacuum furnace at high temperature to form ceramics structure [2]. At the carbonizing process, the phenolic resin changed structure into glassy carbon, which increases fundamental property of woodceramics (corrosion resistance, mechanical strength) reinforces the material and suppresses the fissures and warp (caused by the porous structure characteristic of wood) occurred during thermoforming [3]. The carbonizing condition of woodceramics such as heating rate, carbonizing time, maximum temperature influences the property of woodceramics. Based on the microstructure, the woodceramics have various advantageous properties, such as high electromagnetic shielding effectiveness [4]. The specific heat capacity of woodceramics is related to porosity structure that becomes thermally stable when carbonizing temperature at 2800°C [5]. The bending strength increased with increasing carbonization temperature above 500°C, while the electrical resistivity drastically decreased from insulator to conductor range with increasing carbonization temperature above 800°C. Humidity and gas absorption and infrared radiation properties are also performance advantages that are expected to be used widely in industrial applications as reported in Chapter 1 [4, 6-11].

Woodceramics attracted a lot of attention in the eco-materials field, because they are made from various woody scrap materials or biomass that are not generally suitable for recycling process. Obviously, this development technique will be beneficial for reducing resource usage and environmental protection.

In this chapter shows the development of functional carbon materials as woodceramics from agricultural biomass in Thailand are attempted to develop by woodceramics technology. In this research biomass from Thai rubber tree scrap (leaves, branches, stem, roots) and coconut shell are used. The fabrication parameters (weight fraction of phenolic resin powder to charcoal powder, and various carbonizing temperature in the

vacuum furnace) of woodceramics are varied by design. The microstructure of woodceramics, chemical analysis, physical properties and mechanical properties of woodceramics were investigated in detail.

3.2 Fabrication of Woodceramics from Thai rubber trees and experimental procedure

The biomass from Thai rubber trees was collected from three main parts, (leaves, branches, roots, and residues stem) by wood processing. The flow diagram of woodceramics fabrication was shown in Figure 3.1. The first step is preparing small pieces by cutting with a basic cutting tool. The pieces are kept outside under sun light to remove moisture from the materials. The fabricated charcoal from Thai rubber trees were put inside the oxygen control furnace and carbonized at 600° C for carbonizing time of 4 hours [12]. To fabricate charcoal powder, the product from the first carbonizing process were crushed into small pieces by a mechanical crushing machine as shown in Figure 3.2. The ceramics ball mills jar equipment was used to form very fine charcoal powder, which were made to sieved at 250 µm.

To remove moisture, charcoal powder was kept in dryer machine at heating temperature of 60 °C at a hold for 180 minutes. The design of weight fraction of biomass charcoal powder to phenolic resin were, 60:40, 70:30 and 80:20 respectively.

The biomass charcoal and phenolic mixtures were mixed to homogeneously using the ceramics ball mills. The amount of mixtures (biomass charcoal and phenolic resin) poured in a ceramics jar set to 100 g. Rotation mixing speed of the mills was 600 rpm and mixing time was 10 minutes.

To form the bulk shape pre-woodceramics two kinds of molds were used. One is a graphite mold to form circular shape whose diameter was 10 mm. of diameter. The other was a steel mold to form rectangular shape whose width, length and thickness were 25 mm, 94 mm and 10 mm. respectively.

Preparing biomass Charcoal

Cutting Thai rubber wood into small pieces

Drying under sun light

Carbonizing at 600°C
4 hour under oxygen control furnace

Crushing and put in ceramics ball mills jar

"Biomass charcoal powder"

Preparing to forming woodceramics

Drying for 3 hours at 60°C
in dryer furnace for humidity control

Mixing with phenolic resin
(charcoal: resin)
60:40, 70:30, 80:20

Forming under Hot Press Mold
10 MPa , 453 K, 10 minutes

Carbonizing in oxygen control furnace
for 4 hour
673K, 873K, 1073K, 1273K

Heating rate 5°C/min

"Woodceramics"

Figure 3.1 Flow chart of fabrication process of woodceramics from rubber trees biomass.
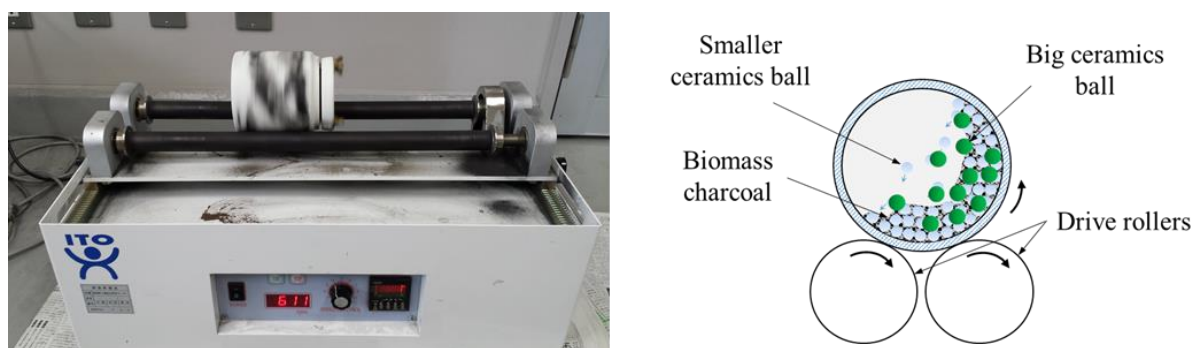
Figure 3.2 Photographs of ball milling process to form charcoal powder from Thai rubber trees biomass.

To fabricate the bulk shape woodceramics the mixed powder filled in a mold set. The amount of mixed powder was controlled by weight scale. The mold is installed in a press machine as shown in Figure 3.3. The temperature of the press machine was increased and kept at 180 °C. The forming pressure was slowly increased to 10 MPa in the maximum, then hold for 10 minutes to melt the phenol resin completely. After processing the bulk shape products were cooled down to room temperature under ambient atmosphere surrounding and then taken out from the mold [3, 13].

The bulk solid shape products woodceramics were carbonized at various temperatures to form woodceramics structure. In this study, the carbonization temperatures were designed to change from 1000 °C to 2800 °C under vacuum [14-16]. The carbonization condition were operated with heating rate at 5°C /minutes [17]. The final products are porous carbonaceous materials called "woodceramics".

A scanning electron microscope (SEM) was used to observe the surface morphology of the woodceramics. The chemical analyses were carried out by energy dispersive X-ray spectroscopy (EDX). For water absorption measurement, samples kept dired at 60 °C for 120 minutes, were immersed in de-ionized water for 24 hours and the amount of water absorption was determined by measuring the weight gained after immersion. The microstrucutre of all fabricated samples were investigated by X-ray diffraction measurement, which characterizes crystal structure and interplanar spacing of graphite basal plane. The effect of carbonizing temperature on behaviors of woodceramics was measured using thermogravimetric (TGA) equipment under a nitrogen flow at a heating rate of 10°C/minutes from room temperature to 1000 °C. Raman spectra of woodceramics was taken to characterize the carbon species, in which integrated intensity ratio, $R=I_D/I_G$, was calculated in terms of the peak internsity of 1360 cm^{-1} (D-band) and 1590 cm^{-1} (G-band) [20]. The electric resistivity of WCMs derived from Thai rubber trees were measured by Mitsubishi Chemical; Laresta-GP MCP-T600. The mechanical properties of woodceramics were measured by compressive test.
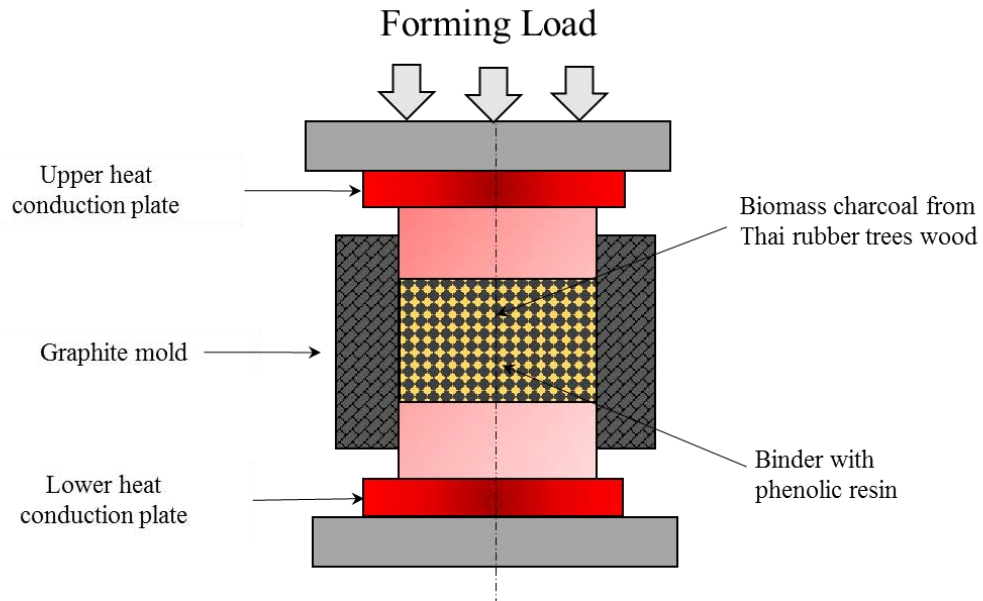
Figure 3.3 Schematic of hot press mold for fabricate woodceramics from biomass charcoal originated from Thai rubber trees.

3.3 Results and discussion

3.3.1 Scanning electron microscopy

The scanning electron microscope shows micrographs of the cross sectional surface of WCMs from biomass originated from Thai rubber trees with various carbonizing temperature are shown in Figure 3.4. As already show in SEM photo, the increasing carbonizing temperatures from (a), carbonized at 600 °C woodceramics have closed surfaces after phenolic resin complete melting and curig, (b) is carbonized at 800 °C woodceramics start to open pores on the surface, and (c) is carbonized at 1000 °C, the woodceramics have more a porous structure, which was confirmed by SEM photo. At the high carbonization temperature, the large amount of volatiles of phenol resin in sample disappears, then increasing mesopores (2-50 nm) and macropores ($\geqslant$ 50nm) in the WCMs increased [18-21].
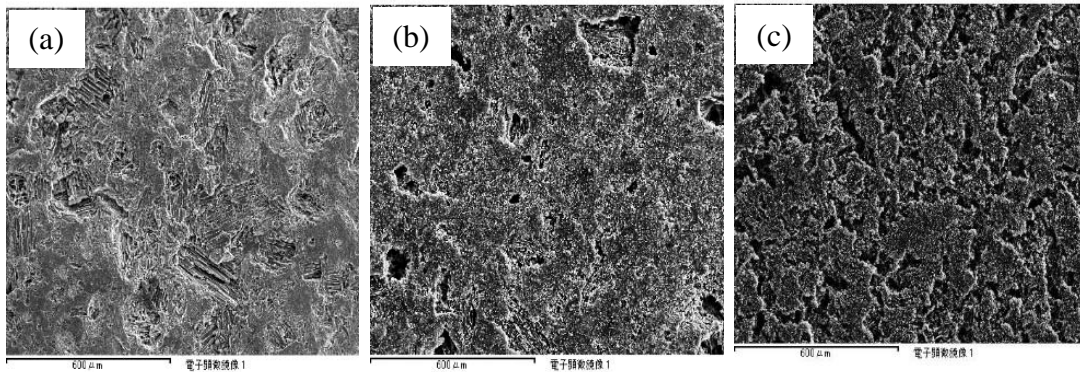
Figure 3.4 SEM images of woodceramics fabrication from biomass originated from
Thai rubber trees at different carbonization temperatures, (a) at 600 °C, (b) at 800 °C
and (c) 1000 °C

3.3.2 Energy Dispersive using X-Ray

Table 3.1 shows the relationship of carbon and oxygen in weight percentage for the
WCMs at different carbonizing temperatures. The EDX results show that carbon
concentration increased with increasing carbonization temperature. On the other hand,
the percentage of oxygen in woodceramics was decreased by increasing the
carbonization temperature. Figure 3.5 shows the relationship between ratio of carbon
and oxygen concentration as a function of carbonization temperature. This function can
be used to design woodceramics to support special applications, which require the high
carbon content inside the woodceramics such as synthesis carbon thin films by use
woodceramics as source material for generated carbon element in the process.

Table.3.1 Shows the chemical composition in WMCs with various carbonization
temperatures.

Carbonizing temp.(°C)	Elemental Composition of WCMs (wt%)				
	C	O	Si	Ca	Other
1000	74.88	14.66	0.3	8.39	1.77
2000	86.34	6.96	3.36	0.37	2.97
2800	96.24	3.33	0.12	0.31	0
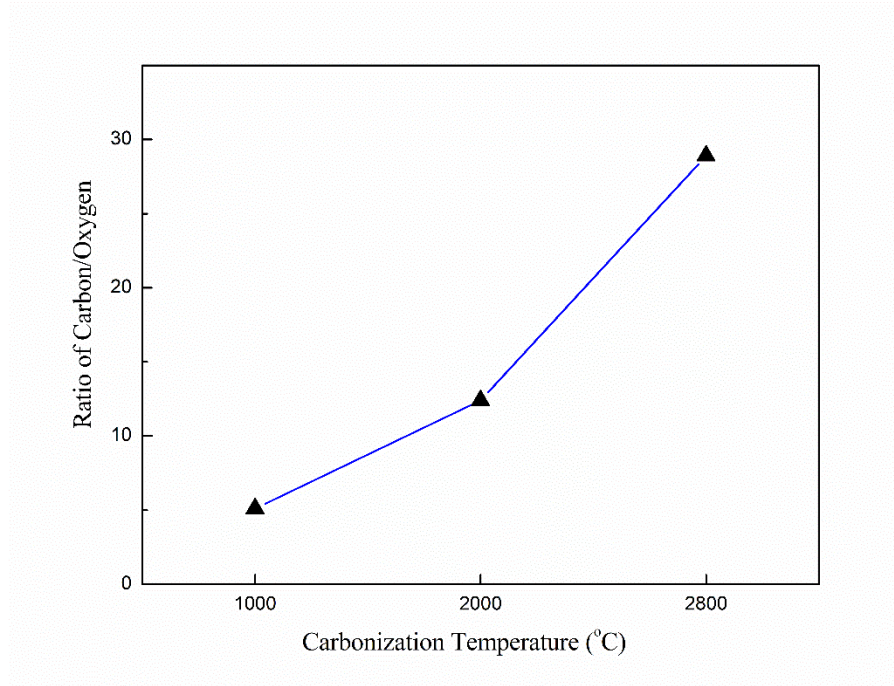
Figure 3.5 Relationship of carbon to oxygen composition in woodceramics fabricated biomass charcoal originated from Thai rubber trees with carbonization temperature.

3.3.3 X-ray diffraction measurement

The WCMs fabricated biomass charcoal originated from Thai rubber trees with various weight ratio of phenolic resin and carbonization temperature. For the WCMs with carbonization lower than 1000 °C, all of X-ray patterns were show that non-crystalline structure or amorphous solid form as shown in Figure 3.6. The WCMs were fabricated with various carbonization temperature are shown in Figure 3.7. The graphitic peak (002) showing that the higher carbonization temperature, high intensity peak at $2\theta =$ 26.4°, which indicated the interplanar spacing of the crystalline smaller than low temperature. The woodceramics fabricated from Thai rubber tree wood consist of three micro structure components that correspond to amorphous, turbostatic, and graphite. When increasing the carbonization temperature, the graphite and turbostratic carbon component increase and the amorphous decreased. This result suggests that carbonization temperature effectively completes graphitized structure [15, 23, 24].
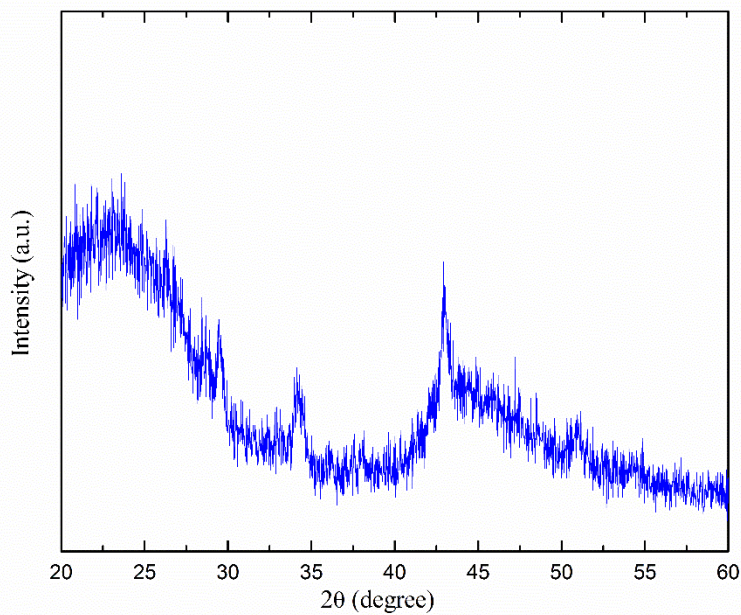
Figure 3.6 XRD patterns of woodceramics fabricated from biomass originated from Thai rubber trees.
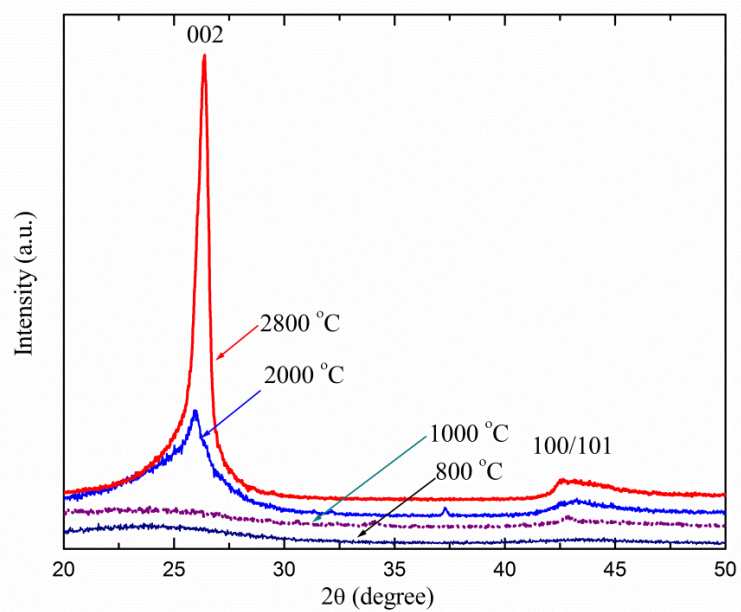
Figure 3.7 XRD patterns of woodceramics carbonized at different temperatures.

3.3.4 Raman spectroscopy

Raman spectra of woodceramics with weigh fraction of 40 percentage of phenolic resin carbonized at different temperature 1000 °C, 2000 °C, and 2800 °C for 4 hours are shown in Figures 3.8. The broad D and G-bands of graphitic carbon materials are the main features to be studied. The several research paper reported that D-band occurred degree of intensity around 1360 cm^{-1} and 1590 cm^{-1} for G-band. The G-band corresponding to large graphite crystals, D-band related to disordered carbon belong to aromatic ring in perfect graphite [20, 25, 26].

The Raman spectra peak of woodceramics originated from biomass Thai rubber trees and coconut shell charcoal indicated that Raman shift peak located at the same shift and I_D/I_G value not different as shown in Figure 3.8 (a). While increasing carbonization temperature for woodceramics originated from rubber tree the peaks corresponding to D and G band were sharpen with a substantial decrease in I_D/I_G value from 1.10 (1000 °C) to 0.69 (2800 °C) as shown in Figure 3.8 (b). The Raman shift peak indicates that the graphitization degree and graphite crystallite size (L_a) significantly increased with increasing carbonization temperature. It has been known that the graphite carbon is normally formed at a higher temperature of about 2500 °C. Figure 3.8 (c) show the Raman spectra of WCMS derived from various raw materials, Thai rubber tree, Apple tree, saw dust, and architecture waste in Aomori were mixed with weight fraction 40% of phenolic resin and carbonized at 1000 °C. The spectra result show that WCMS were composed of two evident peaks at about 1600 and 1348 cm^{-1}, which are assigned to the G band and D band, respectively. The I_D/I_G ratio was found to be about 1.06, 1.00, 1.00, and 1.00 for the WCMS derived from Thai rubber tree, architecture waste, sawdust, and apple, respectively with carbonized at 1000 °C. Among them, WCMs derived from architecture waste char had the highest I_D/I_G ratio, indicating more disorder structure when compared to WCMs derived from other raw materials.
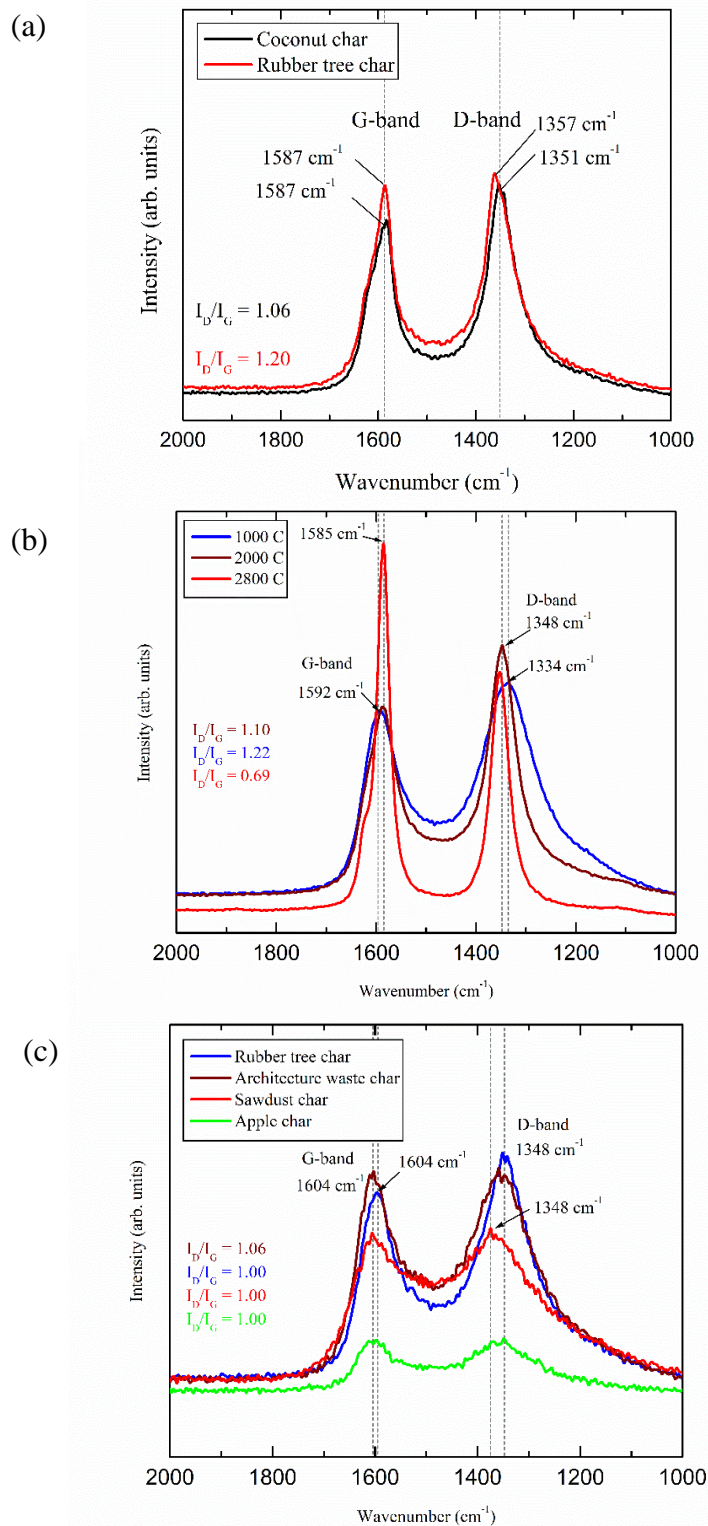
Figure 3.8 Raman spectra comparison of WCMs (a) originated from rubber tree and coconut shell, (b) originated from rubber tree with different carbonization temperatures, and (c) originated from various materials.

3.3.5 Physical property analysis

The woodceramics fabricated from biomass originated from Thai rubber trees at 40
percentage of phenolic resin in weight fraction and carbonized at 1000 °C. As
woodceramics is porous material, the volume density and amount of water absorbed
indicated some physical properties of woodceramics and result are shown in Figure 3.9.
The amount of water absorption was determined by measuring the weight gained after
immersed in de-ionized water for 24 hours. The amount of water absorbed varied from
12 to 18 wt% with increasing the weight fraction ratio of charcoal to phenolic resin,
also increased the volume density of woodceramics. The water absorption increased
with decreasing volume density. The carbonizing temperature also affected to water
absorption. It change volume densities and porosity of WCMs at high temperature [22].
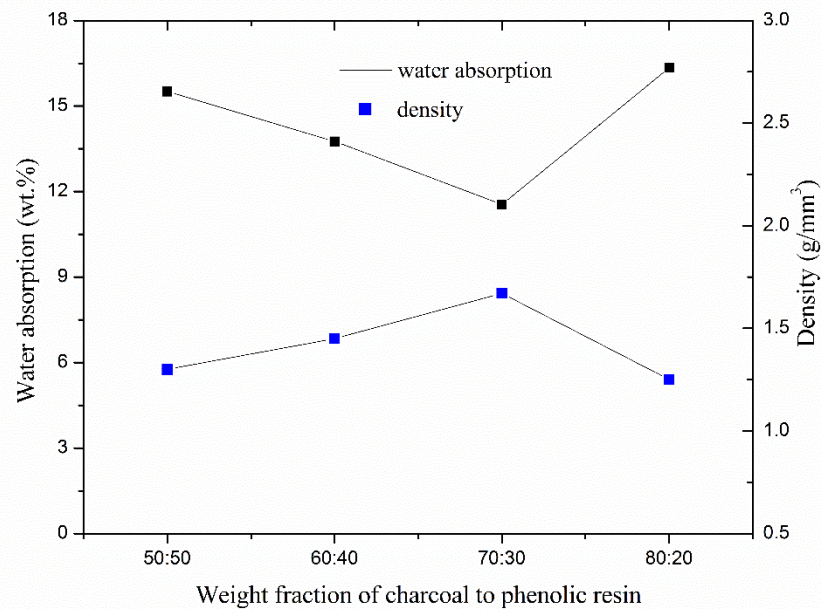
Figure 3.9 Relationship of volume density and water absorption of
woodceramics with varied phenolic resin carbonized at 1000 °C.

The electric resistivity of WCMs derived from Thai rubber tree carbonized at 1000 °C
with specimen size with width = 2.5 cm. thickness = 0.5 cm. and length = 8.5 cm were

measured. The electrical resistivity was 8.637 x 10^{-2} Ω.cm. The electrical resistivity were decrease with increasing carbonization temperature. In the same way to increased weight fraction ratio of phenolic resin decreases the electrical resistivity in woodceramics because phenolic resin changed to glassy carbon, that have lower resistivity than wood carbon [8]. Therefore, higher carbonization temperature improved electric conductivity of WCMs [27].

Woodceramics composite materials whose physical properties are like brittle material, so atomic or molecular bonds cannot be re-formed when external load is applied. Therefore, under compression test, the crystalline plane begins to slip, catastrophic failure occurs and the material fractures [28].

The bending test results of WCMs derived from Thai rubber trees carbonized at various temperatures shown in Figure 3.10 suggested that higher carbonizing temperature increased the compressive strength and bending strength. High weight fraction of phenolic resin also increased. Then it is well known that carbonization process changed the microstructure of phenolic resin to glassy carbon. The glassy carbon is higher strength than that of amorphous carbon, supporting woodceramics to resist the external load.
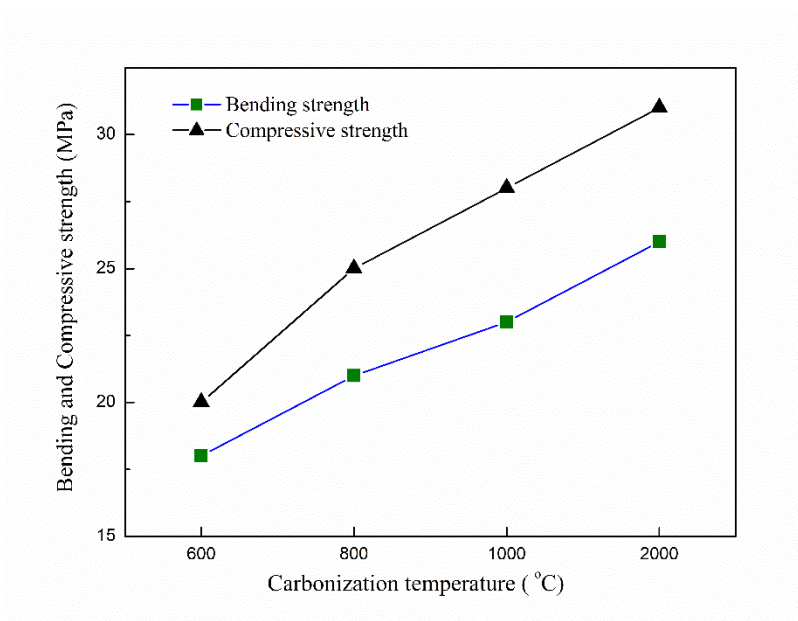
Figure 3.10 Effect of carbonization temperature on bending and compressive strength of WCMs derived from Thai rubber tree.

The dimensional change and weight loss of woodceramics are an effect of carbonization temperature. The details in the previous section, that moisture and decomposition of gas and impurity element are lost during carbonizing process. Figure 3.11, shown that high carbonization temperature, high dimension shrinkage.
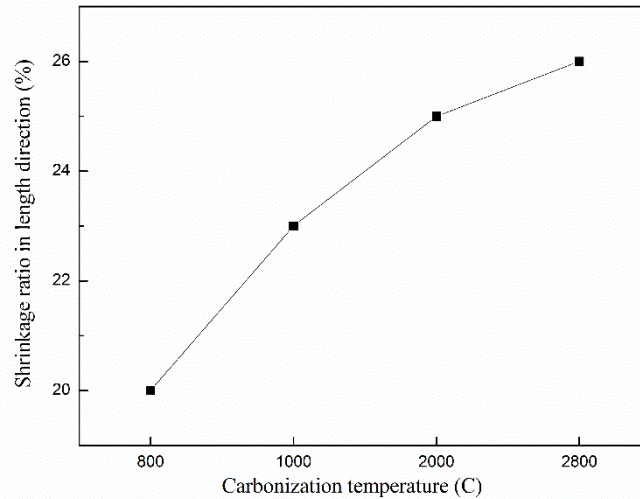
Figure 3.11 Volume density change of WCMs with different carbonization temperature.

3.4 Conclusion

The woodceramics are successfully prepared using raw biomass material from Thai rubber trees. The woodceramics have a topologically uniformly interconnected porous microstructure that is typical of carbon structure. With increasing carbonization temperature, the peak intensity of the XRD pattern becomes stronger and shifts to higher angles, and the (0 0 2) interplanar spacing of graphite in woodceramics and the dimensions of carbonized wood powders decreased. The effective weight ratio of phenolic resin to charcoal powder on the XRD pattern of woodceramics is slight, but improves the forming ability of woodceramics significantly, and results in a more uniformly porous microstructure. With increasing carbonization temperature, the open porosity of woodceramics increase was confirmed by SEM. The carbonization temperature had great effects on the WCMs properties. With increasing carbonization

temperature, higher dimensional shrinkage occurred. The volume density is decreased but specific surface area increased. The graphite peak (002) interplanar spacing of the basal plane decreased with increasing carbonization temperature. High carbonization temperature increased ratio of oxygen to carbon element in WCMs. Therefore, it could be conclude that the woodceramics fabricated from rubber trees has potential to be used as functional carbon materials for future application.

References

[1] T. Okabe, K. Kakishita, H. Simizu, K. Ogawa, Y. Nishimoto, A. Takasaki, T. Suda, M. Fushitani, H. Togawa, M. Sata and R. Yamamoto, "Current status and application of woodceramics made from biomass," *Trans. Mat. Res. Soc. of Japan,* vol. 38, pp. 191-194, 2013.

[2] K. Shibata, T. Okabe, K. Saito, T. Okayama, M. Shimada, A. Yamamura and R. Yamamoto, "Electromagnetic Shielding Properitesd of Woodceramics made from Watespaper," *Journal of Porous MAterials,* vol. 4, pp. 269-275, 1997.

[3] T. Okabe, K. Saito and K. Hokkirigawa, "New porous carbon materials, woodceramics: Development and fundamental properties," *Journal of Porous Materials,* vol. 2, pp. 207-213, 1996.

[4] K. Shibata, T. Okabe, K. Saito, T. Okayama, M. Shimada, A. Yamamura and R. Yamamoto, "Electromagnetic Shielding Properitesd of Woodceramics made from Watespaper," *Journal of Porous MAterials,* vol. 4, pp. 269-275, 1997.

[5] M. Kano, M. Momoto, T. Okabe and K. Saito, "Specific heat capacity of new porous carbon materials: woodceramics," *Thermochimica acta,* vol. 292, pp. 175-177, 1997.

[6] A. Hashimoto, A. Takasaki, S. Uematsu and T. Okabe, "Production of Titanium Oxide Layers on Woodceramics by Plasma Thermal Spraying," *Transsaction of the Materials Research Society of Japan,* vol. 34, no. 4, pp. 655-658, 2009.

[7] A. Takasaki and T. Okabe, "Hydrogen desorption properties of woodceramics," *Trans. Mat. Res. Soc. of Japan,* vol. 34, no. 4, pp. 675-678, 2009.

[8] J. Qian, Zh. Jin and J. Wang, "Structure and basic properties of woodceramics maade from phenolic resin-basswood powder composite," *Materials Science and Engineering,* vol. A 368, pp. 71-79, 2004.

[9] K. Kasai, H. Endo, K. Shibata and M. Otsuka, "Mechanical and electrical properties of carbon films prepared by radio frequency magnetron sputtering of woodceramics," *Journal of Ceramics Socirty of Japan,* vol. 108, no. 1, pp. 32-35, 2000.

[10] R. Ozao, Y. Nishimoto, W.P. Pan and T. Okabe, "Thermoanalytical characterization of carbon/carbon hybrid material, apple woodceramics," *Thermochimica Acta,* vol. 440, pp. 75-80, 2006.

[11] A. Takasaki, S. Iijima, T. Yamane and T. Okabe, "Hydrogen adsorption by woodceramics produced from biomass," *Journal of Shanghai Jiaotong University,* vol. 17, no. 3, pp. 330-333, 2012.

[12] T. Okabe, K. Saito, and K. Hokkirigawa, "The effect of burning temperature on the structural changes of woodceramics," *Joural of porous materials,* vol. 2, pp. 215-221, 1996.

[13] W. Zhou and Y. Yu, "Study of Fe/Woodceramics Composites," dalam *International Conference on Biobase Material Science and Engineering*, Changsha, Chaina, 2012.

[14] K. Hata, K. Shibata, T. Okabe, K. Saito and M. Otsuka, "Laser beam machining of porous woodceramics," *Journal of porous materials,* vol. 5, pp. 65-75, 1998.

[15] H.M. Cheng, H. Endo, T. Okabe, K. Saito and G.B. Zheng, "Graphitization behavior of wood ceramics and bamboo ceramics as determined by X-ray diffraction," *Journal of porous materials,* vol. 6, pp. 233-237, 1999.

[16] T. Hirose, T.X. Fan, T. Okabe and M. Yoshimura, "Effect of carbonization temperature on the basic of woodceramics impregnated with liquefied wood," *Journal of materials science,* vol. 36, pp. 4145-4149, 2001.

[17] T. Hirose, T. Fan, T. Okabe and M. Yoshimura, "Effect of Carbonizing Speed on the Property Change of Woodceramics Impregnated with Liquefacient Wood," *Materials Letters,* vol. 52, pp. 229-233, 2002.

[18] M. Singh and J.A. Salem, "Mechanical properties and microstructure of biomorphic silicon carbide caramics fabricated from wood precursors," *Journal of European Ceramics ,* vol. 22, pp. 2709-2717, 2002.

[19] O. Ishida, D.Y. Kim, S. Kuga, Y. Nishiyama and R. Malcolm Brown Jr.[2], "Microfibrillar carbon from native cellulose," *Cellulose, Kluwer Academic Publishers, Netherlands,* vol. 11, pp. 475-480, 2004.

[20] L.B. Zhang, W. Li, J.H. Peng, N. Li, J.Zh. Pu, Sh.M. Zhang and Sh.H. Guo, "Raman spectroscopic investigation of the woodceramics derived from carbonized tabacco stems/phenolic resin composite," *Materials and Design,* vol. 29, pp. 2066-2071, 2008.

[21] H.M. Mozammel, O. Masahiro and S.C.Bhattacharya, "Activated Charcoal from coconut shell using ZnCl2 activation," *Biomass and Bioenergy,* vol. 22, pp. 397-400, 2002.

[22] J. Guo, Y. Luo, A.Ch. Lua, R.A. Chi, Y.L. Chen, X. Bao and Sh.X. Xiang, "Adsorption of hydrogen sulphide (H2S) by activated carbons derived from oil-palm shell," *Carbon,* vol. 45, pp. 330-336, 2007.

[23] N. Mohamad, L.L. Chung, L.K. Teong and A.R. Mohamad, "Synthesis of activated carbon from lignocellulosic biomass and its applications in air pollution control- a review," *Journal of Environmental Chemical Engineering,* vol. 1, pp. 658-666, 2013.

[24] S. Kakuta, H. Ono, M. kushibiki, T. Okabe, H. Degawa, H. Hatanaka, Y. Iwamoto, M. Ogawa, A.Takasaki and M. Murakami, "Development of bean refuse origin ceramics materials," *Trans. of the Mats. Res. Soc. of Japan,* vol. 31, no. 4, pp. 949-952, 2006.

[25] E.J. Mittemeijer, P. Scardi, Diffraction Analysis of the Microstructure of Materials, Berlin, German: Springer, 2003, Print..

[26] W. D. Callister, Materials Science and Engineering an Introduction, 3rd Ed., New York, United State: John Wiley and Sons, Inc., 1994, Print..

[27] K. Shibata, K. Kasai, T. Okabe and K. Saito, "Electrical resitivity of porous carbon materials woodceramics at law temperature," *Journal of porous materials,* vol. 2, pp. 287-290, 1996.

[28] ENTEGRIS, "Properties and characteristic of graphite," Entegris, Inc., USA, 2013.

Chapter 4

Production of Amorphous Carbon Films using Woodceramics

4.1 Introduction

Amorphous carbon is one of classification for carbon structure that have non-crystalline structure, unsystematic, glassy structure, that is substantially graphite except for not form in a crystalline structure [1], whose main constituent of substances are charcoal, lampblack (soot) and activated carbon. At the atmosphere, carbon material takes the form of graphite, that each atom are bonded in trigonal form to three others in a plane composed of fused hexagonal rings, similarly to those in aromatic hydrocarbons [2].

The development of carbon thin film depositions and growth techniques are well known as amorphous carbon (a-C) thin films. The a-C thin film is a disordered phase of carbon, containing carbon atoms mostly in graphite-like sp^2 and diamond-like sp^3 hybridization sites [3]. The relative concentration of sp^2 or sp^3 hybridized bonds and the atomic connectivity within the films influences to the physical and mechanical properties of a-C films [4]. Figure 4.1 present details of phase diagram for sp^2 and sp^3 bonding categorized to tetrahedral amorphous carbon (ta-C), hydrogenated amorphous carbon (a-C:H) and amorphous carbon (a-C) [5]. The attractive properties of a-C thin films, high surface hardness, chemical inertness, corrosion resistance, low friction coefficient, high thermal conductivity and optical transparency [6, 7]. The a-C thin films have widespread applications as protective coating for some products such as magnetic storage disks, cutting tools, biomedical and micro-electromechanical (MEMs) parts, and automobile components as presented in Figure 4.2. The amorphous carbon films have been coated by several method as chemical vapor deposition (CVD) and the physical vapor deposition (PVD).

Figure 4.1 Phase diagram of ternary bond in amorphous carbon and hydrogen hybridized thin films [5].

Figure 4.2 Photograph of application carbon thin films coated over automotive components [8].

Many of the previous research and papers investigated production of a-C films by radio frequency (RF) magnetron sputtering technique. The RF magnetron sputtering is one technique to produce amorphous carbon films with high deposition rates at low deposition temperature with high forming quality [9]. The process of RF magnetron sputtering involves low-cost fabrication with easy control parameters for film growth, and is suitable for large-scale films deposition. The RF magnetron sputtering process is a extremely technique which allows for the sputtering of a large category of materials with a high deposition rate of film thickness uniformity [10]. The sputtering process is

particle to particle collisions determinate involve an elastic transfer of momentum, which can be utilized to apply a carbon layer to the substrate [11]. The ions are derived from either an ion gas or from exciting a neutral gas into plasma. The ions are accelerated derived from argon gas to bombarding target material, they dislodge target atoms and other ions. The atoms was ejected and moving attach themselves to the surface substrate, and the layer thin film from target material were produced as shown in Figure 4.3.
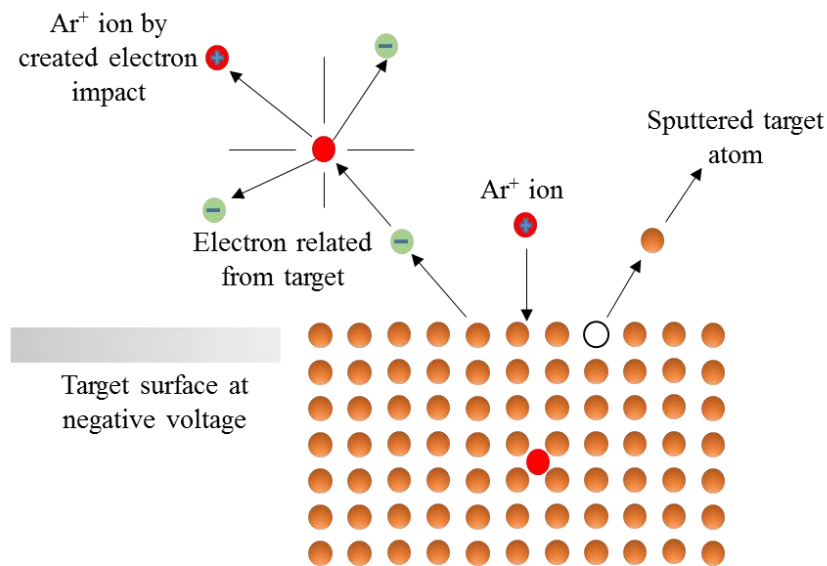
Figure 4.3 Schematic diagram of sputtering at the molecular level.

Woodceramics, a new kind of porous carbon material, consist of high percentages of carbon contents after carbonizing at high temperatures in the vacuum furnace as mentioned in Chapter 3. The woodceramics have a topologically uniform interconnected porous network microstructure, and typical non-graphitizable carbon containing C=C bonds, C-O-C bonds and C-H structure [12, 13].

This study is to explore further areas of application for woodceramics fabricated from biomass originated from Thai rubber trees. The objective of this investigation is to introduce a different target material to fabricate the a-C films. Author attempted to perform low cost deposition of amorphous carbon films onto silicon wafer (Si) substrate by a RF magnetron sputtering technique using woodceramics products from the

research in the previous chapter as a target, which could replace costly high purity graphite. The aim of this study is to investigate the microstructures and the characteristics of produced films by analysis of X-ray diffraction. The Raman spectroscopy is used to determine the concentration of a-C films, together with an X-ray photoelectron spectroscopy was used to identify the sp^2/sp^3 ratio. Some fundamental mechanical properties such as hardness and friction coefficient were also measured. This approach has the potential to add to the value of woodceramics fabricated from Thai rubber trees.

4.2 Experimental Procedures

PREPARING THE TARGET MATERIAL FROM WCMS

The WCMs fabricated from biomass charcoal originated from Thai rubber tree wood, the fabrication details are in the previous Chapter, that was used to prepare the target materials to produce amorphous carbon (a-C) films. The fabrication condition of WCMs have 40% weight fraction of phenolic resin to biomass charcoal from rubber trees and carbonized at 1000 °C. Figure 4.4 show the WCMs was prepared to 10 mm. in diameters and 5 mm. in thickness to fit in size of the supporter base on the RF sputtering machine, which was used in this study.
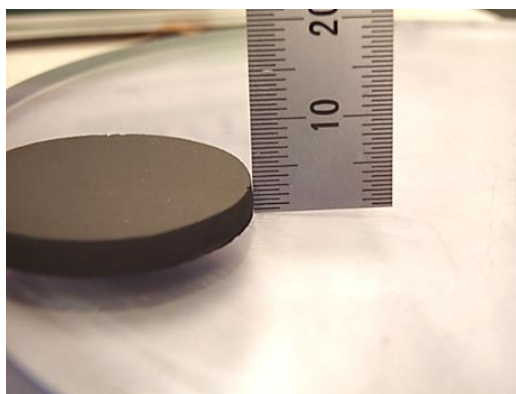
Figure 4.4 Preparing target material from woodceramics for using in process of RF magnetron sputtering.

FABRICATION OF AMORPHOUS CARBON FILMS

The amorphous carbon films in this study were deposited using a RF magnetron sputtering method made by SS Alloys company model PLASMAN ; CSP-III-SPTS-2. The machine specification was a RF power of 100 W, and frequency of 13.56 MHZ. The main parameters for prepare a-C films are coordinate in Figure 4.5. The substrates were silicon wafers, which were cleaned by ultrasonic cleaner for 15 minutes to remove oil and dust from the substrate surface. The distance between the target and substrate setting was 32 mm. The installed schematics and illustrations of sputtering were presented in Figure 4.6 and 4.7. For the deposition of a-C films, first the system was evacuated hamber to 4.5×10^{-3} Pa (4.5×10^{-5} mbar) by the ULVAC vacuum pump. The pure argon gas started flowing at 20 mL/minutes into the chamber in order to clean the substrate. The flow rate of argon gas decreased to 15 mL/minute. The films were deposited at room temperature by slowly increasing RF power to 70 W, and the surfaces were pre-sputtered for 5 minutes before the actual coating. After the pre-coating process the RF power was slowly raised to 120 W, the power was kept constant and kept deposition time following each coating condition. The deposition times used in this study were designed for three condition, 60, 90, and 120 minutes respectively.
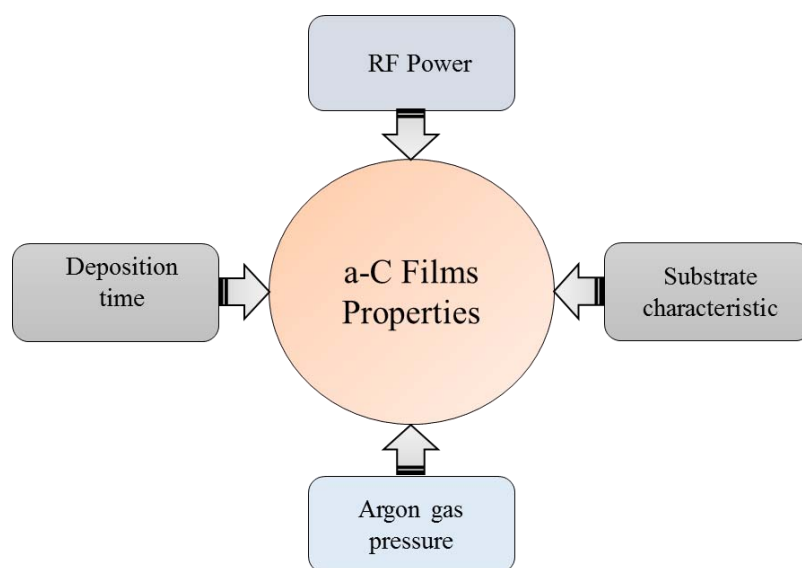
Figure 4.5 Parameters of the RF magnetron deposition operation used to produce a-C films.
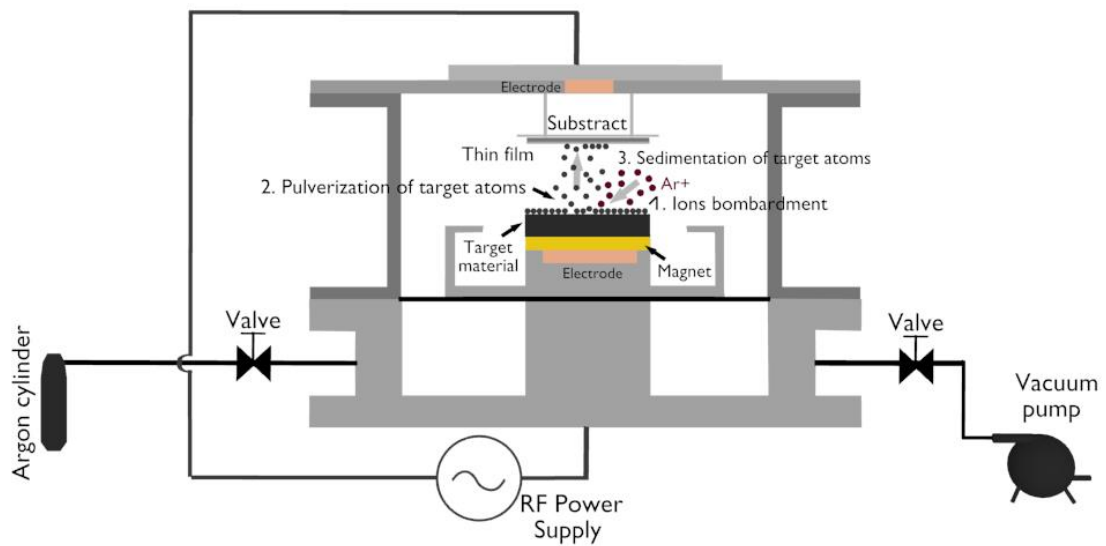
Figure 4.6 Schematic representation of RF magnetron sputtering process.
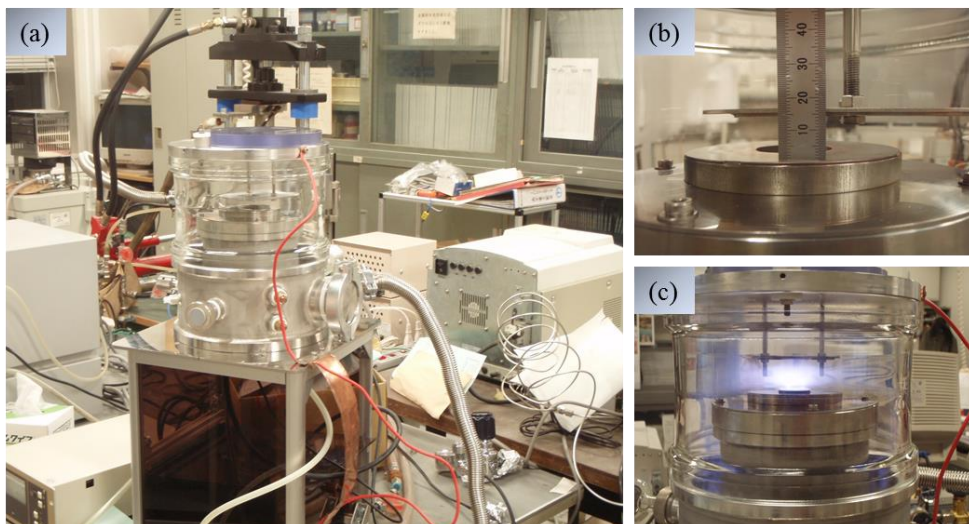
Figure 4.7 Photograph of RF magnetron sputtering (a) sputtering machine, (b) distance of target to substrate, and (c) actual plasma deposition of a-C films.

ANALYSIS

The microstructural analysis and chemical composition of a-C films were measurement by the scanning electron microscope (SEM), X-ray diffraction (XRD) to determine the crystal structures of the films using Cu-Kα radiation at 40kV and 45mA at room

temperature(wave length of 1.541 Å). The Raman spectra were obtained using a
JASCO NRS-2100 laser Raman spectrophotometer, which was operated at a laser
wavelength of 488 nm. The laser power was 30 mW and the spot size was 2 mm. The
spectra were taken from 1100 to 2000 cm^{-1} with a resolution of 2 cm^{-1}. X-ray
photoelectron spectroscopy (XPS) studies were also carried out using a Shimadzu
Kratos Axis-Ultra DLD. The XPS peak positions that reflect the electron binding
energies for specific atomic levels can be used to identify the chemical states of the
structure.

In order to characterization the physical and mechanical properties, the fundamental of
the films were measured using a ball-on-disk friction tester (CSEM; Tribotester). In the
friction test use dry sliding carried made of type 440C stainless steel (diameter of 6.0
mm) under a normal applied load of 3 N, and the disk rotation speed 6000 rpm. The
tests were performed under room condition with 30–45% humidity. The hardness were
measured with a Vickers's microhardness tester.

4.3 Results and discussion

4.3.1 Scanning electron microscope

The amorphous carbon films were fabricated onto a silicon wafer with RF magnetron
sputtering method using woodceramics from rubber trees as a target, as presented in
Figure 4.8. The appearances of a-C film are functions of film thickness, and the
thickness related to deposition time and sputtering parameters. The surface of Si
substrate after being deposited for 60 minutes is shown in Figure 4.9, the scanning
electron microscope indicates that the carbon particulate distributed on the Si surface
notes the density of carbon particle effective to the optical transparency of a-C films.
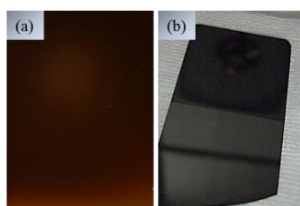
Figure 4.8 Photograph of a-C films coated on the surface of silicon wafer (a) and (b)
are from 60 minutes deposited condition.
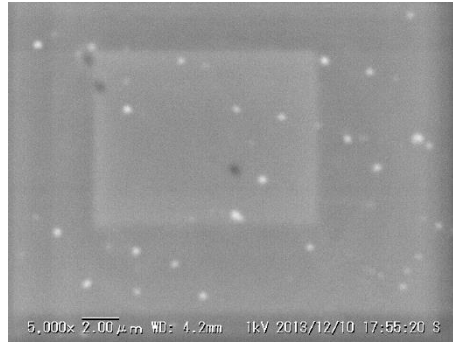
Figure 4.9 The SEM image of a-C films deposited at 60 minutes show a particulate of carbon on silicon wafer surface.

4.3.2 X-ray diffraction

The results of XRD pattern investigations of the deposited films before and after etching with argon ion with 3.8 kV, 20 mA, were shown in Figure 4.10. The pattern of graphite powder was included in this figure for a comparison to show that there was one strong peak at 26.38° and two weakpeaks at 42.30° and 44.31°, which correspond to diffractions from (002), (100) and (101) crystal plane of the graphite [14, 15].
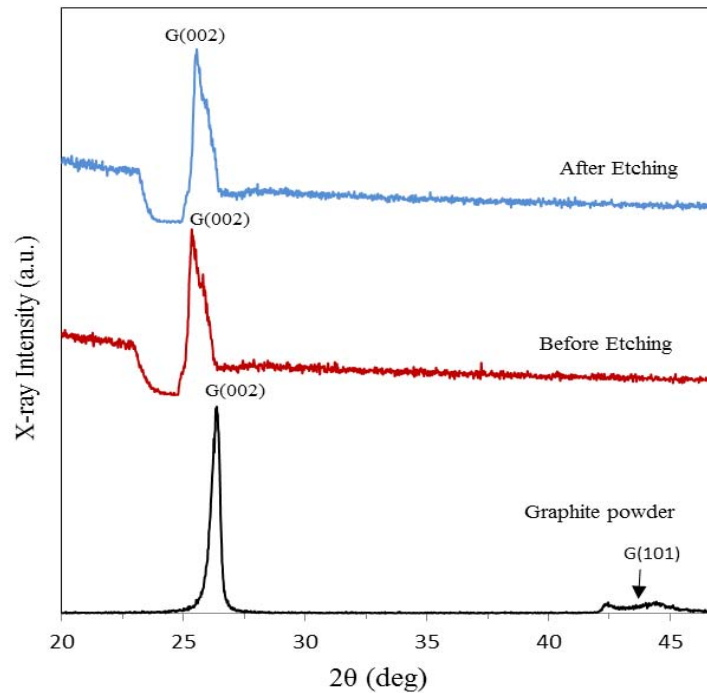
Figure 4.10 X-ray diffraction patterns for the amorphous carbon films before and after etching, comparing with one for graphite powder.

On the other hand, for the deposited substrates, a broad peak is observed at 25.36°~26.05°. These peak correspond to the (002) crystal plane of the graphite. For the deposited substrate only this peak was detected. Furthermore, any other diffraction peaks generally observed for the typical graphite crystal possessing a high crystallinity cannot be detected, indicating that the local structure of the deposited films were turbostratic structures or amorphous.

4.3.3 Raman spectroscopy

Raman spectrum indicated valuable information with regards to atomic bonds and level structure of the molecule[15]. Especially in the nanostructures of a-C films, it has a high potential to defining the structure of carbon films, which is highly sensitive to changes in the bonding configuration of bonding atom structure. The Raman spectroscopy for amorphous carbon films report previously, generally, consisted of two peaks around 1345-1355 cm^{-1} and 1570-1590 cm^{-1}, which correspond to D band and G band, respectively. The result of Raman spectroscopy for a deposited film was shown in Figure 4.11. There were two peaks centered at 1387.22 cm^{-1} and 1575.36 cm^{-1}. The G band peak is belong to graphite like bonding of sp^2 micro domains (bond stretching of all pairs sp^2 atoms in both rings and chains), while the D peak is belong to the bond angle disorder carbon bonding sp^2 graphite like micro domains induced by the linking with sp^3 carbon atom (breathing modes of sp^2 atoms in rings). The intensity ratio of D and G peaks, I_D/I_G, the full width half maximum (FWHM) are used to determine the structure of the different carbon base materials following Equation 4.1 indicated that after the etching process the percentage of sp^3 concentration increased from 79.04 to 81.16 respectively. However, it is difficult to analyze present data because of the overlapping of broad D and G peaks [4, 5, 7, 16-19] .

Table 4.1 Raman results of sp^3 content ratio in a-C film before and after etching.

Condition of etching	Intensity of broad peak		Sp^3 amount (%)
	$I_{(D)}$	$I_{(G)}$	
Before	1.1466	1.4507	79.04
After	1.4154	1.7439	81.16
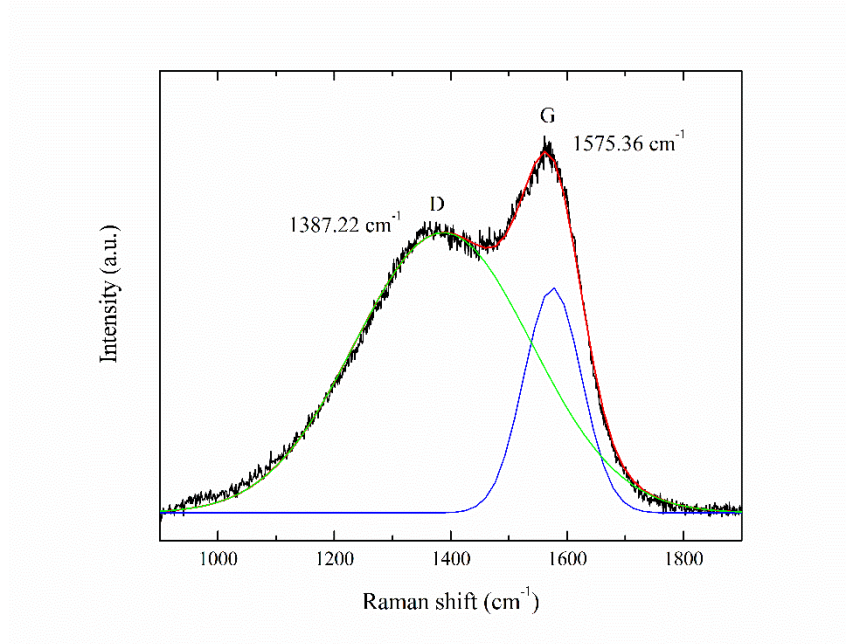
Figure 4.11 Raman spectrum of the deposited a-C films.

$$fraction\ of\ sp^3 = \frac{I_{(D)}}{I_{(G)}} \times 100 \qquad (4.1)$$

4.3.4 X-ray photoelectron spectroscopy (XPS)

XPS analysis, which is ordinarily known in the electron spectroscopy for chemical analysis (ESCA), is the most forceful and dependability tool used for analyzing the composition of amorphous carbon thin film. XPS survey spectra of film before and after etching are shown in Fig. 5. The etching was performed to remove a contaminated surface layer. It was found that the film at the utmost surface contained much more oxygen than at the inner region of the surface. The C1s spectrum of deposited films before and after process etching by argon ions are report in Figure 4.12, (a) and (b) respectively. In recently, various research groups have proposed the decomposition of the C1s peak into one sp^2 bonding corresponding to graphite in amorphous or hydrogenated amorphous carbon and sp^3 bonding corresponding to tetrahedral amorphous carbon. The sp^3 bonding can be determined from the ratio of the peak area over the total C1s peak area [20, 21]. The broad C1s spectra is deconvoluted into three kinds of curves, which correspond to binding energies for sp^2, sp^3 and C-O bonding using a Gaussian and a Lorentzian method.
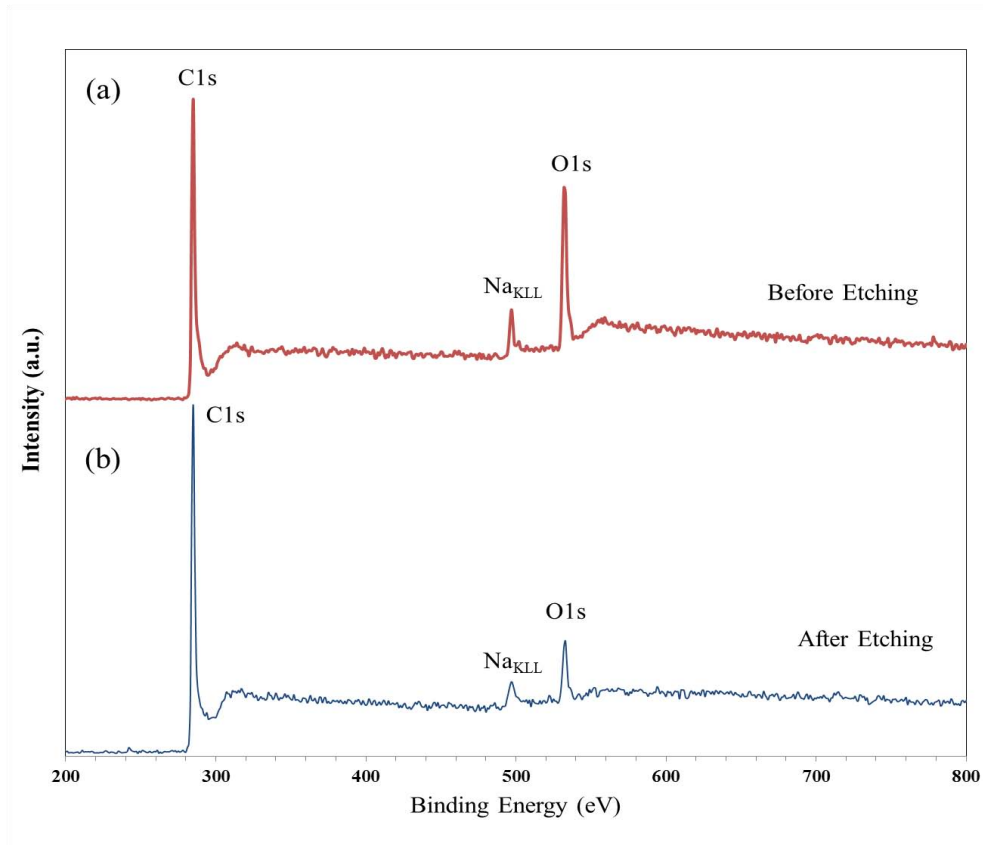
Figure 4.12 XPS spectra of a-C films, (a) before and (b) after etching.

Table 4.2, summarizes the peak position and spectrum area for each peak containing amorphous carbon (a-C) and tetrahedral amorphous carbon (ta-C) respect to ratio of sp^3 before and after etching as presented in Figure 4.13 (a) before etching in pure argon gas and (b) after etching. The mathematical model to calculate the ratio of sp^3 is the following Equation 4.2. Before etching, ratios of sp^3, sp^2 and CO bonding were about 31 %, 27 % and 27 % respectively, while those after etching were 56 %, 12 % and 17 % respectively. There seems to be much CO contaminated phase in the present films. The ratio of sp^3 was about 53 % before etching by argon ions, but it increased to 82 % after etching, probably because of a decrease in surface contamination and/or an oxygen-rich film. It has been reported that films surface layers are often slightly richer in sp^2 bonding than in the bulk [22-24], which agrees well with present results. It is well know from several research papers, that the a-C films had the hardness of highly tetrahedral coordinated carbon films due to the presence of sp^3 bond [25-34].
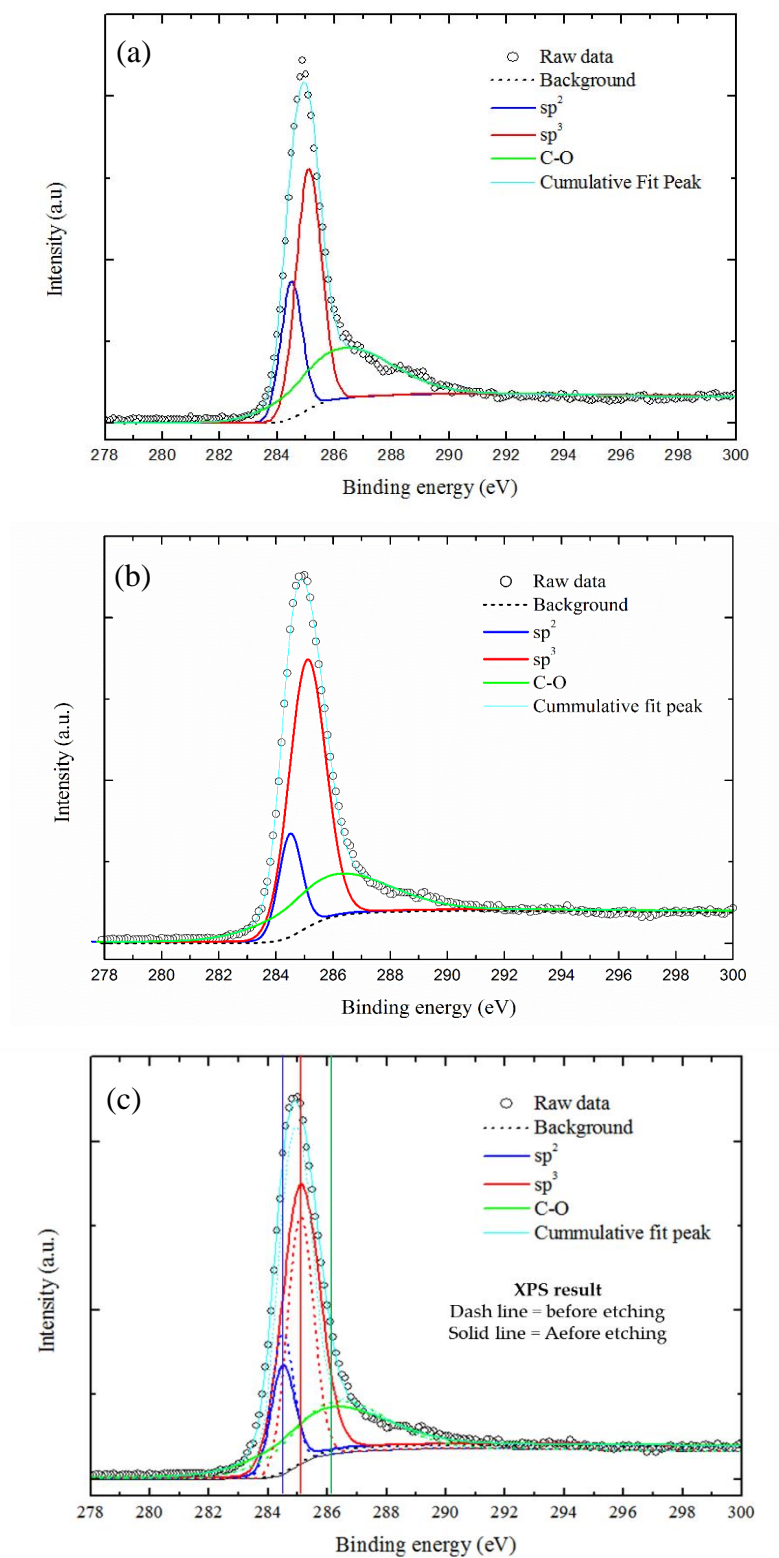
Figure 4.13 The deconvolution of XPS C1*s* peak of the amorphous carbon

films, (a) before etching, (b) after etching, and (c) combined before and after etching.

Table 4.2 Peak position, spectrum integrated area of each peak for C1s spectrum before and after etching, and ratio of sp^3 bonding before and after etching.

Specimen condition	Bonding structure	Binding energy (eV)	Spectrum area (cps eV)	Ratio of sp3 (%)
Before etching	sp3	285.103	6621.6	53.5122
	sp2	284.584	5752.4	
	C-O	286.014	5839.1	
After etching	sp3	285.22	14174.5	81.9975
	sp2	284.591	3112.0	
	C-O	285.772	4189.6	

$$sp^3 \ ratio = \frac{sp^3 \ area}{sp^3 \ area + sp^2 \ area} \qquad (4.2)$$

4.3.5 Mechanical and tribological

The average film thickness deposited on the substrate was approximately 200-400 nm due to limited coating time at 120 minutes. The maximum Vickers hardness of amorphous carbon films measured was found 11.87 GPa. The hardness of the amorphous carbon films fabricated from similar method was found 11-22 Gpa [35]. The dynamic friction coefficient measured was 0.25; the films were unstable and failed easily after 8 minutes of the test because of the thickness of the films. As a result, the results of the friction coefficient were higher than theory and literatures reported for amorphous carbon film at 0.05-0.2 [9].
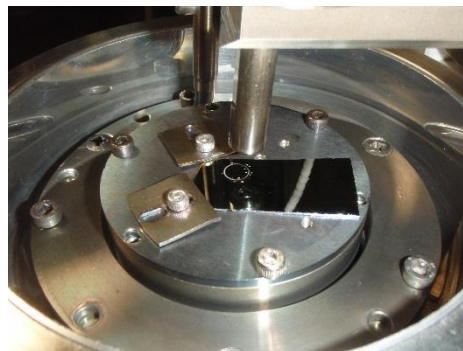
Figure 4.14 Photograph of ball on disk test to determine friction coefficient for a-C films.

4.4 Conclusion

The a-C thin films with high concentration of sp^2 or sp^3 hybridized bonds were fabricated by RF magnetron sputtering using woodceramics as a target. Studies produced amorphous carbon films by magnetron sputtering using woodceramics fabricated from biomass charcoal originating from Thai rubber trees. The films were composed of a turbostratic structure, or amorphous carbon, whose carbon electron configurations were sp^2 and sp^3. The ratio of sp^3 bonding was about 53 % before etching by argon ions, but it increased to 82 % after treatment to the surface layer via the etching process. The average film thickness deposited on the substrate was approximately 200-400 nm. Which was slightly increased as a result of an increase of sputtering time. The maximum Vickers hardness and the dynamic friction coefficient measured were 11.87 GPa and 0.25 respectively.

References

[1] D. William and Jr. Callister, Materials Science and Engineering an Introduction, 3rd Ed., New York, United State: John Wiley and Sons, Inc., 1994, Print..

[2] Wikipedia, "Carbon," Wikipedia free encyclopedia, 14 January 2015. [Online]. Available: http://en.wikipedia.org/wiki/Carbon. [Diakses 15 January 2015].

[3] J.W. Suk, Sh. Murali, J. An and R.S. Ruoff, "Mechanical measurements of ultra-thin amorphous carbon membranes using scanning atomic force microscopy," *Carbon,* vol. 50, pp. 2220-2225, 2012.

[4] M.A. Capano and N.T. McDevitt, "Characterization of amorphous carbon thin films," *J. Vac. Sci. Technol. A,* vol. 14, no. 2, pp. 431-435, 1996.

[5] J. Robertson, "Diamond-Like Amorphous Carbon," *Materials Science and Engineering,* vol. R 37, pp. 129-281, 2002.

[6] A. Grill, "Diamond-like carbon state of the art," *Diamond and related materials,* vol. 8, pp. 428-434, 1999.

[7] A. Carlo and J. Robertson, "Raman spectroscopy of amorphous, nanostructureed, diamond-like carbon, and nanodiamond," *Phil. Trans. R. Soc. Lond.,* vol. 362, pp. 2477-2512, 2004.

[8] A. Bachmann, "Sulzer Metco Announces New DLC Coating That Helps Achieve EU6 Emission Limit," SULZER, 31 July 2013. [Online]. Available:

http://www.sulzer.com/en/Newsroom/Business-News/2013/130731-New-DLC-Coating-Helps-Achieve-EU6-Emission-Limit. [Diakses 15 January 2015].

[9] H.M. Wang, Zh. Wei, Y.H. long and L.Q. liang, "Tribological properties of DLC films prepared by magnetron sputtering," *Physics Procedia,* vol. 18, pp. 274-278, 2011.

[10] K.T. Wojciechowski, R. Zybala, R. Mania and J. Morgiel, "DLC layers prepared by the PVD magnetron sputtering technique," *Journal of Achievements in Materials and Manufacturing Engineering,* vol. 37, no. 2, pp. 726-729, 2009.

[11] J. Kirschbrown, "RF/DC Magnetron Sputtering," 20 September 2007. [Online]. Available: http://www.unc.edu/~justink/RFDC_Sputtering.pdf. [Diakses 15 January 2015].

[12] J. Qian, Zh. Jin and J. Wang, "Structure and basic properties of woodceramics maade from phenolic resin-basswood powder composite," *Materials Science and Engineering,* vol. A 368, pp. 71-79, 2004.

[13] H.M. Cheng, H. Endo, T. Okabe, K. Saito and G.B. Zheng, "Graphitization behavior of wood ceramics and bamboo ceramics as determined by X-ray diffraction," *Journal of porous materials,* vol. 6, pp. 233-237, 1999.

[14] H. Pang, X. Wang, G. Zhang, H. Chen, G. Lv and S. Yang, "Characterization of diamond-like carbon films by SEM, XRD and raman spectroscopy," *Applied Surface Science,* vol. 256, pp. 6403-6407, 2010.

[15] M. Kamiko, K. Aotani, R. Suenaga, J.W. Koo and J.G. Ha, "Ag surfactant effects of TiO2 films prepared by sputter deposition," *Vacuum,* vol. 86, no. 4, pp. 438-442, 2011.

[16] G. Musa, R. Vladoiu, V. Ciupina and J. JAnik, "Raman spectra of carbon thin fikms," *Journal of Optoelectronics and advanced materials,* vol. 8, no. 2, pp. 621-623, 2006.

[17] M. Veres, S. Toth, M. Fule, J. Dobranszky, L. MAjor and M. Koos, "Raman analysis of diamond like carbon films deposited onto corrosion resistant alloys used for coronary stent fabrication," *Materials Science Forum ,* Vol. %1 dari %2537-538, pp. 277-283, 2007.

[18] S. Chowdhury, M.T. Laugier and I.Z. Rahman, "Characterization of DLC coating depisited by rf magnetron sputtering," *Journal of Materials Processing and Technology,* Vol. %1 dari %2153-154, pp. 804-810, 2004.

[19] R. Paul, S.N. Das, S. Dalui, R.N. Gayen, R.K. Roy, R. Bhar and A.K. Pal, "Synthesis of DLC films with different sp2/sp3 ratios and their hydrophobic behaviour," *J. Phys. D: Appl. Phys.,* vol. 41, pp. 1-7, 2008.

[20] D. Guo, K. Cai, L..T Li, Y. Huang, Zh.I. Gui and H.S. Zhu, "Evaluation of diamond like carbon films electrodeposited on an Al substrate from the liquid phase with pulse-modulated power," *Carbon,* vol. 39, pp. 1395-1398, 2001.

[21] R.M. Dey, M. Pandey, D. Bhattacharyya, D.S. Patil and S.K. Kulkarni, "Diamond like carbon coatings deposited by microwave plasma CVD XPS and ellipsometric stuies," *Bull. Mater. Sci.,* vol. 30, no. 6, pp. 541-546, 2007.

[22] F.C. Marques and R.G. Lacerda, "Hardness and Stress of Amorphous Carbon Films Deposited by Glow Discharge and Ion Beam Assisting Deposition," *Brazial Journal of Physics,* vol. 30, no. 3, pp. 527-232, 2000.

[23] T. t. surface, "Coating," Northeast Coating Technology, 2015. [Online]. Available: http://www.northeastcoating.com/products/dlc-coating/coatings. [Diakses 15 January 2015].

[24] N. Paik, "Raman and XPS studies of DLC films prepared by a magnetron sputter-type negative ion source," *Surface and Coating Technology,* vol. 200, pp. 2170-2174, 2005.

[25] X. Fan, K. Nose, D. Diao and T. Yoshida, "Nanoindentation behaviors of amorphous carbon films containing nanocrystalline graphite and diamond clusters prepared by radio frequency sputtering," *Applied Surface Science,* vol. 273, pp. 816-823, 2013.

[26] A. Lazauskas, V. Grigaliuns, S. Meskinis, F. Ecarla and J. Baltrusaitis, "Surface morphology, cohesive and adhesive properties of amorphous hydrogenated carbon nanocomposite films," *Applied Suraface Science,* vol. 276, pp. 543-549, 2013.

[27] X. Yan, T. Xu, G. Chen, Sh. Yang and H. Liu, "Study of structure, tribological properties and growth mechanism of DLC and nitrogen-doped DLC films deposited by electrochemical technique," *Applied Surface Science,* vol. 236, pp. 328-335, 2004.

[28] C.K.Park, S.M. Chang, H.S. Uhm, S.H. Seo and J.S. Park, "XPS and XRR studies on microstructures and intrfaces of DLC films deposited by FCVA method," *Thin Solid Films,* Vol. %1 dari %2421-421, pp. 235-240, 2002.

[29] M.H. Ahmed, J.A. Byrne and J. McLaughlin, "Evaluation of glycine adsorption on diamond like carbon (DLC) and fluorinated DLC deposited by plasma-enhanced chemical vapour deposition (PECVD)," *Surface and Coating Technology,* vol. 209, pp. 8-14, 2012.

[30] P.L.Wong, F. He and X. Zhou, "Interpretation of the hardness of worn DLC particles using micro-raman spectroscopy," *Tribology International,* vol. 43, pp. 1806-1810, 2010.

[31] M.H. Ahmad, J.A. Byrne, J.A.D. Mclauglin, A. Elhissi and W. Ahmed, "Comparison between FTIR and XPS characterization of amino acid glycine adsorption onto diamond like carbon (DLC) and silicon doped DLC," *Applied Surface Science,* vol. 273, pp. 507-514, 2013.

[32] M. Wang, Y. Zhao, R. Xu, M. Zhang, R.K.Y. Fu and P.K. Chu, "Direct formaation of amine functionality on DLC films and surface cyto-compatibility," *Diamond & Related Materials,* vol. 38, pp. 28-31, 2013.

[33] J.Filik, P.W. May, S.R.J. Pearce, R.K. Wild and K.R. Hallam, "XPS and laser raman analysis of hydrogenated amorphous carbon films," *Diamond and Related Materials,* vol. 12, pp. 974-978, 2003.

[34] M. Yang, M.J. Marino, V.J. Bojan, O.L. Erylmaz, A. Erdemir and S.H. Kim, "Quantification of aoxygenated species on a diamond-like carbon (DLC) surface," *Applied Surface Science,* vol. 257, pp. 7633-7638, 2011.

[35] J. Cui, L. Qiang, B. Zhang, X. Ling, T. Yang and J. Zhang, "Mechanical and tribological properties of Ti-DLC films with different Ti content by magnetron sputtering technique," *Applied Surface Science,* vol. 258, pp. 5025-5030, 2012.

Chapter 5

Electrochemical Deposition of Nickel and Copper on Woodceramics

5.1 Introduction

Electrochemical deposition or electroplating are the method of provide a metal coating layer onto metal surface or other surface of materials. This is a process that has been used in various industries. The electrochemical deposition is including variety technique and physic principle, including chemistry, physics, metallurgy, and electrical engineering. This method are apply electric current to the solution of metal to dissolved metal cations after this process layer of metal form to coating on surface of coating product. The concept of plating also used for electrical oxidation of anions onto a body of substrate materials. The principle of process is primarily used to change the appearance surface and the properties of sample (e.g. adhesion and wear resistance, corrosion resistance, tribology, aesthetic qualities, etc.), however, the process also suitable for to increasing the thickness on undersized parts or to form objects by electrochemical deposition [1, 2]. Electrochemical depositions with different operation parameters such as solution temperature, pH and electric density have potential to produce different kinds of deposited structure [3]. The basic concepts of electrochemical deposition consists of cathode (negative polarity), anode (positive polarity), a power supply unit and an electrolyte as shown in Figure 5.1. The main apparatus and procedure are drop sample in a metal solution which is called electrolyte. Cathode, acting as the melt metal ions in the electrolyte solution and reduced between the interface of solution and the cathode, such that they starting to plating onto the cathode. The action of metal coating which is function to the anode dissolved and the rate at which the cathode is plated. This concept explain that the ions in the metallic solution bath are continuously replenished by anode side. The electrochemical deposition is generally a single metallic element. In addition cyanides and non-metal
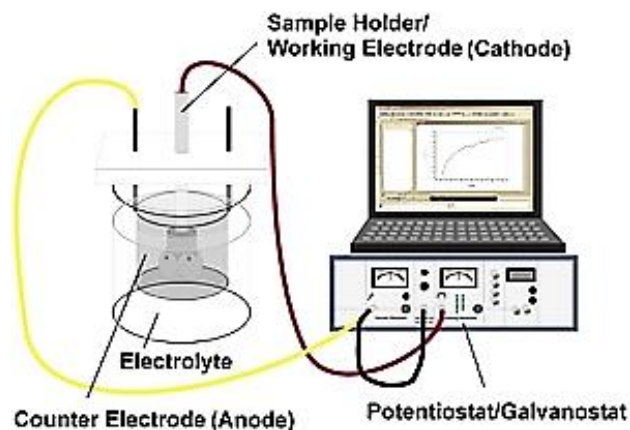
Figure 5.1 Schematic process of electrochemical deposition [5].

In addition, some technique such as carbonates and phosphates possibility to added for improve the electric conductivity [4]. The main purposes of electrochemical deposition are:

- o   Improvement the appearance of sample.
- o   Surface protection.
- o   Addition special surface properties.
- o   Engineering or mechanical properties.

Basic properties of copper is a ductile metal with very high thermal and great electrical conductivity.   [6]. The electrochemical deposition of copper is one technique to fabricate a layer of copper on the substrate surface. Base on that properties as higher current, the hydrogen bubbles will form on materials to be plated, leaving surface imperfectly. In generally, they have variety of chemicals technique are apply to improve plating uniformity or improve bright properties. Lacking of some form of additive, it is almost difficult to generate a smoothly coating surface. These addition process can be anything from dish soap to proprietor element compounds [7].

Nickel material is a silvery-white lustrous metal that have slight golden tinge and have great physical properties such as hardness and ductile properties. The nickel material are used in many application industrial and consumer products, including stainless steel, alnico magnets, coinage, rechargeable batteries, electric guitar strings, microphone capsules, and special alloys. It is also used for plating and as a green tint in glass [8]. Nickel electroplating is simple coating process to generate a thin layer of nickel onto a

substrate surface. The layer of nickel can be decorative, improve corrosion resistance, wear resistance, or be used to build up worn or increase thickness parts for recover original surface [9].

The use of eco-material such as woodceramics has become a matter of increasing interest in the recent year. Various attempts have been made to utilize the high efficiency of woodceramics.

In this chapter I explore the application of woodceramics by electrochemical deposition of nickel or copper layers on woodceramics originating from Thai rubber tree wood was attempted. The film's layer structure and morphology were examined by X-ray diffraction and scanning electron microscopy. The mechanical strength of woodceramics after deposited with nickel or copper were investigated by the compression test. Finally, the practical application of woodceramics with deposited with nickel or copper will be discussed.

5.2 Experimental Procedure

The substrate material that is used in metallic deposition is woodceramics, which is fabricated from biomass charcoal originated from Thai rubber trees wood. The fabrication details are 40 percentage of phenolic resin to biomass charcoal in weight fraction and carbonized at $1000\,^{\circ}\mathrm{C}$ as detailed in Chapter 1. The specimens are prepared in rectangular shape in dimensions of 10 mm. x 10 mm. x 20 mm. The specimens were cleaned with an ultrasonic cleaner equipment for remove dust and oil from the surface, then put in a dryer machine at 60° holding time 120 minutes.

The electrochemical process used in this study involved two kinds of metallic elements copper, and nickel. The electrolyte of both metals is in the formulas $CuSO_4$ (copper sulfate) and $NiSO_4$ (nickel sulfate). The sulfate solution concentration was decided at 10% and 20% which were used in this study. Anode and cathode in the electrochemical deposition process are connected to an external power supply of direct current of electricity. The anode connected to positive of power supply, and the cathode is connected to woodceramics. Switched on the power , the metal starting to oxidized to form cations with a positive charge as shown in Figure 5.2.

The main parameter for electrochemical deposition of nickel and copper has direct relation to the thickness and surface properties. The control parameters were as follows in Table 5.1. The deposition times used in this studies were 30 minutes and 60 minutes.
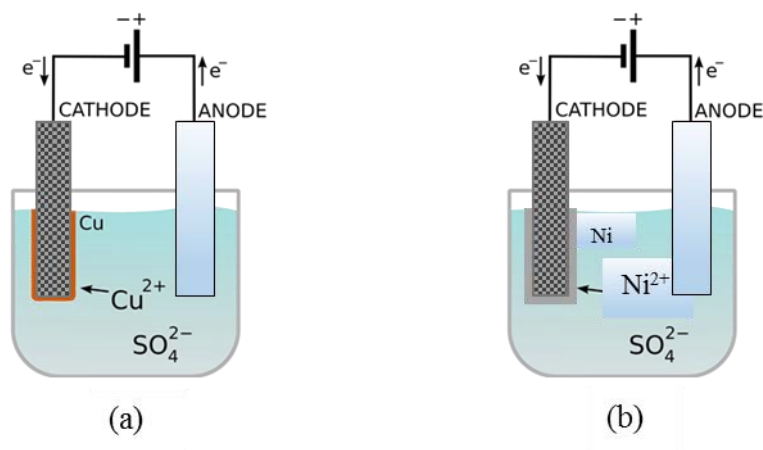

Figure 5.2 Schematic process of electrochemical deposition of (a) copper plating, and (b) nickel plating.

Figure 5.3 Photograph process of electrochemical deposition of copper.

Table 5.1 Operating condition of electrochemical deposition for copper and nickel.

Parameters	Level
Temperature (°C)	40-65
Cathode current density (A/cm^2)	0.02-0.1
pH	3.0-4.5

The current density for electrochemical deposition was kept at 0.02 A/cm^2, and concentration of the solutions as well as deposition time were varied. This is comparable to a galvanic cell acting in reverse. The specimen to be coating is the cathode of the circuit. In this concept, the anode is made of the metal to be plated on the specimen. All components are drop under the solution called an electrolyte that allow the flow of electricity as shown in figure 5.3. The metallic powders that were used in this research are copper (II) sulfate penthahydrate ($CuSO_4 \cdot 5H_2O$), 99.5% of purity) and nickel (II) sulfate hexahydrate ($NiSO_4 \cdot 6H_2O$), 99% of purity were purchased from KANTO Chemical Co.Inc. X-ray diffraction measurements were used to investigated the crystal structure of samples before and after deposition, using a Rigaku Ultima IV (Cu-Kα radiation (wave length of 1.541 Å) at 40kV and 45mA) at room temperature. The scanning electron microscope (SEM) made by a KEYENCE company model VE-9800, was used to investigate the surface morphology of specimens. A compression test is used to evaluate the mechanical properties of woodceramics after deposited with copper and nickel respectively.

5.3 Results and discussion

Woodceramics after electrochemical deposition process contain the same colors as the original metallic coating. The nickel deposited surface on woodceramics have flat and smooth surface appearance. The copper deposited surfaces have high deposition rate and have consistent surface thickness as shown in Figure Figure 5.4.
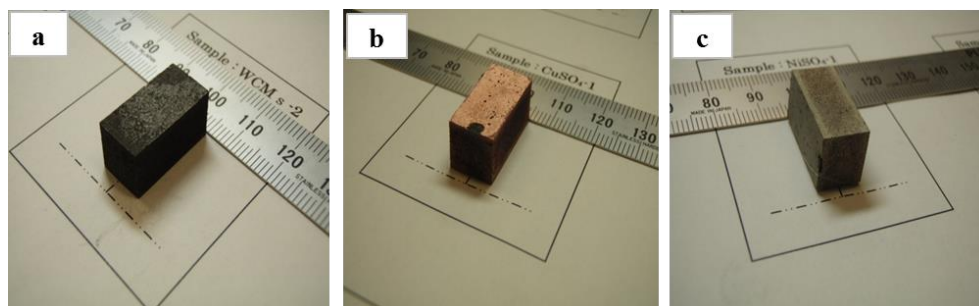
Figure 5.4 The photographs of specimens (a) before deposition, (b) after deposition with copper, and (c) after deposition with nickel.
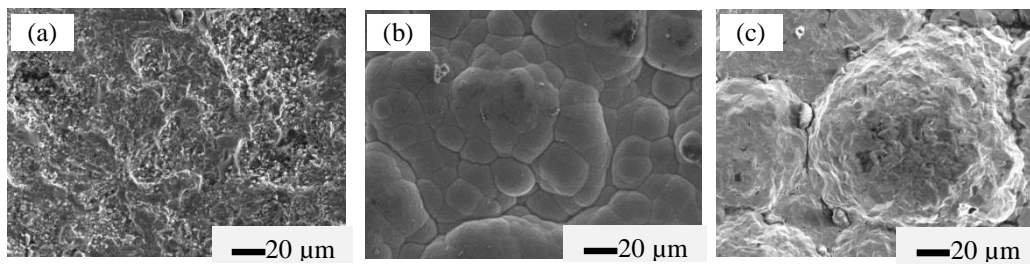
Figure 5.5 SEM micrographs of coated surface with various metallic and deposition time at sulfate solution concentration in 20% (a) without deposition , (b) NiSO$_4$ deposition time 60 min. and (c) CuSO$_4$ deposition time 60 min.

CuSO$_4$ 10%, 30min.   CuSO$_4$ 20%, 30min.   CuSO$_4$ 20%, 60 min.
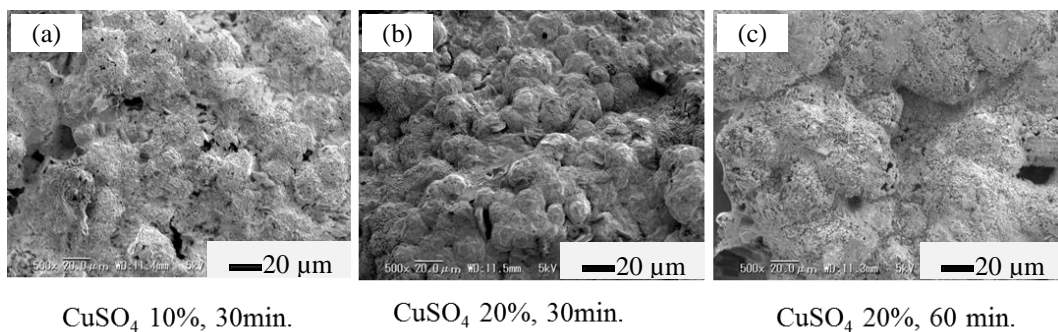
Figure 5.6 SEM micrographs of coated surface with various metallic, deposition time, and sulfate solution concentration (a) CuSO4 10% deposition time 30 min. , (b) CuSO4 20% deposition time 30 min. and (c) CuSO4 20% deposition time 60 min.

5.3.1 Scanning electron microscope (SEM)

The scanning electron microscopic micrographs of specimen surface are shown in Figure 5.5 for, (a) original woodceramics without deposition, (b) suraface after deposited with nickel sulfate with 20% of concentration solution for 60 minutes, and (c) copper deposited surface with the same deposition parameters. The SEM results indicated that nickel surfaces contain smaller grain sizes that support obtaining a smooth surface after deposition. However, the copper surface confirmed that large grain size that comes from copper is very easy to increase the deposition rate on the woodceramics surface. The layer of both metallic elements slightly increased with increased deposition time and concentration of nickel or copper sulfate solution. Figure 5.6 shows micrographs for the ssample for different of solution concentration and

deposition time. With an increasing concentration of copper sulfate, the thickness of
the copper layer slightly increased, and at the same concentration increasing deposition
time also directly affected to the thickness of the copper layer. The electrochemical
deposition fills in the elements in pores of woodceramics.

5.3.2 X-ray diffraction (XRD)

XRD patterns of woodceramics surfaces after deposition in 20% contration of nickel
sulfate for 60 minutes was shown in Figure 5.7. The result reported that many broad
peaks corresponding to nickel crystalline structure. The strong peak occurred at $2\theta =$
44.52, 51.92, and 76.4 which corresponding to the nickel littice planes (111), (200) and
(220) respectively [10, 11]. The XRD pattern of woodceramics surfaces after being
deposited in copper sulfate with 20% concentration, deposition time of 60 minutes was
shown in Figure 5.8. The three broad strong peaks corresponding to copper crystalline
structure. The strong peak occurred at $2\theta =$ 43.46, 50.58, and 74.24 which
corresponding to the copper planes (111), (200) and (220) lattice planes of the cubic
copper phase respectively [12].
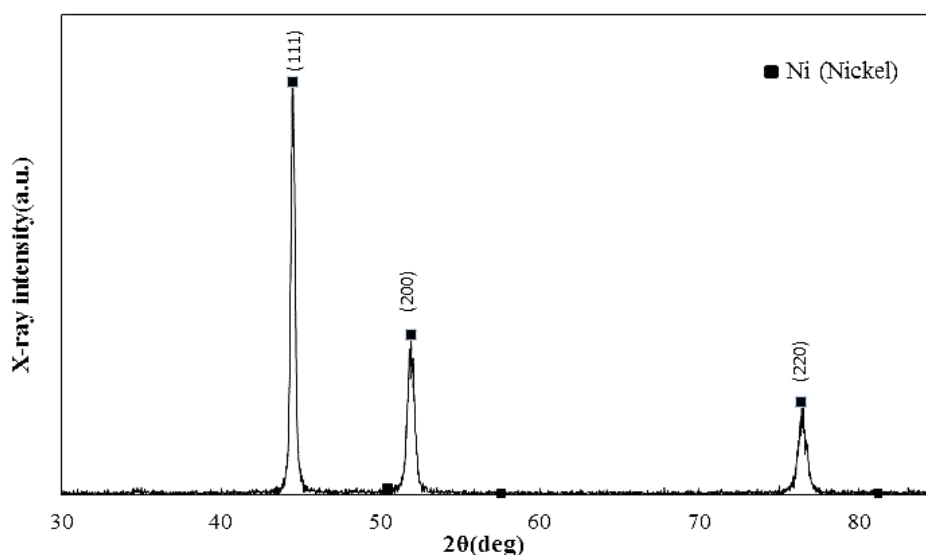
Figure 5.7 X-ray diffraction patterns of electrochemical deposition in $NiSO_4$, 20%
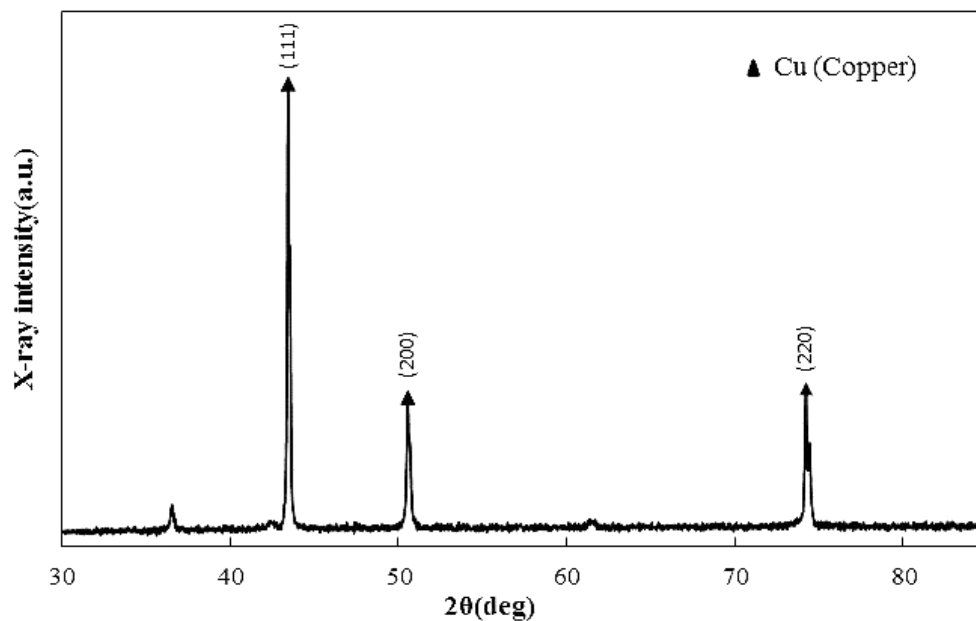concentration solution and deposition time 60 minutes.

Figure 5.8 XRD patterns of woodceramics after electrochemical deposition in CuSO$_4$ 20% concentration solution and deposition time 60 minutes.
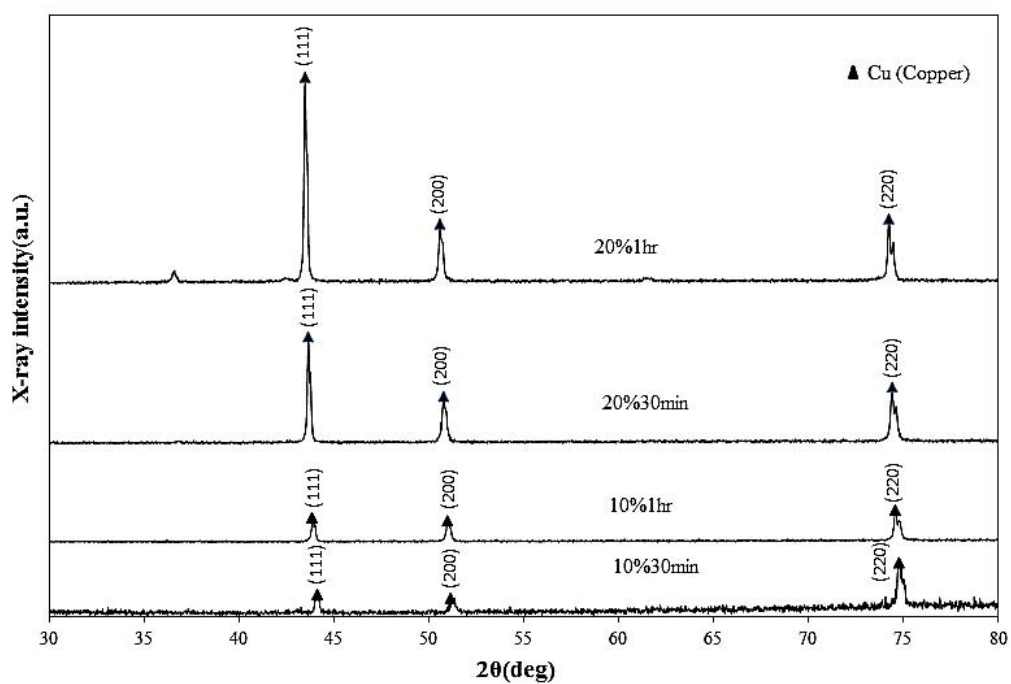

Figure 5.9 X-ray diffraction patterns of woodceramics electrochemically deposited in CuSO$_4$ solution with different concentrations (10 % and 20 %) for 30 min and 60 min.

The X-ray diffraction patterns of woodceramics deposited electrochemically in $CuSO_4$ solution with different concentrations (10 % and 20 %) for 30 min and 60 min are shown in Figure 5.9. Even for shorter deposition time, diffraction peaks can be labeled as Cu, and no graphite peaks due to the woodceramics can be identified. The intensities of diffraction peaks corrsponding to Cu increase when increasing concentration of the solution as well as deposition time. Higher concentration and longer deposition time are effective to produce thicker deposition layers, although optimization is needed (a weak peak observed after 60 min in 20 % $CuSO_4$ solution is probably due to a contamination as mentioend earlier).

For both woodceramics, the strongest three diffraction peaks can be labeled as either Ni or Cu (crystal structure of Ni and Cu is fcc), although a weak peak, probably due to a contamination, is observed at about 36 degree after deposition in $CuSO_4$ solution. It is found that Cu or Ni layers are successfully deposited on the woodceramics samples. No graphite peaks can be identified, while the woodceramics consist of a graphite-like structure whose actual structure is a turbostratic one, in which the stacking distance of carbon layers are random. This means that the deposited layers were thick enough that the X-ray beam did not penetrate the woodceramics beneath the metallic layers [13]. The mass gains after deposition for 60 minutes measured by a balance were about 0.36 g and 0.45 g in $NiSO_4$ and $CuSO_4$ solutions, respectively (corresponding coating rates are about 6.0 mg/min and 7.5 mg/min respectively).

5.3.3 Mechanical properties

Although the maximum compressive strength of woodceramics before electrochemical deposition as shown in Figure 5.10 are about 28 MPa, those after deposition in $NiSO_4$ and $CuSO_4$ are 40 MPa and 35 MPa respectively. On the other hand, the strain to failure for the woodceramics after deposition in $NiSO_4$ and $CuSO_4$ are about 0.1 and 0.12 respectively, while before deposition are 0.07. The electrochemical deposition improved compression properties of the woodceramics that have brittle nature. It was found that the compressive strength increased while increasing concentration of the solutions and deposition time.
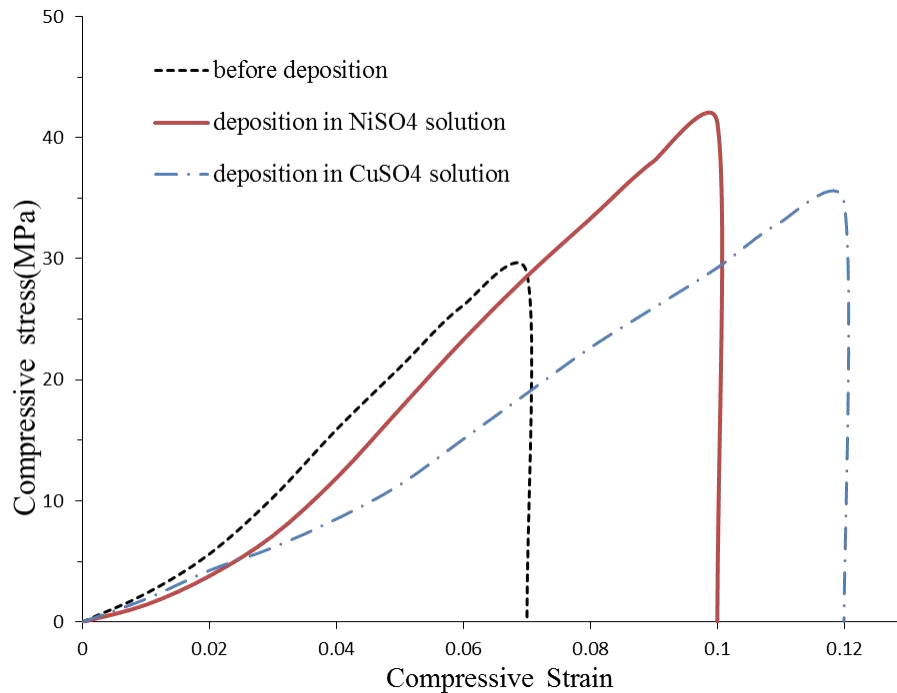
Figure 5.10 Comparison of compressive strength with various surface modification for woodceramics before and after deposition in $NiSO_4$ and $CuSO_4$.

(a)   (b)
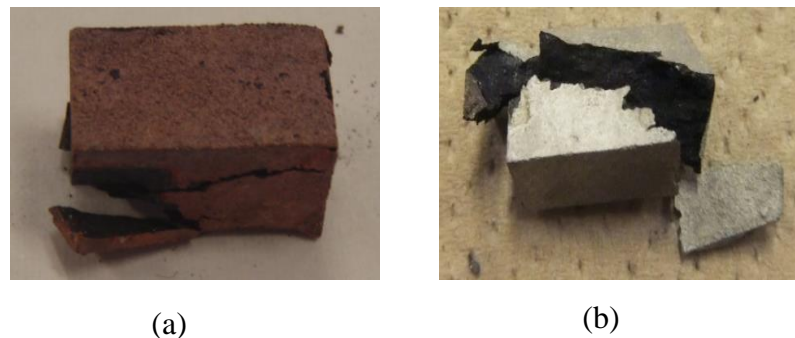
Figure 5.11 Photograph of fracture regions of the tested specimens (a) $CuSO_4$ deposition, and (b) $NiSO_4$ deposition .

The appearance of fracture regions of woodceramics after electrochemical deposition in copper sulfate and nickel sulfate were shown in Figure 5.11. Based on the fundamentals that coating materials like nickel have high hardness and mechanical strength compared with copper, we look at the cracking regions through the core of a specimen [14]. In other words, woodceramics deposited in copper sulfate have not completely broken in to small pieces, that has a functional effect with the fundamental

properties of copper having high plastic deformation, low impact strength, and high stiffness properties [15].

5.4 Conclusion

Nickel (Ni) or copper (Cu) layers could be deposited on woodceramics by electrochemical deposition in either $NiSO_4$ or $CuSO_4$ solution. Thicker metallic deposition layers were produced after longer deposition time in higher concentration of the solution. The mass gains after deposition for 60 min were about 0.36 g and 0.45 g in $NiSO_4$ and $CuSO_4$ solutions (concentration was 20 %). The maximum compressive strengths for the woodceramics in $NiSO_4$ and $CuSO_4$ solution (concentration was 20 %) were 45 MPa and 35 MPa, respectively, while that before the deposition it was about 28 MPa. The compressive stress of the samples increased with increasing concentration of the solutions and coating time.

It is believed that electrochemical deposition changes the chemical, physical, and mechanical properties of the workpiece. Furthermore, nickel deposition would improve corrosion resistance.

References

[1] Wikipedia, "Electroplating," Wikmedia Foundation, 10 November 2014. [Online]. Available: http://en.wikipedia.org/wiki/Electroplating. [Diakses 26 November 2014].

[2] M. Paunovic and M. Schlesinger, Fundamentals of Electrochemical Deposition, USA: A John Wiley & Sons, Inc. Publication, 2006.

[3] Ch. R.K. Rao and D.C. Trivedi, "Chemical and electrochemical depositio of platinum group metals and their application," *Coordination chemestry reviews,* vol. 249, pp. 613-631, 2005.

[4] N. W. E. contributors, "Electroplating," New World Encyclopedia, 17 September 2013. [Online]. Available: http://www.newworldencyclopedia.org/entry/Electroplating. [Diakses 12 January 2015].

[5] C. Moseke, "Biointerface Engineering," FMZ University of Würzburg, 7 January 2015. [Online]. Available: http://www.fmz.uni-

wuerzburg.de/index.php?show=research_engineering&lang=en. [Diakses 12 January 2015].

[6]   "Copper," Wikipedia website, 8 December 2014. [Online]. Available: http://en.wikipedia.org/wiki/Copper. [Diakses 10 January 2015].

[7]   Wikipedia, "Copper plating," Wikipedia, 24 November 2014. [Online]. Available: http://en.wikipedia.org/wiki/Copper_plating. [Diakses 12 January 2015].

[8]   "Nickel," Wikipedis, 10 January 2015. [Online]. Available: http://en.wikipedia.org/wiki/Nickel. [Diakses 12 January 2015].

[9]   Wikipedia, "Nickel plating," Wikipedia, 24 August 2014. [Online]. Available: http://en.wikipedia.org/wiki/Nickel_electroplating. [Diakses 12 January 2015].

[10]   D. William and Jr. Callister, Materials Science and Engineering an Introduction, 3rd Ed., New York, United State: John Wiley and Sons, Inc., 1994, Print..

[11]   N.D. Nikolic, Z. Rakocevic, D.R. Durovic and K.I. Popov , "Reflectio and structural characteristics of semi-bright and mirror bright nickel coating," *J.Serb.Chem.Soc,* vol. 67, no. JSCS-2964, pp. 437-443, 2002.

[12]   A.Rittermeier, Sh. Miao, M.K. Schorter, X. Zhang, M.W.E. Van Der Berg, Sh. Kundu, Y. Wang, S. Schimpf, E. Loffler, R. A. Fischer and M. Muhler, "The formation of colloidal copper nanoparticles stabilized by zinc stearate: one-pot single-step synthesis and characterization of the core–shell particles," *Phys.Chem.Chem.Phy.,* vol. 11, pp. 8358-8366, 2009.

[13]   A. Takasaki, D. Kaewdook and T. Okabe, "Electrochemical Metallic Deposition on Woodceramics Originated from Biomass," dalam *The 11th Intrnational Conference on Eco-materials (ICEM-11)*, Hanoi, Vietnam, 2013.

[14]   L. Alchin, "Nickel Properties," 21 June 2014. [Online]. Available: http://www.elementalmatter.info/nickel-properties.htm. [Diakses 12 January 2015].

[15]   L. Collini, "Mechanical Properties of Copper Processed by Severe Plastic Deformation," dalam *Copper Alloys - Early Applications and Current Performance -*, Croatia, In Tech , 2012, pp. 93-126.

Chapter 6

Concluding Remarks

6.1 Conclusions of this research work

Thailand is a middle income country where having agriculture is instrumental to economic development. Biomass from agricultural residue in Thailand is an important topic to discuss. Four major sources of biomass in Thailand are rice husk/straw, sugar cane, oil parm, and wood waste. The natural rubber trees in Thailand are the main source of biomass from wood waste. The productive life period of rubber trees on plantations is less than 25 years. Old trees are no longer useful and need to be cut away in order to facilitate the growth of new plants. This is the main cause of the increased volume of biomass residue from natural rubber life cycle. Melamine formaldehyde is one of the thermosetting plastics that is widely used in kitchenware in Thailand. The waste from melamine formaldehyde cannot be remelted and therefore the recycling process requires high costs for burning and a lot landfill space, resulting in a serious environmental problem. To address this problem we propose three techniques to fabricate woodceramics and composites resulting from biomass and used melamine formaldehyde. In what follows we summarize these techniques to fabricate environmentally friendly materials in Thailand.

Production of Amorphous Carbon Films using woodceramics.

Amorphous carbon (a-C) thin films are diamond-like carbon (DLC) films with notable physical properties such as high surface scratch resistance, low friction coefficient, and optical transparency. The a-C films have applications in the industry, for instance, as a coating for improvement of electron field emission. Using woodceramics to fabricate a-C films offers enormous potential to reduce operation costs.

Electrochemical Deposition of Ni and Cu on Woodceramics

Woodceramics is a carbon-based hybrid material made of amorphous carbon and glassy carbon. Compared to other composite materials woodceramics exhibits increased performance against abrasion, suitable values of specific heat and heat absorption, high specific surface area, porosity and lightness. The properties of woodceramics can be enhanced by electrochemical deposition with nickel and copper. As a result, compressive strength increases and protection against corrosion improves. A wide range of applications in industry might benefit from using these materials, like fabricating high wear resistant components.

Eco-composite from biomass charcoal and used melamine formaldehyde

Current environmental concerns urge us to design new eco-composite materials that offer mechanical and functional performance. We also need to design materials that are harmless to the environment. Eco-composites are recyclable materials resulting from biomass charcoal powder waste from melamine formaldehyde and phenolic resin. We anticipate a favorable cooperation with companies specializing in melamine formaldehyde products in Thailand.

6.2 Future Works

A next stage of this work would focus on developing new applications for woodceramics and extending the use of raw materials to fabricate woodceramics using different agricultural wastes found in Thailand. Nonetheless, there are some additional considerations to assess in the future, as follows.

The specific surface area of woodceramics increases with porosity. Therefore, for filtering applications, as in municipal waste water treatment processing or in heavy industries, it will be necessary to characterize the specific surface area of woodceramics. The characterization of thermal conductivity would help to guide the design of woodceramics suitable for applications such as heat plates, heat exchanger parts, etc. Porous materials such as woodceramics absorb acoustic waves by means of suppressing and dissipating mechanical waves through these materials. Full characterization of the

acoustic properties will help to design sound proof materials relevant to the construction industry. Proper measurement and characterization of the coefficient of friction (COF) of woodceramics is necessary as well. Wear due to mechanical interactions between surfaces and deformation of surface material as a result of mechanical friction between surfaces is a concern that needs to be addressed to design self-lubricating materials based on woodceramics.

Finally, in Thailand, there are other materials that can be used to fabricate woodceramics. A natural extension of this work would include a variety of raw materials, such as rice straw, rice husk, bagasse, corn, among others.

Appendix

Fabrication of Eco-Composite using charcoal from biomass

Introduction

In the concept of composite materials, most of materials science and engineers have designed to combine variety of metals, ceramics, and polymers to create a new innovation of extraordinary materials. Many kind of composites have been supported to improve all of mechanical properties such as high stiffness, high toughness, and ambient and high temperature resistance. A composite is a multiphase material. One simple scheme for the classification of composite materials is shown in Figure 1, which consists of three main types; particle reinforced, fiber reinforced, and structural composite. Usually, composite materials are composed of the matrix, which is continuous and surrounds the other phase, often indicated in the name of dispersed phase as shown in Figure 2. The physical and mechanical properties of composites materials are a function of the constituent phase, their relative amounts, and the geometry of the dispersed phase [1]. The most important feature of composite materials is that they can be designed and tailored to meet different requirements. As a term, ''eco-composite'' is usually used to describe composite material having environmental and ecological advantages over conventional composites [2].

By definition, an eco-composite may contain natural fiber (NF) and natural polymer. A number of composite materials have been engineered that consist of more than one material type. Many of the recent material developments have involved composite materials [3]. However, in the last period of the composite-materials development only mechanical and functional performance were taken into account in the design and processing.
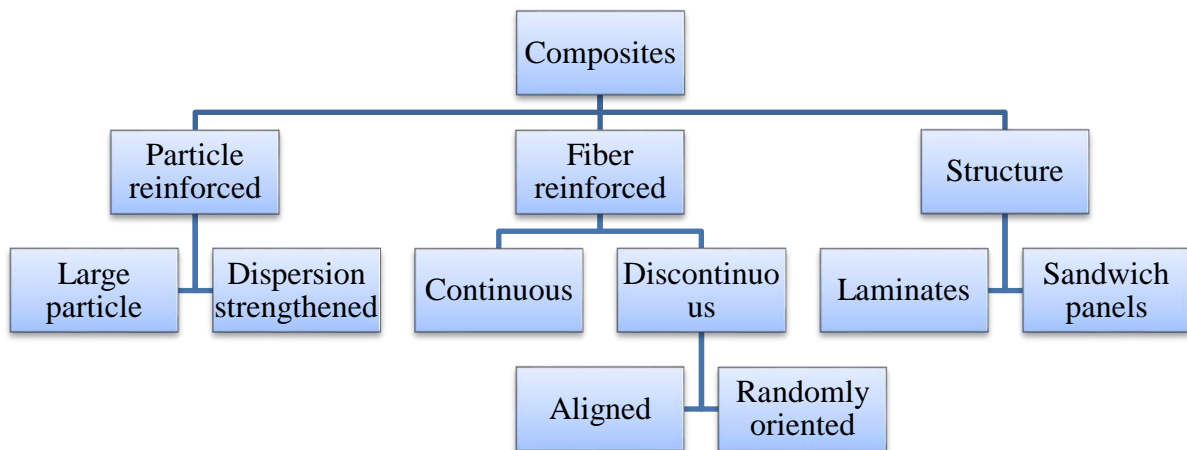
Figure 1 A classification diagram of composite materials.
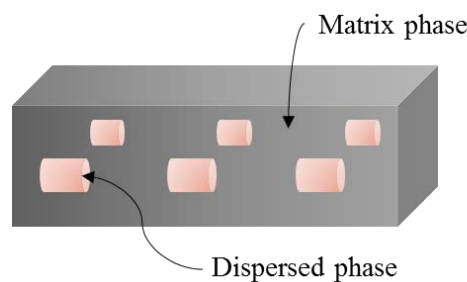
Figure 2 Fundamental phase of composite material.

The idea to fabricate eco-composite materials using biomass charcoal from rubber tree wood and used melamine as reinforcement is shown in Figure 3. This is attractive from the view point of cost and recycling. These advantages include high strength, low weight and low environmental effects. In addition, by using the waste of melamine formaldehyde and biomass charcoal from agricultural residue as reinforced composite can save raw material cost for manufacturer.

Figure 3 Particulate reinforced ecocomposite material system.

Thailand is an agricultural country and a leading producer of crops for exporters, thus the biomass situation in Thailand has continuously increased as mentioned in Chapter 1. The natural rubber plantation area in Thailand has increased more in the last decade since the government launched its planting project. The country also has high potential for expanding the production area and raising production capacity [4]. The natural rubber trees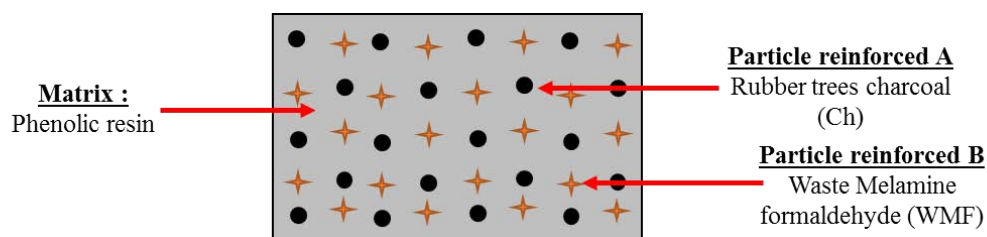 have an economic life less than 25 years, afterwards farmers will cut them down in preparation for the new plant as detailed. The by-product is wood to be supplied to the wood industry. Only the main stem part of rubber trees can be used as an economic wood product. The biomass from rubber trees comes from roots, branches, and leaves. In the years 2009-2012, rubber plantations in Thailand covered 27,000 km^2 [5]. Biomass from rubber tree residues provides a basic energy source for cooking and heating in rural households of traditional Thai style.

The melamine formaldehyde resin is one of the thermosetting plastics, which can not be recycled, which is made from melamine and formaldehyde by polymerization. Thermosetting materials have generally excellent hardness and high thermal resistance. Melamine formaldehyde (MF) materials are widely used in Thailand as kitchen utensils set, laminate floor products, counter bar, cabinetry, top surface coated, textile finishes, paper processing, and binder material. These are some of the application which the melamine formaldehyde have outstanding properties continued to be widely used today. The melamine production industry began in 1973. Raw materials consisted of 3 major components; melamine crystal, alpha cellulose and formaldehyde. Melamine formaldehyde resin was not able to be melted by a heating and pressure forming process

due to three dimensional networks (cross-linking). The general properties of the
melamine formaldehyde added which cellulose were shown in Table 1. The melamine
formaldehyde forming process is to compress and heat simultaneously to the desired
shape by a hot compression molding machine at suitable pressure, temperature, and
time. After formation, the melamine product is transferred to grinding and surface
finishing. During these processes scraps and waste melamine are generated and cannot
be reformed and recycled. Therefore, the disposal is usually done by landfills or burning
that leads to the environmental problems and wastage cost for disposal. It will be more
environmentally friendly if the melamine can be recycled [6, 7].

Table 1 General properties of pure melamine formaldehyde [8].

Melting Temperture	149-204 °C
Specific Gravity	1.47-1.52
Tensile Strength	34-90 MPa
Compression Strength	227-310 MPa
Hardness	M115-M125

The Phenolic resin is a polymer matrix to be used in eco- composite products. The
fundamental properties of phenolic resins provide high mechanical strength at advanced
temperatures in a various the environments and comperative with a multitude of
composite fibers and fillers. Complicated applications benefit by using phenolic resins
in the main part of composite process. The phenolic resins are composed of a wide
variety of structures based on a particular product's reaction. In this research, the
phenolic resin was used as a binder material. The phenolic resin effortlessly penetrates
and adheres to the structure of many organic and inorganic fillers and reinforcements,
which makes it an ideal candidate for variety uses application. A concise thermal
exposal to created crosslinking or thermosetting fabricated attainment of its last
properties. The excellent ability of phenolic resin to wet down and to crosslink through
the fillers and reinforcements provides the desired mechanical, thermal, and chemical
resistance properties. A main properties of thermosetting resin are have ability to
outstanding to high temperature under exterinal load with a little deformation shape. In
general, the phenolic resin propertie are provide the rigid to maintain structural integrity
and dimension stability under severe condition. For this reason, phenolic resin binders

meet the challenges of eco-composite in demand application such as house construction, friction, and machinery parts. The application advantage from the great physical preperties, as well as thermal and chemical resistance properties from phenolic resins include abrasive grinding wheels, friction liner, refractory products, and other mechanical parts used at high temperature or in aggressive environments. In recently, phenolic resin's outstanding compatibility together cellulose fillers has been applied to increase benefit of particleboard, plywood, hardboard, oriented strand board, substrates for melamine laminates, and decking applications. Composites were used for variety applications such as on oil platforms, missile components, and heat shields [9]. The phenolic resin matrix in composite materials generally have lower strength, yet have high potential in impact resistance as shown in Table 2.

Table 2 Mechanical Properties of Composites with various resin [10]

Matrix materials	Flecural strength,MPa	Elongation, %	Notched Izod, J/m
Phenolic resin	228	2	1868
Polyeaster	276	1.75	960
Vinyl ester	310	2	1227

This study is based on the premise that Thailand is the largest producer of natural rubber and a high producer of melamine formaldehyde, which makes a high potential to get raw materials for producing eco-composite. Therefore, the author chose biomass charcoal originating from Thai rubber tree wood waste, used melamine formaldehyde powder, and phenolic resin to fabricate eco-composite material to compare with pure melamine formaldehyde and phenolic resin. The aim of this study is to investigate the microstructures, physical properties and the mechanical properties such as compressive strength by X-ray diffractometry (XRD), scanning electron microscopy (SEM) and mechanical test.

Experimental Procedure

The biomass from rubber trees were cut in small pieces, put in the furnace prepared to carbonizing under oxygen control chamber at 600 °C , holding time was 4 hours to
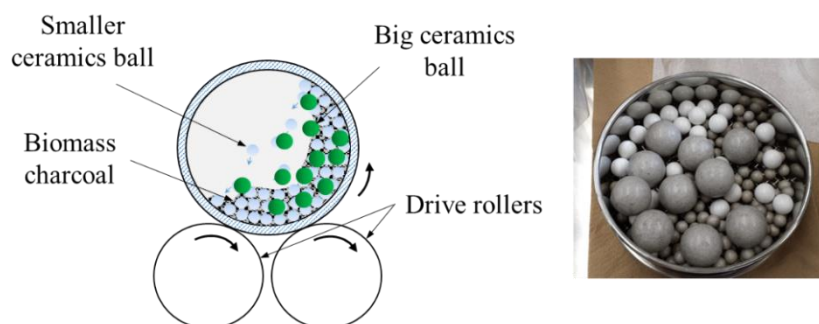
Figure 4 Mechanical crushers machine.

Figure 5 Ceramic ball mill to crush biomass charcoal into powders.

produce biomass charcoal. The biomass charcoal was broken in to small pieces by a mechanical crusher machine as shown in Figure 4. The ceramics ball mill equipment was used to crush the biomass charcoal preparing the powder in finer incriments as shown in Figure 5. The size control was particle size 250 μm by the industrial sieved equipment [11, 12].

The materials used in this study were waste melamine formaldehyde (WMF), or used melamine formaldehyde from the heat molding process in the manufacturer that is supported by the Suranaree Institute of Technology (SUT), Thailand. The prepared process was first broken into small pieces using a ball mill crushers method. These

pieces of waste melamine were again pulverized into finer powder and sieved by shakers to control particles size around 1-150 μm [7, 13].

In addition, pure melamine formaldehyde (PMF) or virgin melamine formaldehyde, whose industrial grade was ME6033 (ready to mix with cellulose and formaldehyde), was also used for comparison with their eco-composite characteristic. Also the phenolic resin was used in this study was industrial phenolic resin received from Aomori Research Institute (AITC).

In order to produce the highest mechanical properties of eco-composite with maximum weight ratio of waste melamine formalehyde and biomass charcoal from rubber trees residues, these experiments were designed to include the following six conditions in weight fraction ratio as shown in Table 3.

Table 3 Design of parameters to fabricate eco-composite.

Sample	The powder mixed in weight fraction ratio (%)			
	WMF	C	PMF	R
WMF/R=50/50	50	X	X	50
WMF/C/R=50/30/20	50	30	X	20
WMF/C/R=30/50/20	30	50	X	20
C/PMF=50/50	X	50	50	X
C/R=50/50	X	50	X	50
PMF/R = 50/50	X	X	50	50

WMF : Waste melamine formaldehyde
Ch : Biomass charcoal
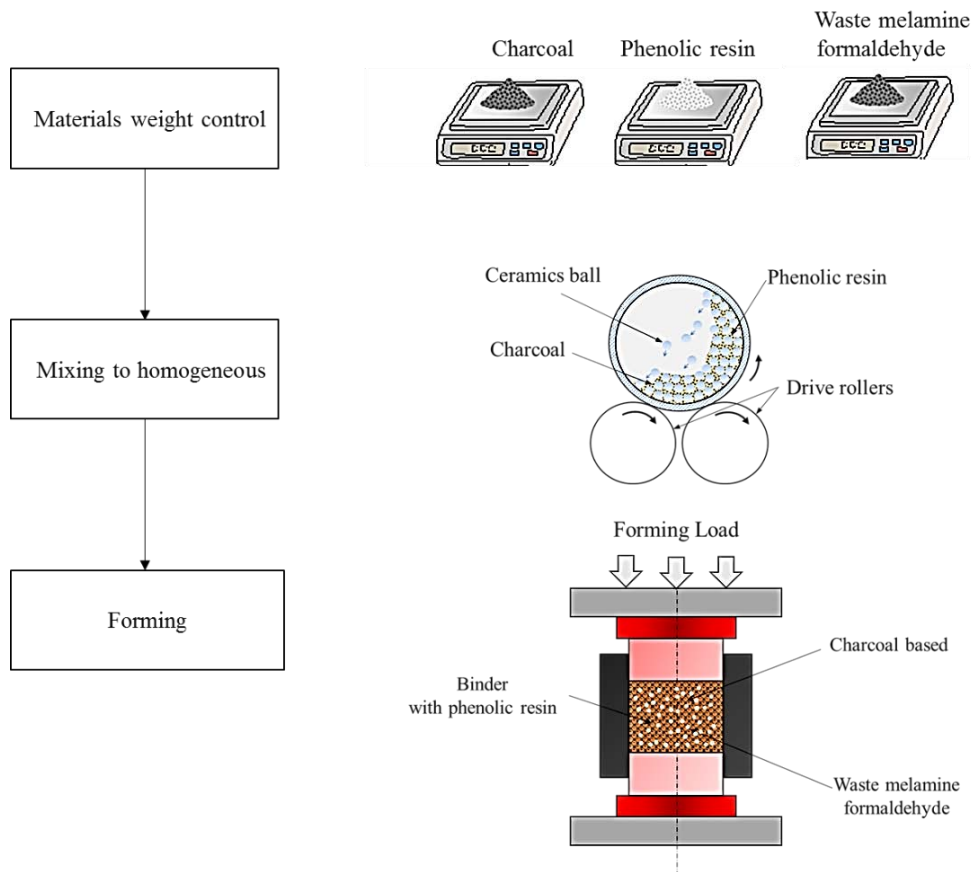PMF : Pure melamine formaldehyde
R : Phenolic resin

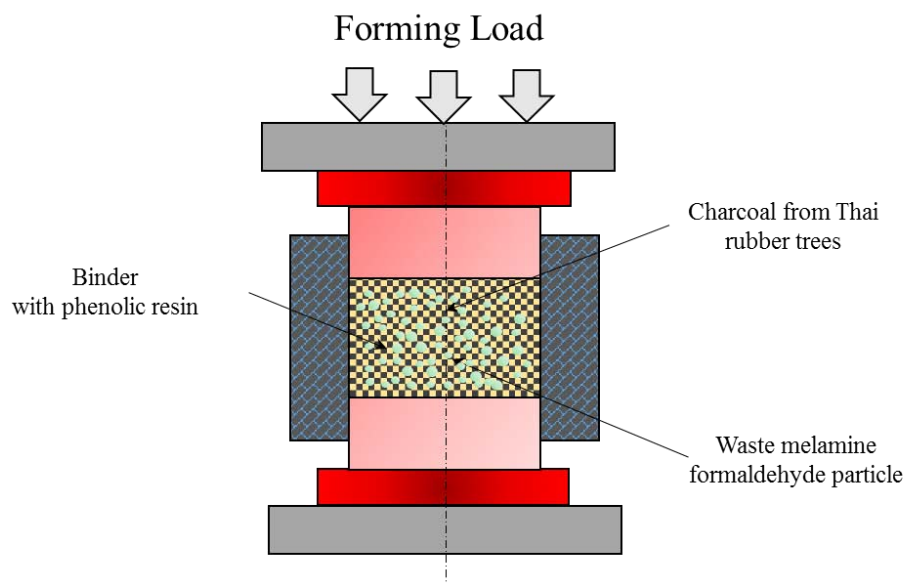Figure 6 Schematic diagram to fabricate eco-composite materials.

Figure 7 The schematic diagram of hot press molding to compaction eco-material.

The fabrication procedure's goal was to control the weight ratio following the designed weight scale. The second step was to place a sample in the dryer machine to control the humidity of sample powder at 60 °C for 120 minutes. The mixing process is very important for the properties of composite. In order to produce homogenous powders, the mixing equipment used was a ball mill jar. The compaction metod of eco-composite used was the hot press molding as shown in Figure 6. The form parameters of bulk shapes were formed by a hot compression mold at a temperature of 523 K and a compression pressure of 30 MPa for 30 min to completed melting phenolic resin to cure the particle of biomass charcoal and waste melamine formaldehyde particles as shown in Figure 7 and 8.

The particle sizes of WMF and PMF were analyzed using a particle size analyzer, a Horiba LA-950V2, which includes two light sources (He-Ne laser (632.8 nm) coupled with a beam expander and a blue monochrome tungsten lamp (405 nm). The X-ray diffraction (XRD) measurement were used by a Rigaku Ultima IV to determine crystal structures of eco-composites using Cu-Kα radiation at 40kV and 45mA at

Eco-composite specimen

Figure 8 Hot press molding to fabricate specimen.

room temperature (wave length of 1.541 Å). The surface morphology of the eco-composite was observed by a scaning electron microscope (SEM), KEYENCE VE-9800, at an accelerating voltage of 10kV. A compression test was also used that was made by a TENSILON TOYO BALDWIN SS-207-AP.

Results and discussion

The particle size distributions of pure melamine formaldehyde and waste melamine formaldehyde were measured by the particle size analyzer. The result are shown in Table 4. It is found that the mean particle size of waste melamine formaldehyde particles is smaller than that the pure melamine formaldehyde.

Table 4 Mean particle size of pure and waste melamine formaldehyde.

	Median Size (μm)	Mean Size (μm)	Standard Deviation. (μm)
Pure melamine formaldehyde	14.98	17.05	8.89
Waste melamine formaldehyde	7.89	9.39	6.41

Based on the waste melamine formaldehyde being of smaller size, this was expected to occur from the characteristic of thermosetting plastic after being forming by heating to over the melting point. Afterwords the polymer structure in micro level has been decomposed [14].

Scanning electron microscopy

The SEM results show biomass charcoal obtained after carbonizing Thai rubber tree wood and its charcoal powders, which were obtained after crushing and milling in Figure 9 (a) and (b) respectively. Although cell structures of the rubber tree still remained after burning, those were completely crushed and broken into fine charcoal powders after crushing and milling to powder.
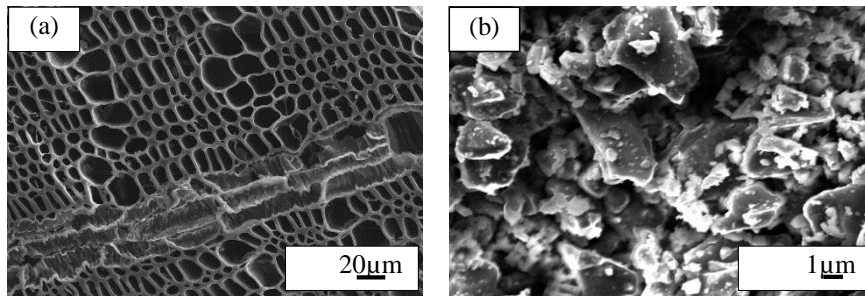
Figure 9 SEM images showing surface of biomass charcoal from rubber tree (a)
image of charcoal after carbonized and (b) after crushed with ceramics ball mills.
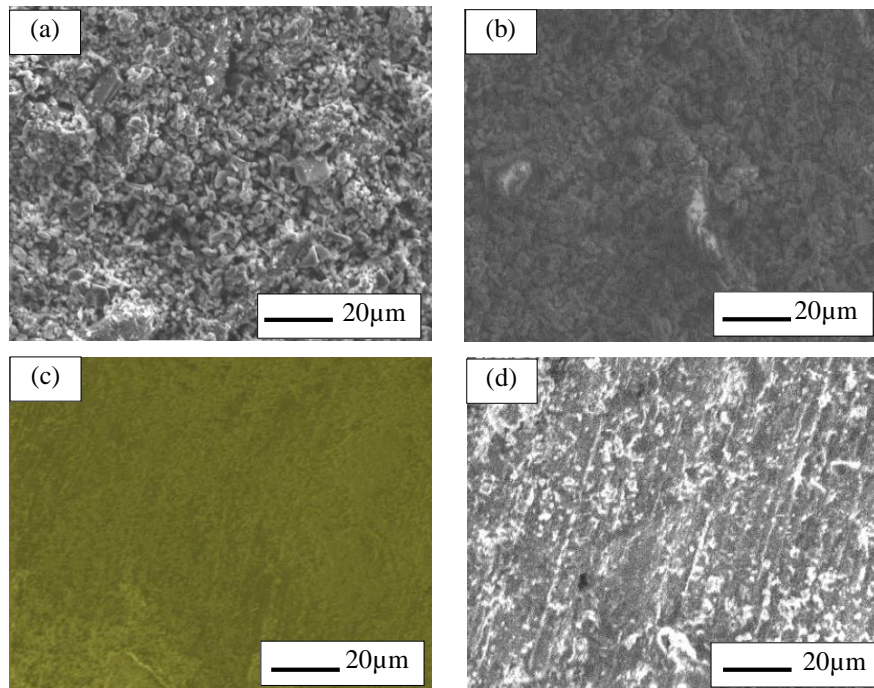
Figure 10 SEM images of microcapsules composite specimens (a) C/R=50/50, (b)
PMF/C=50/50, (c) WMF/R=50/50 and (d) WMF/C/R=50/30/20

The surfaces of eco-composites, along with various materials, and fabricated weight
fraction ratio were observed by an SEM. The SEM micrographs of the sample with the
weight fraction ratio of biomass charcoal and phenolic resin in 50/50 percentage, as can
be seen in Figure 10 (a), shows charcoal still remained inside the composite and some
particle of waste melamine formaldehyde on figure (d) because the fabrication

temperature its not enough to complete the melting of phenolic resin to cure the particle of carbon from biomass charcoal and waste melamine formaldehyde. The images of figure (b) are pure melamine formaldehyde with biomass charcoal. Here, the pure melamine formaldehyde is acting as a binder material instead of phenol resin that can see the black carbon from the biomass charcoal remaining inside. It is suggested from the forming temperature and holding time that fabricated eco-composite are not appropriate for this mixing parameter. For figure (c) particle size of WMF is very fine and the SEM images were shown to have a smooth surface. That, with the effect from the small amount of waste formaldehyde, the completed is homogeneously mixed.

X-ray diffraction

XRD was applied for determination of the degree of the eco-composite after fabricating with various weight fraction ratios. The patterns of the original materials were used to fabricate eco-composite including pure melamine formaldehyde, phenolic resin and biomass charcoal from rubber tree wood as shown in Figure 11. The pattern of pure melamine formaldehyde showed many peaks corresponding to crystalline phase of polymer composition [15].

The XRD patterns of eco-composites after fabrication are shown as Figure 12. The weight fraction ration of WMF/C/R=50/30/20, PMF/R=50/50, WMF/R=50/50, and Ch:R=50/50 are reported that after phenolic resin is cured (above 200°C) it changes to carbonaous phase. The pattern's intensity of composites show a non crystalline structure that suggests amorphous-like graphite. Due to phenolic resin change, this structure is similar to those for charcoal and phenolic resin. The XRD patterns for the composites include some strong peaks, which are due to formation of crystalline of polymers [16].
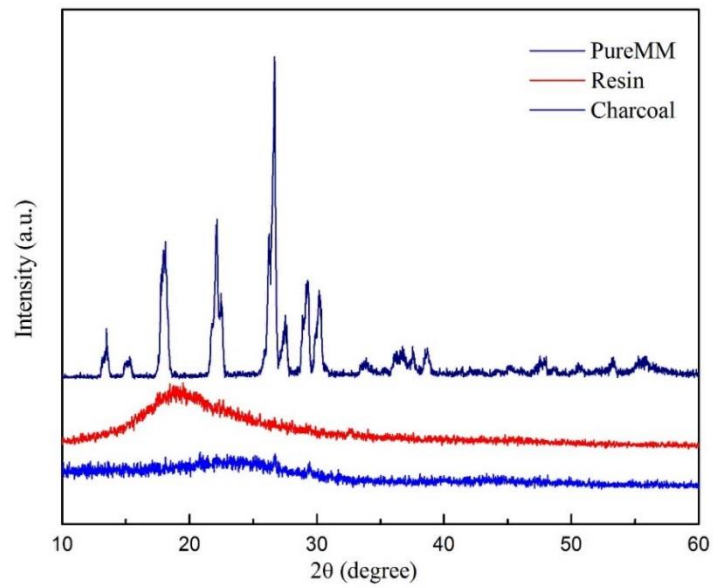
Figure 11 XRD patterns of the original material were used to fabrication eco-composite include of pure melamine formaldehyde, phenolic resin and biomass charcoal from rubber trees wood.
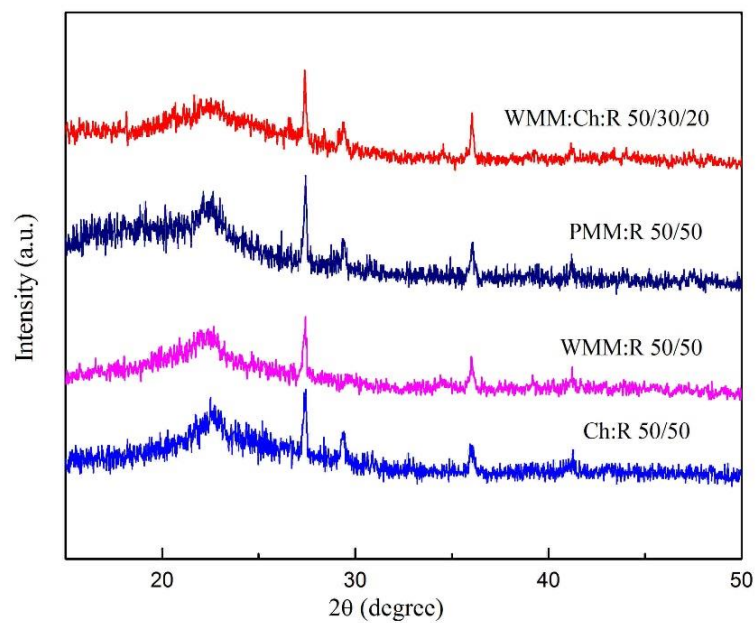

Figure 12 X-ray diffraction patterns for charcoal, phenol resin, and composites comsisted of WMF/R=50/50 and WMF/C/R=50/30/20.

Compressive strength

The compressive test was performed on four specimens, each with different compositions of eco-composite to check the deviation in compressive strength. The compressive stress and strain curves for the composites consisted of WMF/C/R=50/30/20, WMF/R=50/50, PMF/R=50/50, and Ch:R=50/50 and are show in Figure 13. It can be seen that compressive stress increased linearly with copressive strain until failure. The maximum compressive strength, 37.5 MPa, was obtained from the composite consisting of the maximum weight fraction of waste melamine formaldehyde whose ratio was WMF/C/R=50/30/20. The compressive stress of the sample mixed with waste malamine formaldehyde and phenolic resin whose ratio was WMF/R=50/50 gave 45.28 MPa as shown in Figure 14. The compressive stress of the sample mixed with pure melamine formaldehyde and phenolic resin, was about 23.75 MPa as shown in Figure 15. The compressive stress of the sample of biomass charcoal was mixed with phenolic resin giving lowest compressive strength at 11.76 MPa as shown in Figure 16. The particle reinforced materials as waste melamine formaldehyde, pure melamine formaldehyde and biomass charcoal powder have potential to increase the compressive strength of eco-composite. The waste malamine formaldehyde is thermosetting plastic that, when formed by heating, will keep solid structure and have high initial hardness. The pure malamine formaldehyde, after being forming and cued with phenolic resin also gives the results of high compressive strength compared with that of biomass charcoal mixed with phenolic rein. The key qualities of this eco-composite design concept are to use the maximum amount of waste melamine formaldehyde and biomass charcoal to increase compressive strength.

Figure 13 Compressive stress - strain curves for eco-composite whose mixture in weight fraction was WMF/C/R=50/30/20.

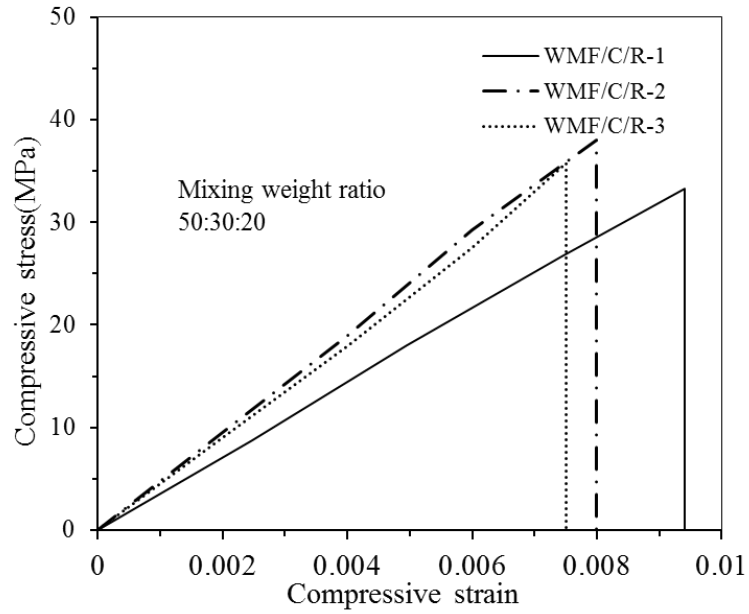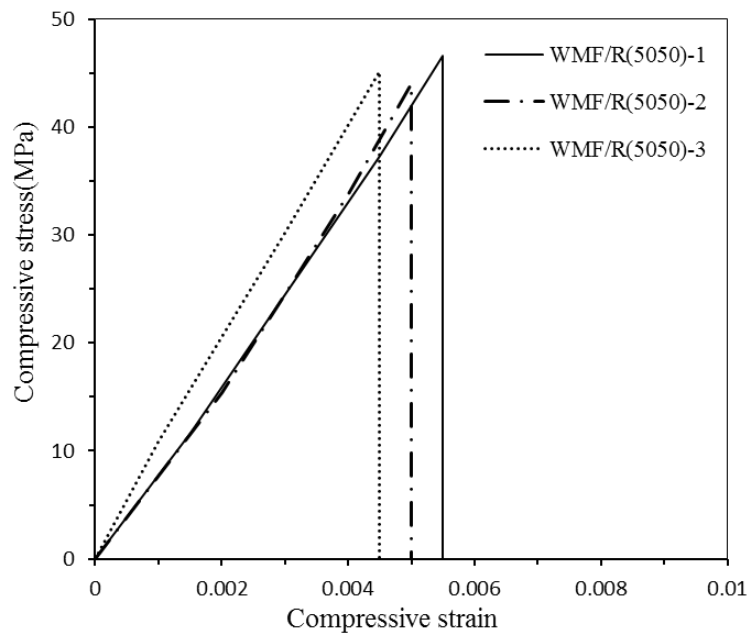Figure 14 Compressive stress - strain curves eco-composite whose mixture in weight fraction was WMF:R=50/50
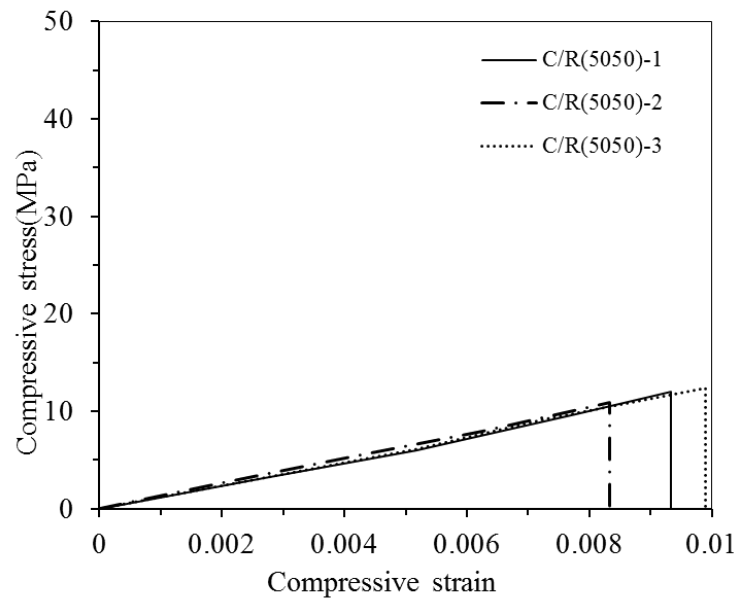
Figure 15 Compressive stress - strain curves for eco-composite whose mixture in weight fraction was PMF:R=50/50.
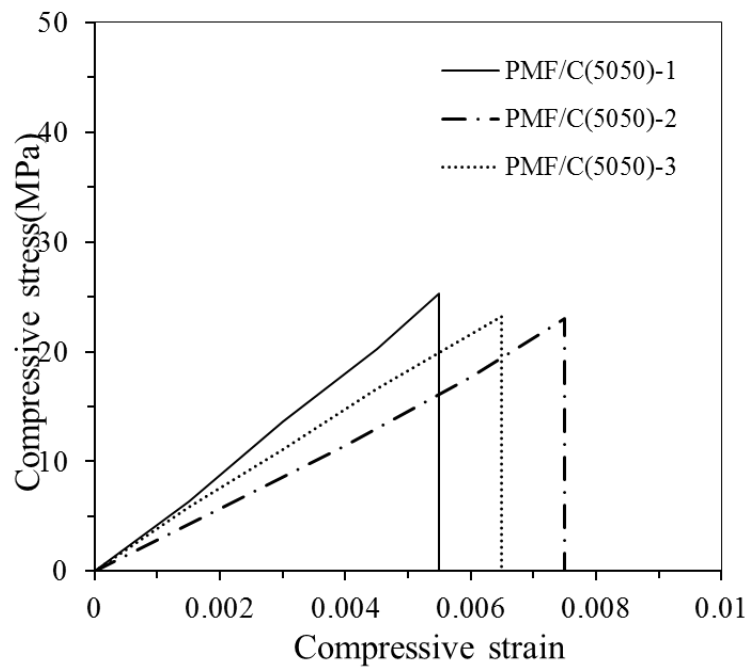

Figure 16 Compressive stress - strain curves for the the eco-composite whose mixture in weight fraction was C:R=50/50.

Ozone treatment

The ozone treatment was one of the techniques used to modify the surface activity of biomass charcoal in powder. The ultraviolet (UV) ozone has dramatic effect on the nature of surface oxidation, leading to the production of quinines, esters, and hydroxy function group [17]. The ozone treatment has improved the interfacial adhesion between a particle element of carbon, which was the reason to increase the compressive strength of eco-composite [18, 19]. Also UV ozone technique increased oxygen concentration and adhension of biomass charcoal with phenol resin matrix in eco-composite [20]. In this study, the ultraviolet (UV) ozone generation process was applied to biomass charcoal powder before mixing with particle reinforced materisls to fabricate eco-composites. The results of compressive strength were shown in Figure 17.
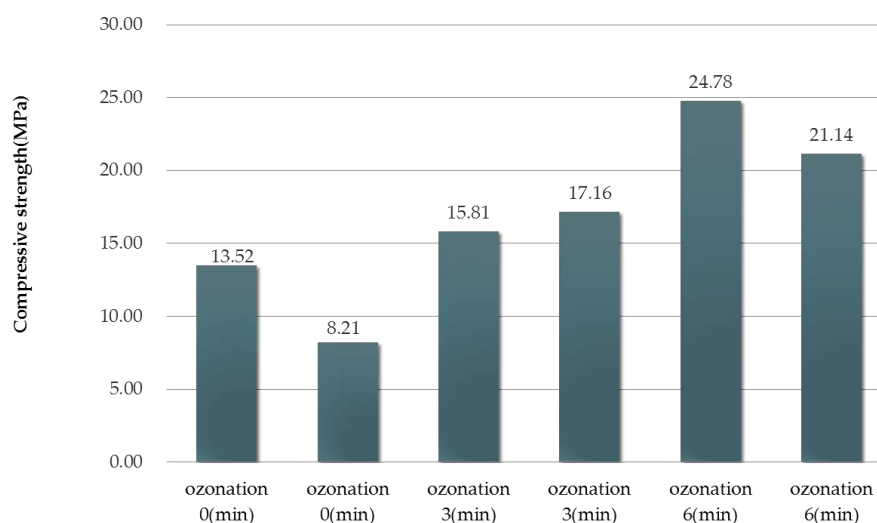

Figure 17 Compressive strength of WCMs effect from Ozone treting method.

Conclusion

Attempts to synthesize Eco-composites using waste malamine formaldehyde and biomass charcoal powder originating from Thai rubber tree wood as particle reinforcing materials were made. The waste malamine formaldehyde is a thermosetting plastic, that

keeps solidity shape permanently after being formed. The curing materials (pure melamine formaldehyde or phenolic resin powders) were designed for use with different weight fractions to binder materials. The microstructures of solid composites whose formed and compressive strengths were mainly investigated. Waste malamine formaldehyde content in eco-composite increases compressive strength. The maximum weight fraction of waste melamine formaldehyde to synthesize the composite was 50% in weight. The highest compressive strength of 35.7 MPa was obtained from a composite mixed with waste melamine formaldehyde (waste melamine formaldehyde /charcoal/phenol resin: 50/30/20), while those with pure melamine formaldehyde (virgin MF/charcoal: 50/50) and phenolic resin (phenolic resin/charcoal: 50/50) were 24.1 MPa and 11.5 MPa respectively.

These eco-composite materials provide high compressive strength when the volume of waste malamine forldehyde was increased. The consideration of toxicity, safety, and environmental factors of the eco-composite is important and should be investigated in the future.

References

[1] D. William and Jr. Callister, Materials Science and Engineering an Introduction, 3rd Ed., New York, United State: John Wiley and Sons, Inc., 1994, Print..

[2] X.H. Nguyen, T. Honda, "Classification of Eco-Materials in the perspectives of sustainability," dalam *The 3 International Symposium on Environmental Conscious Design and Inverse Manufacturing*, Japan, 2003.

[3] G. Bogoeva Gaceva, M. Avella, M. Malinconico, A. Buzarovska, A. Grozdanov and G. Gentile, "Natural Fiber Eco-Composites," *Polymer Composite,* pp. 98-107, 2007.

[4] Ch. Saengruksawong, S. Khamyong, N. Anongrak and J. Pinthong, "Growths and carbon stocks or para rubber plantations on phonpisai soil series in Northeastern Thailand," *Rubber Thai Journal,* vol. 1, pp. 1-18, 2012.

[5] T. T. R. Association, "Production of natural rubber in Thailand," August 2014. [Online]. Available: http://www.thainr.com/en/index.php?detail=stat-thai. [Diakses 12 September 2014].

[6] S. Siwadamrongpong, W. Boongsood, M. Mahai and K. Wonglane, "Influence of pre-heating in cold forming of melamine," dalam *The 7th South East Asian Technological University Consortium Symposium (SEATUC-7)*, Bandung, Indonesia, 2013.

[7] Ch.Chaitongrat, S. Siwadamrongpoong, M.Mahai and K.Wonglane, "Thermal properties of recycled material from waste melamine formed by hot molding process," dalam *7th SEATUC Symposium*, Indonesia, March,2013.

[8] S.H.Goodman, Handbook of Thermoset Plastic 2nd, California, United State of America: Raytheon Systems Company EI Segundo, 1998.

[9] P. Company, "Plastic Engineering Company; Phenolic Resin," Plenco Company, [Online]. Available: https://www.plenco.com/phenolic-novolac-resol-resins.htm. [Diakses 6 January 2015].

[10] F.H. Mark and others, "Phenolic Resins," dalam *Encyclopedia of polymer science and technology; Plastics, resins, rubbers, fibers*, New York, John Wiley & Sons, 1968, p. 358.

[11] R. Ozao, Y. Nishimoto, W. Pan and T. Okabe, "Thermoanalytical characterization of carbon/carbon hybrid material, apple woodceramics," *Thermochimica Acta,* vol. 440, pp. 75-80, 2006.

[12] T. Okabew, K. Kakishita, H. Simizu, K. Ogawa, Y. Nishimoto, A. Takasaki, T. Suda, M. Fushitani, H. Togawa, M. Sata and R. Yamamoto, "Current status and application of woodceramics made from biomass," *Trans. Mat. Res. Soc. of Japan,* vol. 38, pp. 191-194, 2013.

[13] F. Salaun and I. Vroman, "Influence of core materials on the thermal properties of melamine-formaldehyde microcapsules," *European Polymer Journal,* vol. 44, pp. 849-860, 2008.

[14] S. Pickering, "Recycling technologies for thermoset compositematerials-current status," *Composites : Part A,* vol. 37, pp. 1206-1215, 2006.

[15] T.R. Lakshminarayayanan and M.P. Gupta, "X-Ray Diffraction studies on Shellac/Melamine Resin Blends," *Journal of Applied Polymer Science,* vol. 19, pp. 3385-3386, 1975.

[16] J. Qian, Zh. Jin and J. Wang, "Structure and basic properties of woodceramics maade from phenolic resin-basswood powder composite," *Materials Science and Engineering ,* vol. A 368, pp. 71-79, 2004.

[17] E. Najafi, J.Y. Kim, S.H. Han and K. Shin, "UV-Ozone treatment of multi-walled carbon nanotubes for enhanced organic solvent dispersion," *Colloids and Surfaces,* vol. 284, pp. 373-378, 2006.

[18] Zh. Jin, Zh. Zhang and L. Meng, "Effects of ozone method treating carbon fibers on mechanical properties of carbon/carbon composite," *Materials Chemistry and Physics,* vol. 97, pp. 167-172, 2006.

[19] T.H. Benney, T. J. Bandosz and S.S. Wong, "Effect of ozonolysis on the pore structure, surface chemistry, and bundling of single-walled carbon nanotubes," *Journal of Colloid and Interface Science,* vol. 317, pp. 375-382, 2008.

[20] M.J. Rich, L.T. Drzal, B.P. Rook, P. Askeland and E.K. Drown, "Novel carbon fiber surface treatment with ultraviolet light in ozone to promote composite mechanical properties," dalam *ICCM-17*, Edinburgh, UK, 2009.

List of Publications

Journals

1. **D. Kaewdook**, A. Takasaki and T. Okabe, Deposition of Amorphous Carbon Thin Films by RF Magnetron Sputtering using Woodceramics as Target, Trans. Mat. Res. Soc. Japan, Vol. 39(1), pp. 39-42, March 2014.

International Conference Proceeding

1. **D. Kaewdook**, M. Ookawa, T. Okabe and A. Takasaki, New Applications of Woodceramics Orginated from Waste Thai Hevea Wood, The 5th TSME International Conference on Mechanical Engineering, Thailand, 2014.

2. **D. Kaewdook**, M. Ookawa, A. Takasaki and T. Okabe, Production of Woodceramics using Thai Waste Coconut Shell, and their Physical Properties, The 8th MSAT International Conference on Materials Science and Technology, Thailand, 2014.

3. **D. Kaewdook**, A. Takasaki and T. Okabe, The Characteristics of DLC Films Deposited by RF Magnetron Sputtering using Woodceramics as Target, The 7th SEATUC Symposium, Indonesia, March 2013.

4. **D. Kaewdook**, M. Naoto and A. Takasaki, Development of Functional Carbon Materials as Woodceramics from Thai Rubber Tree Wood, The 7th SEATUC Symposium, Indonesia, March 2013.

5. **D. Kaewdook**, J. Aphirakmethawawong, S. Siwadamrongpong, T. Okabe and A. Takasaki, Fabrication of Composites Consisted of Waste Melamine and Charcoal Originated from Waste Thai Rubber Trees, The 11th Inter.Conf. on Eco-materials(ICEM11), November 2013.

6. A. Takasaki, **D. Kaewdook** and T. Okabe, Electrochemical Metallic Deposition on Woodceramics Originated from Biomass, The 11th Inter.Conf. on Eco-materials(ICEM11), November 2013.

7. **D. Kaewdook**, A. Takasaki and T. Okabe, The Effect of Substrate Surface Roughness on the Mechanical Properties of DLC Film Deposited by RF Magnetron Sputter Ion Plating from Woodceramic as Target, The 2nd TSME International Conference on Mechanical Engineering, Thailand, 2011.

International Conference Presentation

1. **D. Kaewdook**, M. Ookawa, A. Takasaki and T. Okabe, Effect of carbonization temperature on the structure and basic properties of Woodceramics Originated from waste Thai rubber wood, *22nd SYOKUGYOUDI Forum 2014*, Polytechnic University, Tokyo, Japan, October 2014.

2. **D. Kaewdook**, M. Ookawa, A. Takasaki and T. Okabe, Development of Woodceramics Originated from Coconut Shell, *The 15th IUMRS-Inter. Conf.in Asia (IUMRS-ICA 2014)*, Fukuoka, Japan, August 2014

3. **D. Kaewdook**, A. Takasaki and T. Okabe, New Applications of Woodceramics Originated from Biomass, *Practical Education Workshop-2014 (Jissen)*, Tokyo, Japan, August 2014.

4. **D. Kaewdook**, A. Takasaki, H. Miyakawa, T. Hirose and T. Okabe, Development of Woodceramics Originated from Thailand Waste Rubber Tree Wood, *The 23rd Annual Meeting/Academic Symposium of MRS-J*, Yokohama, Japan, December 2013.

5. **D. Kaewdook**, A. Takasaki and T. Okabe, Deposition of DLC Films by RF Magnetron Sputtering using Woodceramics as Target, *The 22nd Academic Symposium of MRS-J*, Yokohama, Japan, September 2012.